HARVARD UNIVERSITY
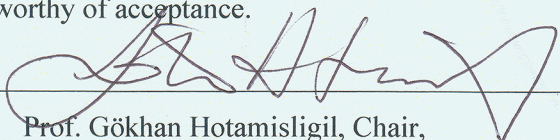## Graduate School of Arts and Sciences

DISSERTATION ACCEPTANCE CERTIFICATE

The undersigned, appointed by the

Committee on Higher Degrees in Biological Sciences in Public Health

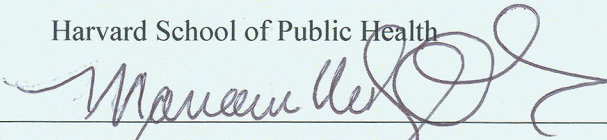have examined a dissertation entitled

"SREBP: A Key Effector of mTORC1 Signaling in Metabolism and Cancer"
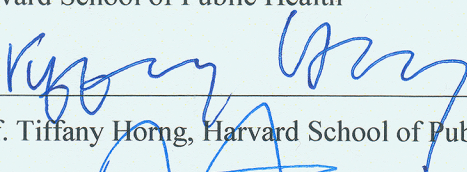
presented by Jessica Lucas Yecies

candidate for the degree of Doctor of Philosophy and hereby certify that it is worthy of acceptance.

Signature _____

Typed name: Prof. Gökhan Hotamisligil, Chair,

Harvard School of Public Health

Signature _____

Typed name: Prof. Marianne Wessling-Resnick,

Harvard School of Public Health

Signature _____

Typed name: Prof. Tiffany Horng, Harvard School of Public Health

Signature _____

Typed name: Prof. David Sabatini, Massachusetts Institute of Technology

Date: November 30, 2011

SREBP: A Key Effector of mTORC1 Signaling

in Metabolism and Cancer

A dissertation presented

by

Jessica Lucas Yecies

to

The Program in Biological Sciences in Public Health

in partial fulfillment of the requirements
for the degree of

Doctor of Philosophy
in the subject of
Biological Sciences in Public Health

Cambridge, Massachusetts

March 2012

Advisor: Brendan D. Manning   **Jessica Lucas Yecies**

SREBP: A Key Effector of mTORC1 Signaling in Metabolism and Cancer

ABSTRACT

The mammalian target of rapamycin complex 1 (mTORC1), a master regulator of cell growth and proliferation, is aberrantly activated in cancer, genetic tumor syndromes and obesity. Much progress has been made to understand the upstream pathways that regulate mTORC1, most of which converge upon its negative regulator, the Tuberous Sclerosis Complex (TSC) 1-TSC2 complex. However, the cell intrinsic consequences of aberrant mTORC1 activation remain poorly characterized. Using systems in which mTORC1 is constitutively activated by genetic loss of TSC1 or TSC2 and pharmacologically inhibited by treatment with an mTORC1-specific inhibitor rapamycin, we have identified that mTORC1 controls specific aspects of cellular metabolism, including glycolysis, the pentose phosphate pathway, and *de novo* lipogenesis. Induction of the pentose phosphate pathway and *de novo* lipogenesis is achieved by activation of a transcriptional program affecting metabolic gene targets of sterol regulatory element-binding protein (SREBP). We have demonstrated that mTORC1 stimulates the accumulation of processed, active SREBP, although details of the molecular mechanism remain to be elucidated.

To understand the physiological and pathological relevance of mTORC1-dependent activation of SREBPs and lipogenesis, we explored these findings in the liver and in cancer. While we find that the induction of hepatic SREBP1c and lipogenesis by insulin requires mTORC1, mTORC1 activation is not sufficient to stimulate hepatic SREBP1c in the absence of Akt signaling, revealing the existence of an additional downstream pathway also required for this induction. We demonstrate that this

mTORC1-independent pathway involves Akt-mediated suppression of *Insig2a*, a liver-specific transcript encoding the SREBP1c inhibitor INSIG2. In cancer, our initial findings demonstrate that mTORC1 plays a role downstream of TSC-deficiency and oncogenic PIK3CA and K-Ras to activate lipogenic SREBP targets and de novo lipogenesis. Further studies of the connection between mTORC1 and SREBPs in disease may offer insights into novel therapeutic approaches.

TABLE OF CONTENTS

CHAPTER 1

Introduction

CHAPTER 2

mTOR Complex 1 Controls Cellular Metabolism

CHAPTER 2 continued

SREBP is responsible for increased lipid biosynthesis, the pentose phosphate pathway, and cell proliferation downstream of mTORC1
mTORC1 activates SREBP1 through S6K1

CHAPTER 3

mTORC1-Dependent and Independent Control of Hepatic SREBP1c

Insulin stimulates hepatic SREBP1c in an mTORC1-dependent manner
Liver-specific deletion of *Tsc1* results in insulin-independent activation of mTORC1
LTsc1KO mice are protected from age- and diet-induced hepatic steatosis
LTsc1KO mice have defects in hepatic induction of SREBP1c and lipogenesis
Elevated hepatic mTORC1 signaling attenuates insulin signaling to Akt
Restoration of Akt signaling to *LTsc1KO* hepatocytes rescues SREBP1c induction
INSIG2a suppression is an mTORC1-independent mechanism regulating SREBP1c downstream of Akt

CHAPTER 4

Discussions and Future Directions

APPENDIX

Chewing the Fat on Tumor Cell Metabolism

For Derek, Mom, Dad and Justin

In memory of Pete Curtin

ACKNOWLEDGEMENTS

I have had a wonderful Ph.D. experience thanks to Brendan, who has been an incredibly supportive advisor. I learned so much from Brendan, who has taught me not only how to do great science but also to effectively communicate my work to others. I am so grateful for the tremendous opportunities Brendan has provided me with, whether to pursue exciting projects, to write papers and reviews, and to speak at conferences. I am really appreciative of his caring guidance and willingness to always provide insightful and thoughtful feedback. I will miss our chats that quickly went off topic towards some exciting discussion of new future directions. I have also to thank him for my acquisition of a liking for both coffee and good beer.

I would like to especially thank my family. My husband, Derek, has always been there to support me, in both the happy and difficult times throughout graduate school and always. I could not have accomplished my Ph.D. without him – and I also mean this literally, as he worked as my very talented technician for a few months. I would like to express my upmost appreciation for my mom, who inspired me to study science and pursue a Ph.D. She has accompanied me throughout my Ph.D. on the other end of the phone during my daily journeys to and from the lab. She has always been there to offer suggestions and advice, both scientific and personal. Thanks also, to my Mom, Dad and brother, Justin, who made long trips up from New York to visit for dinner, which were always a fun escape from weekends in the lab.

Finally, I would like to thank the members of my Dissertation Advisory and Dissertation Defense Committee Drs. Lewis Cantley, Gökhan Hotamisligil, Chih-Hao Lee, Tiffany Horng, Marianne Wessling-Resnick, and David Sabatini for their time, advice, and support.

CHAPTER 1

Introduction

Adapted from:

Yecies, J.L.[1] and Manning, B.D[1]. (2011). mTOR links oncogenic signaling to tumor cell metabolism. *J Mol Med* 89, 221-8.

[1]Department of Genetics and Complex Diseases, Harvard School of Public Health, Boston, MA 02115, USA

SUMMARY

The mammalian target of rapamycin (mTOR) complex 1 (mTORC1) is aberrantly activated in a wide variety of disease states, including cancer, genetic tumor syndromes, and metabolic disorders. As a key regulator of cell growth and proliferation, mTORC1 has been the subject of intense investigation for its role in tumor development and progression. This research has revealed a signaling network of oncogenes and tumor suppressors lying upstream of mTORC1, and oncogenic perturbations to this network result in the aberrant activation of this kinase complex in the majority of human cancers. However, the molecular events downstream of mTORC1 contributing to tumor cell growth and proliferation are just coming to light. In addition to its better-known functions in promoting protein synthesis and suppressing autophagy, mTORC1 has emerged as a key regulator of cellular metabolism. Recent studies have found that mTORC1 activation is sufficient to stimulate an increase in glucose uptake, glycolysis, and de novo lipid biosynthesis, which are considered metabolic hallmarks of cancer, as well as the pentose phosphate pathway. mTORC1's novel role as a regulator of cellular metabolism also has implications for its role in metabolic disorders, such as type 2 diabetes. Here, we focus on the molecular mechanisms of metabolic regulation by mTORC1, and the potential consequences for anabolic tumor growth and therapeutic strategies. We will also briefly summarize the current knowledge of mTORC1's control of systemic metabolism.

BACKGROUND

The successful tumor cell must overcome the metabolic demands of an increased rate of growth and proliferation, often in the face of diminishing access to certain nutrients. In order to adapt and thrive under such conditions, tumor cells

inevitably acquire oncogenic mutations in growth factor and nutrient-sensing signaling

pathways that disconnect metabolic regulation from physiological signals. The

mammalian target of rapamycin (mTOR) is an evolutionarily conserved Ser/Thr kinase

that could play a major role in the metabolic reprogramming of tumor cells. A complex of

mTOR with at least two other essential core components (Raptor and mLST8), known as

mTOR complex 1 or mTORC1, responds to signals relaying the status of extrinsic and

intrinsic cellular growth conditions and has emerged as an upstream control point for

cellular metabolism. Importantly, the mTORC1 pathway is aberrantly activated in the

majority of human tumors (reviewed in [1]), making it poised to influence the metabolic

changes common to tumor cells.

Common oncogenic signaling events activate mTORC1

As a key regulator of cell growth and proliferation, mTORC1 is activated by the

predominant signaling pathways that promote these processes. These include both the

PI3K-Akt and Ras-Erk pathways, which are the most common oncogenic signaling

pathways activated in human cancers. These pathways regulate mTORC1 by

converging on a small G protein switch, involving the tuberous sclerosis complex (TSC)

tumor suppressors TSC1 and TSC2 and the Ras-related small G protein Rheb (Figure 1-

1; reviewed in [2]). TSC2, when in a complex with TSC1, acts as a GTPase-activating

protein (GAP) for Rheb, thereby stimulating its conversion to the inactive GDP bound

form. GTP-bound Rheb is thought to bind directly to mTORC1 and is essential for the

stimulation of mTORC1 kinase activity [3]. Protein kinases downstream of Ras and PI3K,

including Akt, Erk, and RSK, directly phosphorylate TSC2 on a variety of inhibitory sites,

thereby blocking the ability of the TSC1-TSC2 complex to act as a GAP for Rheb. This

results in accumulation of GTP-bound Rheb and acute activation of mTORC1. In

addition to these growth factor signaling pathways, mTORC1 signaling is sensitive to
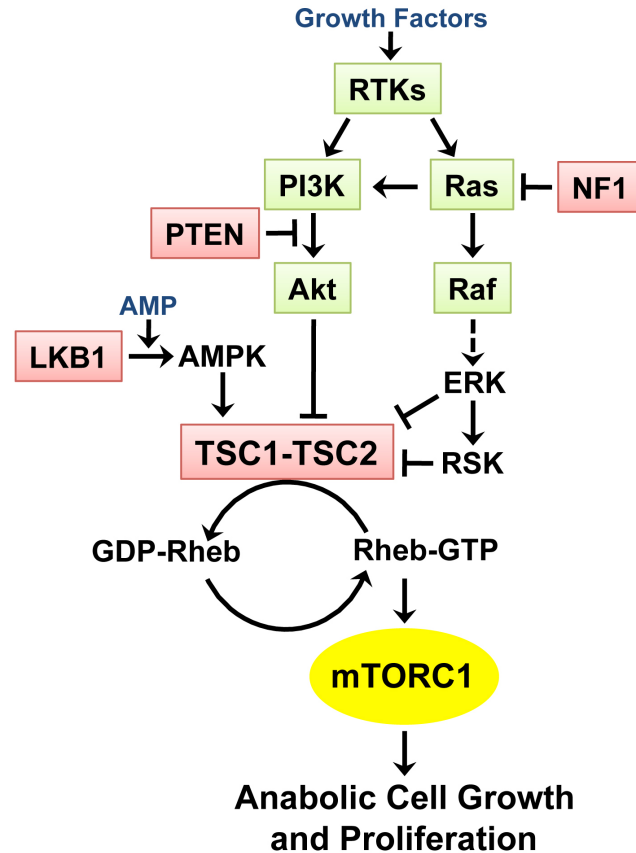
Figure 1-1. A network of oncogenes and tumor suppressors lie upstream of mTORC1. Growth factors bind to and stimulate receptor tyrosine kinases (RTKs), which can activate mTORC1 through both the PI3K-Akt and Ras-Erk signaling pathways. These pathways converge to inhibit the TSC1-TSC2 complex, allowing Rheb-GTP to accumulate and activate mTORC1. Cellular energy depletion is sensed by mTORC1 through a rise in intracellular AMP leading to LKB1-dependent activation of AMPK. AMPK also signals through the TSC1-TSC2 complex, but enhances the activity of this complex, thereby inhibiting mTORC1 in response to energy stress. Within this upstream signaling network lie many oncogenes (depicted in green) and tumor supressors (depicted in red). Oncogenic mutations within this network are common in human tumors, resulting in aberrantly elevated mTORC1 activity contributing to uncontrolled cell growth and proliferation.

intracellular nutrients and energy. While the sensing mechanisms are poorly understood,

mTORC1 senses amino acids in a manner dependent on the Rag GTPases, which

under amino acid replete conditions recruit mTORC1 to lysosomal membranes for

activation by Rheb [4]. Cellular energy levels are sensed by mTORC1, at least in part,

through the AMP-activated protein kinase (AMPK). In response to ATP consumption and

a rise in intracellular AMP levels, AMPK inhibits mTORC1 by phosphorylating TSC2 on

activating sites [5] and the mTORC1 component Raptor on inhibitory sites [6]. Therefore,

the activation status of mTORC1 is influenced by a network of signaling pathways that

sense cellular growth conditions. Aberrantly elevated mTORC1 signaling is detected in

40 to 90% of the ten most frequently occurring human cancers [1]. This is consistent with

the fact that the signaling network lying upstream of mTORC1 is comprised of some of

the most commonly mutated oncogenes and tumor suppressors (Figure 1-1). In addition

to common activating mutations in PI3K and K-Ras, upstream receptor tyrosine kinases

(RTKs) are often subjected to activating mutations and amplifications, and tumor

suppressors that negatively regulate these pathways, such as PTEN and NF1, are

frequently lost. Through activation of the PI3K and/or Ras signaling pathways, these

events lead to growth factor-independent activation of mTORC1. In addition, the LKB1

tumor suppressor, which is mutated in a large percentage of lung cancers, is required for

AMPK activation in response to energy stress, and its loss also leads to aberrant

mTORC1 signaling [7]. In addition to sporadic cancers, mTORC1 is activated in a large

number of genetic tumor syndromes, classified as hamartoma syndromes or

phakomatoses, caused by loss of upstream tumor suppressors, including tuberous

sclerosis complex (TSC1, TSC2), Cowden syndrome (PTEN), neurofibromatosis (NF1,

NF2), and Peutz-Jeghers syndrome (LKB1) (reviewed in [1]). Therefore, as a

convergence point for numerous oncogenes and tumor suppressors, mTORC1 is well-

positioned to control cellular processes common to all tumor cells.

mTORC1 signaling and the metabolic reprogramming of tumor cells

Given the pervasive upregulation of mTORC1 in human tumors, it is important to establish a better understanding of the downstream consequences of mTORC1 activation under both physiological and pathological states. Studies using the mTORC1-specific inhibitor rapamycin have revealed an evolutionarily conserved role for mTORC1 orthologs in the control of cell growth (i.e. an increase in cell size) and proliferation (i.e., an increase in cell number) in organisms from yeast to humans [8]. However, these are complex biological processes, and the specific molecular functions of mTORC1 contributing to these gross physiological outcomes are still being elucidated. Below, we focus on metabolic processes found to be regulated downstream of mTORC1 and their potential to contribute to the bioenergetic and anabolic demands of rapidly growing and proliferating tumor cells.

Protein synthesis

The most recognized function for mTORC1 is the promotion of protein synthesis, which it controls at several levels. While the mechanisms are poorly understood in mammalian cells, mTORC1 plays a conserved role in stimulating ribosome biogenesis. A major point of control for the production of new ribosomes is the translation of mRNAs encoding ribosomal proteins, which share the characteristic of 5' untranslated regions (UTRs) containing sequences rich in pyrimidines, commonly referred to as 5'-terminal oligo pyrimidine (5'TOP) tracts. The translation of these mRNAs, which also include those encoding translation factors, is stimulated by mTORC1 signaling through an unknown mechanism (e.g., reference [9]). In addition, the transcription of rRNA genes can be induced downstream of mTORC1 [10]. Apart from enhancing the protein synthetic capacity of the cell by increasing the number of ribosomes, mTORC1 signaling controls specific aspects of mRNA translation initiation through at least two classes of

direct downstream substrates (reviewed in [11]). mTORC1 phosphorylates and activates

the ribosomal S6 kinases (S6K1 and S6K2), which in turn phosphorylate a number of

downstream targets involved in translation initiation, including ribosomal protein S6,

eIF4B, and PDCD4 (programmed cell death 4). mTORC1 also phosphorylates the

eukaryotic initiation factor 4E (eIF4E)-binding proteins (4E-BP1 and 4E-BP2), which

triggers their release from eIF4E at the 5'-cap of mRNAs, thereby allowing translation

initiation factors to bind (Figure 2-2). However, mTORC1 activation appears to acutely

stimulate the translation of only a subset of mRNAs. Aside from 5'TOP sequences, the

molecular properties dictating this selectivity are poorly defined, but many of the mRNAs

that are particularly sensitive to mTORC1 signaling contain highly structured 5'UTRs.

Importantly, this includes mRNAs encoding proteins that control cell proliferation and

metabolism (e.g., cyclin D1, c-Myc, HIF1α). While the individual translational targets of

mTORC1 signaling will contribute to tumor development and progression, the stimulation

of ribosome biogenesis leading to an overall increase in protein synthesis is likely to be a

major mechanism by which mTORC1 promotes anabolic cell growth and proliferation in

tumor cells.

Autophagy

Autophagy is a catabolic cellular process that facilitates the recycling of

organelles and proteins into their nutrient components (reviewed in [12]). Autophagy

serves as both a quality control process and a mechanism to replenish intracellular

nutrients under conditions of poor nutrient availability. Under nutrient rich conditions,

mTORC1 signaling suppresses autophagy, at least in part, by inhibiting a conserved

protein complex containing the protein kinases ULK1 or ULK2, which is required for the
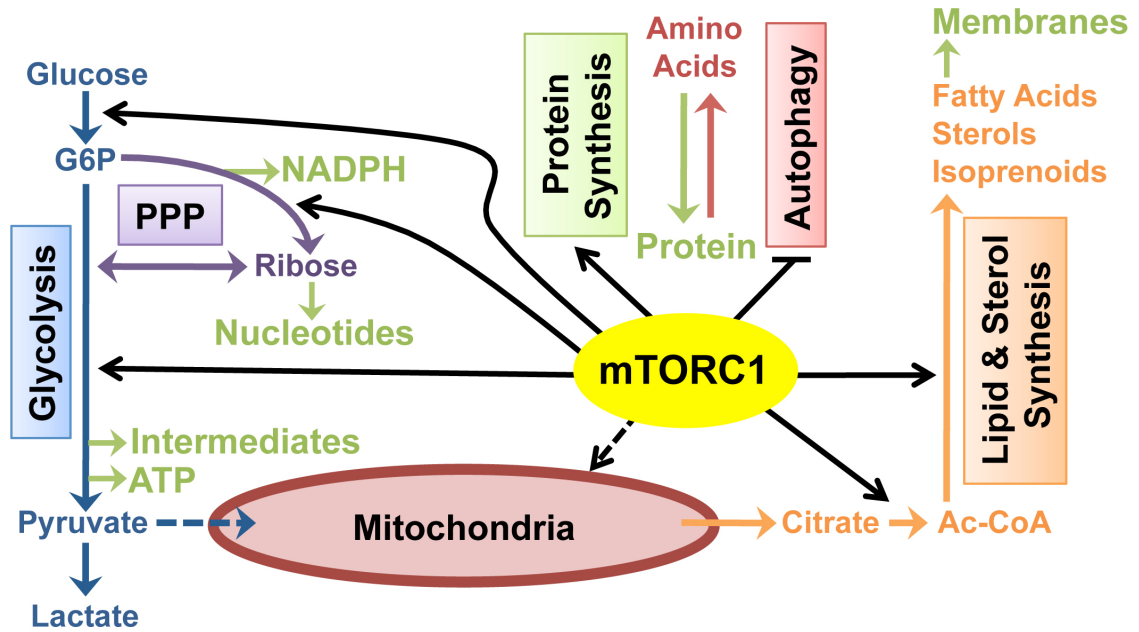
Figure 1-2. mTORC1 regulates many aspects of cellular metabolism. Physiological or pathological activation of mTORC1 results in changes to cellular metabolic processes. In addition to its well-known roles in promoting protein synthesis and inhibiting autophagy, mTORC1 has been found to stimulate glucose uptake, its conversion to glucose 6-phosphate (G6P), and metabolic flux through both glycolysis and the oxidative arm of the pentose phosphate pathway (PPP). Through activation of SREBP, mTORC1 also stimulates the production of cytosolic acetyl-CoA and subsequent lipid and sterol synthesis. The products of these metabolic processes that are most likely to contribute to anabolic growth and proliferation downstream of mTORC1 are depicted in green. See text for details.

induction of autophagy [13]. Autophagy is thought to have prosurvival effects on cells

experiencing metabolic and nutritional stress within established tumors, enabling them to

evade apoptosis [14]. However, autophagy also has tumor suppressive effects, as

defective initiation of autophagy promotes tumorigenesis. Therefore, aberrant activation

of mTORC1 and inhibition of autophagy in the early stages of tumorigenesis could

promote tumor progression.

Glucose Uptake and Glycolysis

One of the most well appreciated metabolic differences between cancer cells and

their cell of origin is a greatly enhanced rate of glucose uptake and its glycolytic

conversion to lactate (reviewed in [15]). This glycolytic switch is driven, in part, by the

hypoxic tumor microenvironment, which dampens the capacity for oxidative metabolism

in the mitochondria. However, this switch to glycolysis is generally maintained when

tumor cells are returned to normoxic conditions following angiogenesis or, as seen most

often, when cultured in the laboratory, suggesting underlying genetic or epigenetic

changes. This phenomenon, known as aerobic glycolysis or the "Warburg effect",

provides tumor cells a proliferative advantage over normal cells under conditions of

intermittent hypoxia within the growing tumor. However, aerobic glycolysis also more

readily provides both the energy (ATP) and building blocks (carbon intermediates) for

rapid anabolic growth and proliferation. The switch to aerobic glycolysis occurs, in large

part, through the global upregulation of genes encoding the enzymes of glycolysis, and

these genes are amongst the most overexpressed in human cancer [16].

Oncogenic events, most notably the activation of the PI3K-Akt-mTORC1

pathway, have been found to promote expression of genes involved in glucose uptake

and glycolysis through normoxic upregulation of the hypoxia-inducible factor (HIF1α)

transcription factor [17-22]. Importantly, activation of mTORC1 increases translation from

the 5'UTR of the mRNA encoding HIF1α and is sufficient to stimulate glycolytic gene

expression and a corresponding increase in flux through glycolysis (Chapter 2; [23]).

Another known translational target of mTORC1 is the oncogenic transcription factor c-

Myc, which can also promote glycolytic gene expression and might contribute to the

induction of glycolysis downstream of mTORC1 in some settings [24, 25]. Therefore,

through its effects on specific transcription factors, mTORC1 activation by upstream

oncogenic signaling pathways could be an underlying mechanism driving the Warburg

effect in some tumors. In the clinic, monitoring glucose uptake into tumors, through FDG-

PET imaging, could serve as an important tool to predict the efficacy of mTORC1

inhibitors [22].

Mitochondrial Metabolism

The glycolytic program of tumor cells is generally accompanied by upregulation

of enzymes involved in further funneling pyruvate, the end product of glycolysis, away

from oxidation in mitochondria. This is achieved in large part through HIF1α-mediated

expression of lactate dehydrogenase (LDH1), which converts pyruvate to lactate, and

pyruvate dehydrogenase (PDH) kinase (PDK1), which inhibits the conversion of

pyruvate to acetyl-CoA by phosphorylating and inhibiting a subunit of PDH (reviewed in

[25]). Activation of mTORC1 promotes the HIF1α-dependent expression of both LDH1

and PDK1 (Chapter 2; [23]) and, therefore, would be predicted to decrease oxidative

metabolism in the mitochondria. However, in some cellular settings, mTORC1 appears

to promote mitochondrial biogenesis and oxidative metabolism [26, 27], and in one

study, short-term inhibition of mTORC1 with rapamycin actually led to an increase in

lactate production and decrease in oxygen consumption [28]. A genetic mouse model

ablating mTORC1 activity specifically in skeletal muscle has also suggested a role for

mTORC1 in mitochondrial function [29]. Further studies focused on the importance of

mTORC1-mediated effects on the mitochondria in tumor models are clearly needed to

understand potential contributions of this regulation to tumor cell metabolism.

Lipid Synthesis

Like the Warburg effect, an increased rate of *de novo* lipid synthesis is another

nearly ubiquitous metabolic change in tumor cells [30]. In contrast to metabolic cell types

designed to produce lipids, such as those comprising the liver and adipose tissue, most

normal cells have very low rates of lipid synthesis, instead obtaining essential lipids from

the diet. The acquired ability of cancer cells to generate their own lipids facilitates the

increased demand for new membranes to support rapid growth and proliferation. The

sterol regulatory element-binding protein (SREBP) transcription factors (SREBP1a,

SREBP1c, and SREBP2) are master regulators of genes involved in lipid and sterol

synthesis. In order to prevent the metabolically costly processes of lipid and sterol

synthesis under conditions of low demand, the SREBPs are tightly regulated through a

complex series of events that have yet to be fully delineated [31]. SREBPs reside as

inactive precursors in the endoplasmic reticulum (ER) in complex with SREBP cleavage-

activating protein (SCAP). Growth factor signaling or depletion of intracellular cholesterol

stimulate SREBP trafficking from the ER to the golgi, where two sequential proteolytic

cleavage events release the mature, active form, which translocates to the nucleus to

turn on target genes.

The PI3K-Akt pathway has been shown to upregulate lipogenic gene expression

in an SREBP-dependent manner [32], and mTORC1 has recently been identified as the

critical downstream effector responsible for SREBP activation (Chapter 2; [23, 33]).

Although the molecular mechanism(s) remains to be elucidated, current data support a

role for mTORC1 signaling in promoting the trafficking or processing of SREBP.

mTORC1 activation has been demonstrated to stimulate *de novo* lipogenesis in an

11

SREBP-dependent manner, and this contributes to both the growth and proliferation of cells downstream of mTORC1 (Chapter 2; [23, 33]). Interestingly, fatty acid synthase (FASN) is encoded by an SREBP target gene and is upregulated at the mRNA level in most types of human cancer [30]. Activation of the PI3K-Akt pathway has been implicated in the increased expression of FASN in prostate cancer cell lines and primary tumors [34, 35]. Future studies will focus on determining whether mTORC1 is primarily responsible for elevated FASN expression and de novo lipid synthesis in some classes of tumors, such as those driven by the PI3K-Akt pathway. However, one recent study has suggested that the elevated activation of SREBP in at least some tumors is resistant to rapamycin [36]. FASN expression can also be readily detected in biopsy samples, and its sensitivity to treatment with mTORC1 inhibitors may prove to be a useful biomarker to predict clinical response to these inhibitors.

The Pentose Phosphate Pathway

While increases in protein synthesis, glycolysis, and de novo lipogenesis are metabolic hallmarks of cancer, contributions from altered regulation of the pentose phosphate pathway are more poorly understood. Increased activity of the rate limiting enzyme of the oxidative arm of the pentose phosphate pathway, glucose 6-phosphate dehydrogenase (G6PD), has been reported in a variety of human tumors (e.g., references [36-38]). Similarly, overexpression and increased activity of transketolase (TKTL1), a key enzyme of the non-oxidative branch of the pentose phosphate pathway, has been found to correlate with increased invasiveness and patient mortality in several cancer types (e.g., references [40-42]). A recent study has found that mTORC1 activation is sufficient to stimulate the expression of genes encoding the enzymes of both the oxidative and non-oxidative branches of the pentose phosphate pathway

(Chapter 2; [23]), although the relevance to cancers displaying elevated mTORC1 signaling remains to be explored.

Activation of the pentose phosphate pathway could contribute to many of the unique metabolic requirements of tumor cells. Through its generation of NADPH, the oxidative arm of the pentose phosphate pathway provides reducing power to drive anabolic metabolism. For instance, large amounts of NADPH are required and consumed during de novo lipid synthesis. In support of a link between the pentose phosphate pathway and lipogenesis, *G6PD* has been suggested to be a transcriptional target of the lipogenic transcription factor SREBP1 [43-45]. Importantly, the induction of *G6PD* expression downstream of mTORC1 was found to be dependent on the ability of mTORC1 to activate SREBP1 (Chapter 2; [23]). How mTORC1 signaling stimulates the other pentose phosphate genes is currently unknown. Pentose phosphate pathway-generated NADPH also protects against oxidative stress by sustaining levels of reduced glutathione. This could be particularly important in tumor cells that might have elevated levels of reactive oxygen species due to metabolic fluctuations influenced by intermittent access to oxygen and nutrients within the tumor. In support of this idea, a recent study demonstrated that the PI3K-Akt pathway reduces oxidative stress and promotes cell survival of mammary epithelial cells detached from the extracellular matrix by increasing flux through the oxidative pentose phosphate pathway [46]. It has been demonstrated that mTORC1 activation is sufficient to stimulate an increase in flux through the oxidative pentose phosphate pathway (Chapter 2; [23]), and future studies will determine the role of this regulation in tumor cell adaptation to the dynamic tumor microenvironment.

Both the oxidative and non-oxidative branches of the pentose phosphate pathway generate ribose, an essential precursor for *de novo* nucleotide biosynthesis. Rapidly dividing tumor cells must generate their own nucleotides to sustain DNA replication and the increased demand for RNA, especially ribosomal RNA. While

mTORC1 stimulates expression of genes encoding enzymes of both branches of the pentose-phosphate pathway, the increase in production of ribose 5-phosphate stimulated by mTORC1 activation was found to come primarily from increased flux through the oxidative branch (Chapter 2; [23]). There is some debate over the relative contributions of the oxidative and non-oxidative arms of the pentose phosphate pathway to the production of ribose for nucleotide biosynthesis within tumor cells. This is an important area for future study in the field of tumor cell metabolism, as it is likely that distinct oncogenic events could differentially regulate the pentose phosphate pathway at various stages of tumor progression. In general, a more detailed understanding of how metabolic flux through the pentose phosphate pathway affects other bioenergetic and anabolic processes, including glycolysis and lipid and nucleotide synthesis are required.

Implications for the treatment of tumors with aberrant mTORC1 activation

Given that mTORC1 activity is elevated in the majority of human tumors, there has been much interest in targeting this kinase complex with highly specific inhibitors, such as rapamycin (sirolimus) and its analogs (e.g., temsirolimus and everolimus). However, while studies are ongoing, these inhibitors have had limited success as cancer therapeutics thus far, and they generally elicit cytostatic rather than cytotoxic responses. An important recent finding is that rapamycin-derived compounds, which are allosteric inhibitors of mTOR, only partially inhibit mTORC1 function [47]. Another potential contributing factor to the limited effectiveness of these compounds as single anti-tumor agents is that they can potently activate the upstream PI3K-Akt pathway by blocking mTORC1-dependent feedback mechanisms. One way around such effects is to target key processes downstream of mTORC1, rather than mTORC1 itself. Downstream metabolic pathways are excellent candidates for such an approach, as mTORC1 activation is sufficient to drive the metabolic changes most common to tumor cells,

including increased rates of glycolysis and protein and lipid synthesis. An increased

dependence on these metabolic pathways distinguishes tumor cells from normal cells

and presents therapeutic opportunities to selectively kill tumor cells.

The coordinated activation of specific metabolic processes by mTORC1 signaling

could represent a mechanism of cellular adaptation to the potentially deleterious effects

of uncontrolled mTORC1 signaling in tumor cells. For example, increased lipid synthesis

may be as important for expanding ER membranes to accommodate an increase in ER

load due to mTORC1-driven protein synthesis as it is for promoting membrane

biogenesis to facilitate cell growth and proliferation. Likewise, activation of the pentose

phosphate pathway may be more critical for maintaining cellular redox homeostasis than

for directly supporting the anabolic processes of de novo lipid and nucleotide

biosynthesis. Therefore, while mTORC1 inhibitors might block adaptive metabolic

processes, they also alleviate the metabolic stress induced by hyperactivation of

mTORC1. To this end, rapamycin has been found to have pro-survival effects on cells

with aberrantly high mTORC1 activity [5, 48, 49]. The induction of autophagy by

rapamycin might also facilitate tumor cell survival under some conditions. Therefore,

targeting the metabolic pathways important for adaptation to the stress of elevated

mTORC1 signaling could elicit potent tumor-specific responses. In support of this idea,

knockdown of SREBP, the transcription factor responsible for the induction of lipid

synthesis and the oxidative pentose phosphate pathway downstream of mTORC1, can

block mTORC1-driven growth and proliferation in cell culture models (Chapter 2; [23,

33]). It will be important to identify the key enzymes induced by SREBP that underlie this

effect and to test the *in vivo* response of tumor cells exhibiting uncontrolled mTORC1

activity to knockdown or genetic ablation of these targets. In theory, the enzymes

comprising the major metabolic pathways downstream of mTORC1 are so-called

druggable targets. Novel and specific pharmacological inhibitors of the rate-limiting and

branch-point enzymes of these pathways will be important for validating these targets in preclinical tumor models. However, it is clear that a deeper understanding of how metabolic pathways are interconnected with and altered by oncogenic signaling pathways is needed to design therapeutic strategies to target tumor cell metabolism.

Beyond cancer: the role of mTORC1 in metabolic disorders

In addition to cancer, elevated mTORC1 activity has also been implicated in states of obesity and insulin resistance that are characterized by dysregulated lipid metabolism [50]. In mouse models of HFD-induced obesity, mTORC1 activity is elevated in insulin-responsive tissues, like the liver and muscle, which correlates with increased IRS phosphorylation and the development of hepatic insulin resistance [51]. The findings from studies of whole body S6K1 and 4E-BP1/2 knockout mice challenged with a HFD suggest that mTORC1-dependent activation of S6K1 and inhibition of 4E-BPs promotes cell intrinsic insulin resistance [52, 53]. S6K1 knockout mice are protected from obesity when fed a HFD or crossed to genetic models of obesity, while 4E-BP double knockouts are more susceptible to HFD-induced adiposity and increased hepatic triglyceride levels.

Additional studies have been performed in genetic models that modulate mTORC1 signaling in a tissue-specific manner to further understand the role of mTORC1 in physiology and disease. mTORC1 coordinates nutrient utilization by promoting insulin secretion from the pancreas and promoting mitochondrial biogenesis in skeletal muscle, while mTORC1 functions to suppress continued food intake in the hypothalamus and to prevent lipolysis in adipose tissue (reviewed in [54]). Although we are beginning to understand the cell intrinsic functions and regulation of mTORC1, further work is needed to completely understand how it is connected to and exerts control over systemic metabolic homeostasis.

ACKNOWLEDGEMENTS

REFERENCES

1.   Menon, S. and Manning, B.D. (2008). Common corruption of the mTOR signaling network in human tumors. Oncogene *27*, S43-S51.

2.   Huang, J. and Manning, B.D. (2008). The TSC1-TSC2 complex: a molecular switchboard controlling cell growth. Biochem J *412.*

3.   Sancak, Y., Thoreen, C.C., Peterson, T.R., Lindquist, R.A., Kang, S.A., Spooner, E., Carr, S.A. and Sabatini, D.M. (2007). PRAS40 Is an Insulin-Regulated Inhibitor of the mTORC1 Protein Kinase. Mol Cell *25*, 903-915.

4.   Sancak, Y., Bar-Peled, L., Zoncu, R., Markhard, A.L., Nada, S. and Sabatini, D.M. (2010). Ragulator-Rag complex targets mTORC1 to the lysosomal surface and is necessary for its activation by amino acids. Cell *141*, 290-303.

5.   Inoki, K., Zhu, T. and Guan, K.L. (2003). TSC2 mediates cellular energy response to control cell growth and survival. Cell *115*, 577-590.

6.   Gwinn, D.M., Shackelford, D.B., Egan, D.F., Mihaylova, M.M., Mery, A., Vasquez, D.S., Turk, B.E. and Shaw, R.J. (2008). AMPK phosphorylation of raptor mediates a metabolic checkpoint. Mol Cell *30*, 214-226.

7.   Shaw, R.J., Bardeesy, N., Manning, B.D., Lopez, L., Kosmatka, M., DePinho, R.A. and Cantley, L.C. (2004). The LKB1 tumor suppressor negatively regulates mTOR signaling. Cancer Cell *6*, 91-99.

8.   Wullschleger, S., Loewith, R. and Hall, M.N. (2006). TOR signaling in growth and metabolism. Cell *124*, 471-484.

9.   Bilanges, B., Argonza-Barrett, R., Kolesnichenko, M., Skinner, C., Nair, M., Chen, M. and Stokoe, D. (2007). Tuberous sclerosis complex proteins 1 and 2 control serum-dependent translation in a TOP-dependent and -independent manner. Mol Cell Biol *27*, 5746-5764.

10.   Mayer, C. and Grummt, I. (2006). Ribosome biogenesis and cell growth: mTOR coordinates transcription by all three classes of nuclear RNA polymerases. Oncogene *25*, 6384-6391.

11. Ma, X.M. and Blenis, J. (2009). Molecular mechanisms of mTOR-mediated translational control. Nat Rev Mol Cell Biol *10*, 307-318.

12. Shanware, N.P., Mullen, A.R., DeBerardinis, R.J., and Abraham, R.T. (2011). Glutamine: pleiotropic roles in tumor growth and stress resistance. J Mol Med *89*, 229-36.

13. Neufeld, T.P. (2010). TOR-dependent control of autophagy: biting the hand that feeds. Current Opinion in Cell Biology *22*, 157-168.

14. Mathew, R., Karantza-Wadsworth, V. and White, E. (2007). Role of autophagy in cancer. Nature Reviews 7, 961-967.

15. Vander Heiden, M.G., Cantley, L.C. and Thompson, C.B. (2009). Understanding the Warburg effect: the metabolic requirements of cell proliferation. Science *324*, 1029-1033.

16. Altenberg, B. and Greulich, K.O. (2004). Genes of glycolysis are ubiquitously overexpressed in 24 cancer classes. Genomics *84*, 1014-1020.

17. Semenza, G.L., Roth, P.H., Fang, H.M. and Wang, G.L. (1994). Transcriptional regulation of genes encoding glycolytic enzymes by hypoxia-inducible factor 1. J Biol Chem *269*, 23757-23763.

18. Zhong, H., Chiles,K., Feldser,D., Laughner, E., Hanrahan, C., Georgescu, M.M., Simons, J.W. and Semenza, G.L. (2000). Modulation of hypoxia-inducible factor 1alpha expression by the epidermal growth factor/phosphatidylinositol 3-kinase/PTEN/AKT/FRAP pathway in human prostate cancer cells: implications for tumor angiogenesis and therapeutics. Cancer Res *60*, 1541-1545.

19. Laughner, E., Taghavi, P., Chiles, K., Mahon, P.C. and Semenza, G.L. (2001). HER2 (neu) signaling increases the rate of hypoxia-inducible factor 1alpha (HIF-1alpha) synthesis: novel mechanism for HIF-1-mediated vascular endothelial growth factor expression. Mol Cell Biol *21*, 3995-4004.

20. Hudson, C.C., Liu, M., Chiang, G.G., Otterness, D.M., Loomis, D.C., Kaper, F., Giaccia, A.J. and Abraham, R.T. (2002). Regulation of hypoxia-inducible factor 1alpha expression and function by the mammalian target of rapamycin. Mol Cell Biol *22*, 7004-7014.

21. Hu, C.J., Wang, L.Y., Chodosh, L.A., Keith, B. and Simon, M.C. (2003). Differential roles of hypoxia-inducible factor 1alpha (HIF-1alpha) and HIF-2alpha in hypoxic gene regulation. Mol Cell Biol *23*, 9361-9374.

22. Majumder, P.K., Febbo, P.G., Bikoff, R., Berger, R., Xue, Q., McMahon, L.M., Manola, J., Brugarolas, J., McDonnell, T.J., Golub, T.R., Loda, M., Lane, H.A. and Sellers, W.R. (2004). mTOR inhibition reverses Akt-dependent prostate intraepithelial neoplasia through regulation of apoptotic and HIF-1-dependent pathways. Nat Med *10*, 594-601.

23.   Duvel, K., Yecies, J.L., Menon, S., Raman, P., Lipovsky, A.I., Souza, A.L., Triantafellow, E., Ma, Q., Gorski, R., Cleaver, S., Vander Heiden, M.G., MacKeigan, J.P., Finan, P.M., Clish, C.B., Murphy, L.O. and Manning, B.D. (2010). Activation of a metabolic gene regulatory network downstream of mTOR complex 1. Mol Cell *39*, 171-183.

24.   West, M.J., Stoneley, M. and Willis, A.E. (1998). Translational induction of the c-myc oncogene via activation of the FRAP/TOR signalling pathway. Oncogene *17*, 769-780.

25.   Gordan, J.D., Thompson, C.B. and Simon, M.C. (2007). HIF and c-Myc: sibling rivals for control of cancer cell metabolism and proliferation. Cancer Cell *12*, 108-113.

26.   Schieke, S.M., Phillips, D., McCoy, J.P., Jr., Aponte, A.M., Shen, R.F., Balaban, R.S. and Finkel, T. (2006). The mammalian target of rapamycin (mTOR) pathway regulates mitochondrial oxygen consumption and oxidative capacity. J Biol Chem *281*, 27643-27652.

27.   Cunningham, J.T., Rodgers, J.T., Arlow, D.H., Vazquez, F., Mootha, V.K. and Puigserver, P. (2007) mTOR controls mitochondrial oxidative function through a YY1-PGC-1alpha transcriptional complex. Nature. **450**, 736-740.

28.   Ramanathan, A. and Schreiber, S.L. (2009). Direct control of mitochondrial function by mTOR. Proc Natl Acad Sci U S A *106*, 22229-22232.

29.   Bentzinger, C.F., Romanino, K., Cloetta, D., Lin, S., Mascarenhas, J. B., Oliveri, F., Xia, J., Casanova, E., Costa, C.F., Brink, M., Zorzato, F., Hall, M.N. and Ruegg, M.A. (2008). Skeletal muscle-specific ablation of raptor, but not of rictor, causes metabolic changes and results in muscle dystrophy. Cell Metab *8*, 411-424.

30.   Menendez, J. A. and Lupu, R. (2007). Fatty acid synthase and the lipogenic phenotype in cancer pathogenesis. Nature Reviews *7*, 763-777.

31.   Raghow, R., Yellaturu, C., Deng, X., Park, E.A. and Elam, M.B. (2008). SREBPs: the crossroads of physiological and pathological lipid homeostasis. Trends in endocrinology and metabolism: TEM *19*, 65-73.

32.   Porstmann, T., Griffiths, B., Chung, Y.L., Delpuech, O., Griffiths, J.R., Downward, J. and Schulze, A. (2005). PKB/Akt induces transcription of enzymes involved in cholesterol and fatty acid biosynthesis via activation of SREBP. Oncogene *24*, 6465-6481.

33.   Porstmann, T., Santos, C.R., Griffiths, B., Cully, M., Wu, M., Leevers, S., Griffiths, J.R., Chung, Y.L. and Schulze, A. (2008). SREBP activity is regulated by mTORC1 and contributes to Akt-dependent cell growth. Cell Metab *8*, 224-236.

34.   Van de Sande, T., De Schrijver, E., Heyns, W., Verhoeven, G. and Swinnen, J.

V. (2002). Role of the phosphatidylinositol 3'-kinase/PTEN/Akt kinase pathway in the overexpression of fatty acid synthase in LNCaP prostate cancer cells. Cancer Res *62*, 642-646.

35. Van de Sande, T., Roskams, T., Lerut, E., Joniau, S., Van Poppel, H., Verhoeven, G. and Swinnen, J. V. (2005). High-level expression of fatty acid synthase in human prostate cancer tissues is linked to activation and nuclear localization of Akt/PKB. The Journal of Pathology *206*, 214-219.

36. Guo, D., Prins, R.M., Dang, J., Kuga, D., Iwanami, A., Soto, H., Lin, K.Y., Huang, T.T., Akhavan, D., Hock, M. B., Zhu, S., Kofman, A.A., Bensinger, S.J., Yong, W.H., Vinters, H.V., Horvath, S., Watson, A.D., Kuhn, J.G., Robins, H.I., Mehta, M.P., Wen, P.Y., DeAngelis, L.M., Prados, M. D., Mellinghoff, I.K., Cloughesy, T. F. and Mischel, P. S. (2009). EGFR signaling through an Akt-SREBP-1-dependent, rapamycin-resistant pathway sensitizes glioblastomas to antilipogenic therapy. Science Signaling *2*, ra82.

37. Zampella, E.J., Bradley, E.L., Jr. and Pretlow, T.G., 2nd. (1982). Glucose-6-phosphate dehydrogenase: a possible clinical indicator for prostatic carcinoma. Cancer *49*, 384-387.

38. Bokun, R., Bakotin, J. and Milasinovic, D. (1987). Semiquantitative cytochemical estimation of glucose-6-phosphate dehydrogenase activity in benign diseases and carcinoma of the breast. Acta Cytologica *31*, 249-252.

39. Dessi, S., Batetta, B., Cherchi, R., Onnis, R., Pisano, M. and Pani, P. (1988). Hexose monophosphate shunt enzymes in lung tumors from normal and glucose-6-phosphate-dehydrogenase-deficient subjects. Oncology *45*, 287-291.

40. Langbein, S., Zerilli, M., Zur Hausen, A., Staiger, W., Rensch-Boschert, K., Lukan, N., Popa, J., Ternullo, M. P., Steidler, A., Weiss, C., Grobholz, R., Willeke, F., Alken, P., Stassi, G., Schubert, P. and Coy, J.F. (2006). Expression of transketolase TKTL1 predicts colon and urothelial cancer patient survival: Warburg effect reinterpreted. British Journal of Cancer *94*, 578-585.

41. Krockenberger, M., Honig, A., Rieger, L., Coy, J. F., Sutterlin, M., Kapp, M., Horn, E., Dietl, J. and Kammerer, U. (2007). Transketolase-like 1 expression correlates with subtypes of ovarian cancer and the presence of distant metastases. Int J Gynecol Cancer *17*, 101-106.

42. Langbein, S., Frederiks, W.M., zur Hausen, A., Popa, J., Lehmann, J., Weiss, C., Alken, P. and Coy, J.F. (2008). Metastasis is promoted by a bioenergetic switch: new targets for progressive renal cell cancer. International Journal of Cancer *122*, 2422-2428.

43. Amemiya-Kudo, M., Shimano, H., Hasty, A.H., Yahagi, N., Yoshikawa, T., Matsuzaka, T., Okazaki, H., Tamura, Y., Iizuka, Y., Ohashi, K., Osuga, J., Harada, K., Gotoda, T., Sato, R., Kimura, S., Ishibashi, S. and Yamada, N. (2002). Transcriptional activities of nuclear SREBP-1a, -1c, and -2 to different target promoters of lipogenic and cholesterogenic genes. Journal of Lipid Research *43*, 1220-1235.

44.   Liang, G., Yang, J., Horton, J.D., Hammer, R.E., Goldstein, J.L. and Brown, M.S. (2002). Diminished hepatic response to fasting/refeeding and liver X receptor agonists in mice with selective deficiency of sterol regulatory element-binding protein-1c. J Biol Chem *277*, 9520-9528.

45.   Shimomura, I., Shimano, H., Korn, B.S., Bashmakov, Y. and Horton, J.D. (1998). Nuclear sterol regulatory element-binding proteins activate genes responsible for the entire program of unsaturated fatty acid biosynthesis in transgenic mouse liver. J Biol Chem *273*, 35299-35306.

46.   Schafer, Z.T., Grassian, A.R., Song, L., Jiang, Z., Gerhart-Hines, Z., Irie, H.Y., Gao, S., Puigserver, P. and Brugge, J.S. (2009). Antioxidant and oncogene rescue of metabolic defects caused by loss of matrix attachment. Nature *461*, 109-113.

47.   Guertin, D. A. and Sabatini, D. M. (2009). The pharmacology of mTOR inhibition. Science Signaling *2*, pe24.

48.   Choo, A.Y., Kim, S.G., Vander Heiden, M.G., Mahoney, S.J., Vu, H., Yoon, S.O., Cantley, L.C. and Blenis, J. (2010). Glucose addiction of TSC null cells is caused by failed mTORC1-dependent balancing of metabolic demand with supply. Mol Cell *38*, 487-499.

49.   Ozcan, U., Ozcan, L., Yilmaz, E., Duvel, K., Sahin, M., Manning, B.D. and Hotamisligil, G.S. (2008) Loss of the tuberous sclerosis complex tumor suppressors triggers the unfolded protein response to regulate insulin signaling and apoptosis. Mol Cell *29*, 541-551.

50.   Korsheninnikova, E., can der Zon, G.C., Voshol, P.J., Janssen, G.M., Havekes, L.M., Grefborst, A., Kuipers, F., Reijngoud, D.J., Romijn, J.A., Ouwens, D.M., and Maassen, J.A. (2006). Sustained activation of the mammalian target of rapamycin nutrient sensing pathway is associated with hepatic insulin resistance, but not with steatosis, in mice. Diabetiologica 49, 3049-57.

51.   Dann, S.G., Selvaraj, A., and Thomas, G. (2007). mTOR Complex1-S6K1 signaling: at the crossroads of obesity, diabetes and cancer. Trends in Mol Med *13*, 252-259.

52.   Um, S.H., Frigerio, F., Watanabe, M., Picard, F., Joaquin, M., Sticker, M., Fumagalli, S., Allegrini, P.R., Kozma, S.C., Auwerx, J.*, et al.* (2004). Absence of S6K1 protects against age and diet-induced obesity while enhancing insulin sensitivity. Nature *431*, 200-205.

53.   LeBacquer, O., Petroulakis E., Pglialunga, S., Poulin, F., Richard, D., Cianflone, K., and Sonenberg, N. (2007) Elevated sensitivity to diet-induced obesity and insulin reistance in mice lacking 4E-BP1 and 4E-BP2. J Clin Invest *117*, 387-396.

53.   Howell, J.J., and Manning, B.D. (2011). mTOR couples cellular nutrient sensing to organismal metabolic homeostasis. Trends Endocrinol Metab *22*, 94-102.

CHAPTER 2

mTOR Complex 1 Controls Cellular Metabolism

Adapted from:

Duvel, K.[1,7], Yecies, J.L. [1,7], Menon, S.[1,8], Raman, P. [2,8], Lipovsky, A.I.[1,5], Souza, A.L. [3], Triantafellow, E.[2], Ma, Q.[2], Gorski, R.[2], Cleaver, S.[2], Vander Heiden, M.G.[4], MacKeigan, J.P.[2,6], Finan, P.M.[2], Clish, C.B.[3], Murphy, L.O.[2], and Manning, B.D[1]. (2010). Activation of a metabolic gene regulatory network downstream of mTOR complex 1. *Molecular Cell* 39, 171–183.

[1]Department of Genetics and Complex Diseases, Harvard School of Public Health, Boston, MA 02115; [2]Developmental and Molecular Pathways, Novartis Institutes for BioMedical Research, Cambridge, MA 02139; [3]Metabolite Profiling Initiative, Broad Institute of MIT and Harvard, Cambridge, MA 02142;

[4]The David H. Koch Institute for Integrative Cancer Research at MIT, Cambridge, MA 02142;

[5]Current Address: Department of Genetics, Yale University School of Medicine, New Haven, CT 06520;

[6]Current Address: Laboratory of Systems Biology, Van Andel Research Institute;

[7]These authors contributed equally to this work

[8]These authors contributed equally to this work

JLY performed the experiments in Figures 2-1B; 2-3D-F; 2-4E, 2-5C and D; 2-7A, B, and F; 2-9A and G; 2-10E; 2-11; 2-12. Author contributions are noted in figure legends.

SUMMARY

Aberrant activation of the mammalian target of rapamycin complex 1 (mTORC1) is a common molecular event in a variety of pathological settings, including genetic tumor syndromes, cancer, and obesity. However, the cell intrinsic consequences of mTORC1 activation remain poorly defined. Through a combination of unbiased genomic, metabolomic, and bioinformatic approaches, we demonstrate that mTORC1 activation is sufficient to stimulate specific metabolic pathways, including glycolysis, the oxidative arm of the pentose phosphate pathway, and *de novo* lipid biosynthesis. This is achieved through the activation of a transcriptional program affecting metabolic gene targets of hypoxia-inducible factor (HIF1α) and sterol regulatory element-binding protein (SREBP1 and SREBP2). We find that SREBP1 and 2 promote proliferation downstream of mTORC1, and the activation of these transcription factors is mediated by S6K1. Therefore, in addition to promoting protein synthesis, mTORC1 activates specific bioenergetic and anabolic cellular processes that are likely to contribute to human physiology and disease.

BACKGROUND

The mammalian target of rapamycin (mTOR) is an evolutionarily conserved Ser/Thr kinase that has been implicated in a diverse array of physiological processes and pathological states. Aberrantly elevated mTOR activity is a common molecular defect detected in the majority of human cancers [1], under conditions of obesity [2], and in genetic syndromes with a high incidence of cognitive deficits and autism spectrum disorders [3]. While this increased activation of mTOR is believed to contribute to the development and progression of these diseases, the downstream consequences of mTOR activation at the molecular, cellular, and organismal levels are poorly understood.

The mTOR kinase exists within two physically and functionally distinct protein complexes, mTORC1 and mTORC2, which differ in their regulation, downstream targets, and sensitivity to the allosteric mTOR inhibitor rapamycin [4]. mTORC1 consists of the core essential components mTOR, Raptor, and mLST8 and is acutely sensitive to rapamycin. Pharmacological and genetic studies have demonstrated that mTORC1 activation increases cell growth (i.e., an increase in cell mass) in diverse organisms from yeast to human [5]. However, mTORC1 inhibition using rapamycin causes most mammalian cells to arrest in the G1 phase of the cell cycle, thereby demonstrating that mTORC1 activity also promotes cell proliferation. While the molecular mechanisms by which mTORC1 promotes anabolic cell growth and proliferation are not fully understood, two classes of direct downstream targets of mTORC1 have been well characterized. Specifically as part of mTORC1, mTOR directly phosphorylates the ribosomal protein S6 kinases (S6K1 and S6K2) and the eukaryotic initiation factor 4E (eIF4E)-binding proteins (4E-BP1 and 4E-BP2), both of which control specific steps in the initiation of cap-dependent translation [6]. Phosphorylation of the S6Ks downstream of mTORC1 leads to their activation, whereas phosphorylation of the 4E-BPs lead to their inhibition and release from eIF4E at the 5' cap of mRNAs. mTORC2 is comprised of the core essential components mTOR, Rictor, mSIN1, and mLST8. Within this complex, mTOR is not directly inhibited by rapamycin, but mTORC2 assembly is blocked by prolonged exposure to this compound [7]. The known downstream targets of mTORC2 are all AGC family kinases, including Akt, SGK1, and PKCα [4]. The focus of this current study is on downstream events specific to mTORC1 signaling.

The aberrant increase in mTORC1 signaling detected in a variety of human disease states is due to genetic or environmental factors leading to frequent misregulation of upstream signaling pathways that, in large part, converge on a small G protein switch essential for the proper control of mTORC1 activation. In its GTP-bound

state, the Ras-related GTPase Rheb is a potent and essential activator of mTORC1

[8,9]. Rheb is tightly regulated by a GTPase-activating protein (GAP) called TSC2 (or

tuberin). Along with its binding partner TSC1 (or hamartin), TSC2 is encoded by a tumor

suppressor gene mutated in the genetic tumor syndrome tuberous sclerosis complex

(TSC; [10]). TSC2 has specific GAP activity toward Rheb, which is greatly enhanced by

binding to TSC1, thereby inactivating Rheb and, in turn, mTORC1. As a key regulator of

anabolic growth and proliferation, mTORC1 is exquisitely sensitive to cellular growth

conditions, such as the presence or absence of growth factors, nutrients, energy, and

stress. Many of the signaling pathways that relay the status of these conditions to

mTORC1 do so, at least in part, through specific phosphorylation events on the TSC1-

TSC2 complex that affect the ability of this complex to act as a GAP for Rheb [9].

Reciprocal to its inhibitory effects on mTORC1, the TSC1-TSC2 complex promotes the

activation of mTORC2 through an as yet unknown mechanism that can be separated

from its effects on Rheb and mTORC1 [11, 12].

Importantly, genetic loss of either TSC1 or TSC2 leads to constitutive activation

of mTORC1 that is largely insensitive to perturbations in cellular growth conditions [9].

This is most obvious under conditions of growth factor withdrawal, where mTORC1

signaling is attenuated in normal cells but remains fully stimulated in cells lacking a

functional TSC1-TSC2 complex or overexpressing Rheb (e.g., [13-16]. Consistent with

its role in the activation of mTORC2, TSC-deficient cells exhibit defects in mTORC2

activity, even in the presence of growth factors [11, 12]. In this study, we take advantage

of these major differences in mTOR signaling between *Tsc1* and *Tsc2* null cells and their

wild-type counterparts to isolate mTORC1 activity from mTORC2 and other growth

factor-stimulated signaling pathways. By comparing TSC-deficient cells to wild-type cells

in the absence of growth factors, we have an mTORC1 gain-of-function model that,

when combined with rapamycin, can be used to reveal cellular processes that mTORC1

activation is sufficient to induce. Through a combination of genomic, metabolomic, and

bioinformatic analyses, we find that mTORC1 activation on its own can stimulate a gene

network that alters specific metabolic pathways.

RESULTS

A genomic approach to identify transcriptional targets downstream of mTORC1

Cells lacking TSC1 or TSC2 exhibit growth-factor independent activation of

mTORC1 (Figure 2-1A). In order to identify mTORC1-dependent transcriptional

changes, we compared wild-type MEFs to $Tsc1^{-/-}$ and $Tsc2^{-/-}$ MEFs following serum

starvation, where mTORC1 signaling is off in wild-type cells and fully active in TSC-

deficient cells (P-S6K1; Figure 2-1B). Importantly, under these conditions, mTORC2

targets are off in all of these cell lines, as Akt-S473 phosphorylation is lost and SGK1

protein levels are nearly undetectable. All cell lines were serum-starved for 24 h, and the

$Tsc1^{-/-}$ and $Tsc2^{-/-}$ cells were treated with a time course of rapamycin prior to the isolation

of mRNA for microarray analysis. The use of both $Tsc1$ and $Tsc2$ null cells provides an

added degree of stringency and controls for non-specific differences in these

independently derived lines [14,16]. In order to be classified as an mTORC1-regulated

transcript in this study, a gene probe must meet four independent criteria at a P-

value<0.01: 1) different in $Tsc1^{-/-}$ versus wild-type; 2) different in $Tsc2^{-/-}$ versus wild-type;

3) reverted toward wild-type levels by rapamycin in $Tsc1^{-/-}$; 4) reverted toward wild-type

levels by rapamycin in $Tsc2^{-/-}$ (Figure 2-1C). Strikingly, only 239 of the 39,000 gene

probes analyzed, representing 205 genes, met these conditions (available online).

These are shown in the scatter plot in Figure 2-1D (blue dots) in relation to all others

(gray dots). These 205 genes include those that are decreased in TSC1- and TSC2-

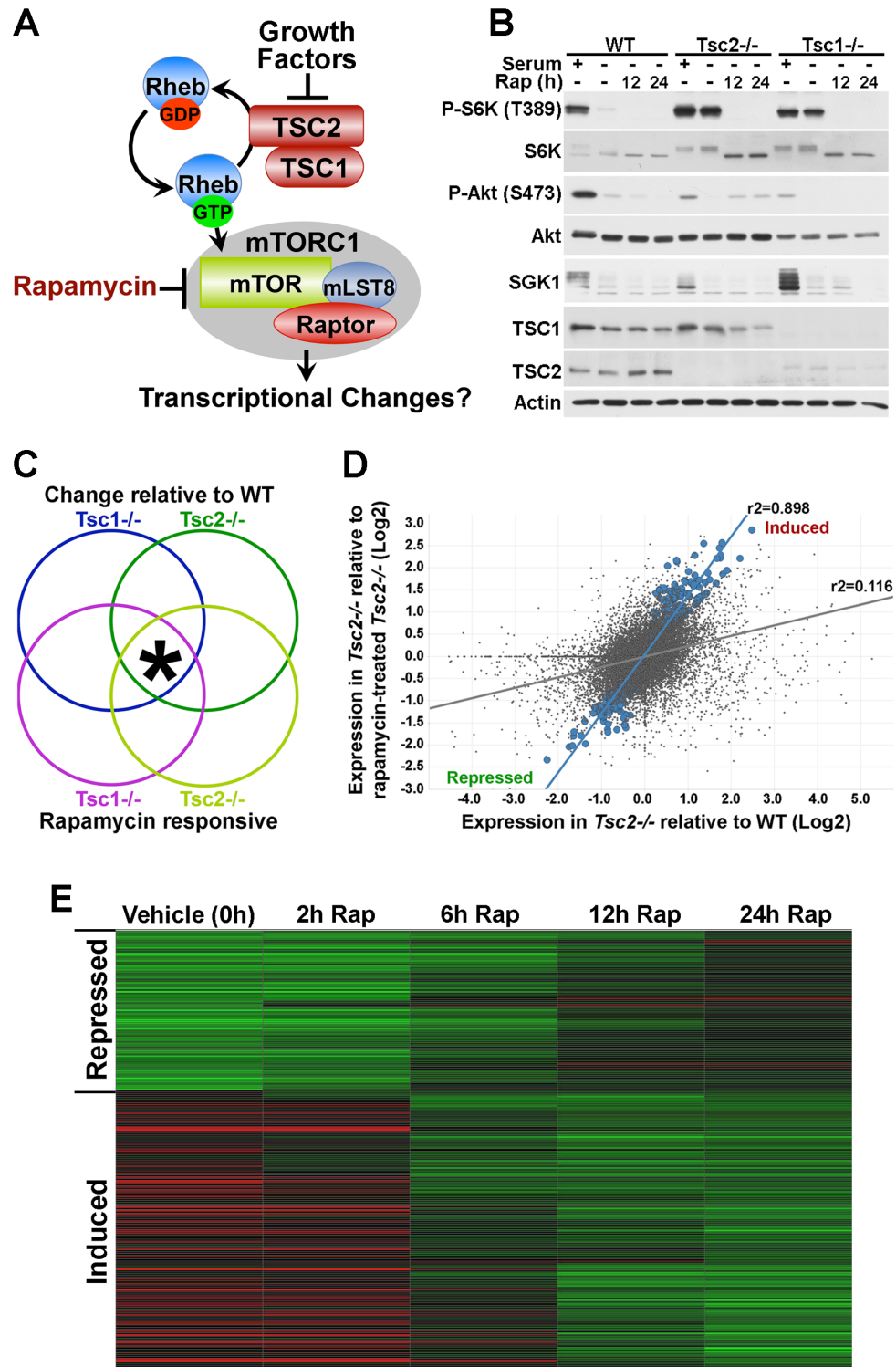deficient cells and stimulated by rapamycin (75 mTORC1-repressed genes) and those

Figure 2-1. **A genomics approach to identify mTORC1-regulated transcripts.**

A) Model of mTORC1 regulation downstream of growth factors.

Figure 2-1 continued

B) Growth factor-independent mTOR signaling in $Tsc1^{-/-}$ and $Tsc2^{-/-}$ MEFs. MEF lines were serum starved for 24 h in the presence of vehicle (-) or 20-nM rapamycin (12 or 24 h) and, where indicated, were stimulated with 10% serum for the final 1 h. **(JLY)**

C) Hypothetical Venn diagram of the four major changes in gene expression detected in this study. mTORC1-regulated transcripts were classified as those that met all four of these criteria at a statistical cut of p<0.01 (*).

D) Scatter plot of the expression levels (log_2) of the 39,000 gene probes comparing vehicle-treated $Tsc2^{-/-}$ cells to vehicle-treated wild-type controls (x-axis) and vehicle-treated $Tsc2^{-/-}$ cells to rapamycin-treated (24 h) $Tsc2^{-/-}$ cells (y-axis). The larger blue dots depict the pattern of the 239 gene probes meeting the criteria described in (B). The gray dots depict the expression pattern of the whole dataset. **(PR)**

E) Heat map of the 239 probes found to be regulated by mTORC1 signaling in this study, showing their expression levels and response to a rapamycin time course in $Tsc2^{-/-}$ cells. Expression levels shown are representative of the log_2 average obtained from independent replicates per time point. The brightness of green and red represents the degree to which expression is respectively lower or higher in the $Tsc2^{-/-}$ cells relative to vehicle treated wild-type cells. **(AIL, PR)**

that are increased in these cells and inhibited by rapamycin (130 mTORC1-induced

genes). The rapamycin time course revealed that the majority of these mTORC1-

regulated genes were responsive to rapamycin at 6 to 12 h of treatment in both $Tsc2^{-/-}$

(Figure 2-1E) and $Tsc1^{-/-}$ (Figure 2-2) cells.

mTORC1 induces genes encoding the enzymes of specific metabolic pathways

To identify functional groups that are enriched amongst the mTORC1-regulated

genes, a gene set enrichment analysis (GSEA) was performed on a larger set of genes

meeting the above criteria for being induced or repressed by mTORC1 signaling at a P-

value<0.05 (Table 2-1). Interestingly, within the top 20 mTORC1-induced gene sets are

specific metabolic pathways, including the pentose phosphate pathway ($P<7\text{x}10^{-8}$), fatty

acid biosynthesis ($P<5\text{x}10^{-6}$), glycolysis ($P<0.0002$), and cholesterol biosynthesis

($P<0.0031$). Indeed, a survey of mTORC1-induced genes found many encoding the

enzymes of glycolysis (Figure 2-3A), the pentose phosphate pathway (Figure 2-3B), and

sterol and fatty acid biosynthesis (Figure 2-3C) to be elevated in both $Tsc1^{-/-}$ and $Tsc2^{-/-}$

cells and rapamycin sensitive. The mTORC1-dependent induction of many of these

genes was verified by qRT-PCR (representative genes shown in Figures 2-3D-F). In

addition, the regulation of representative genes from these metabolic pathways was

further confirmed in three independent genetic settings of mTORC1 activation, including

$Tsc2^{-/-}$ MEFs reconstituted with empty vector or human $TSC2$ (Figure 2-4A), HeLa cells

with a stable shRNA-mediated knockdown of $TSC2$ (Figure 2-4B), and HEK-293 cells

over-expressing Rheb (Figure 2-4C). In all three systems, activation of mTORC1

signaling led to increased expression of genes of glycolysis, the pentose phosphate
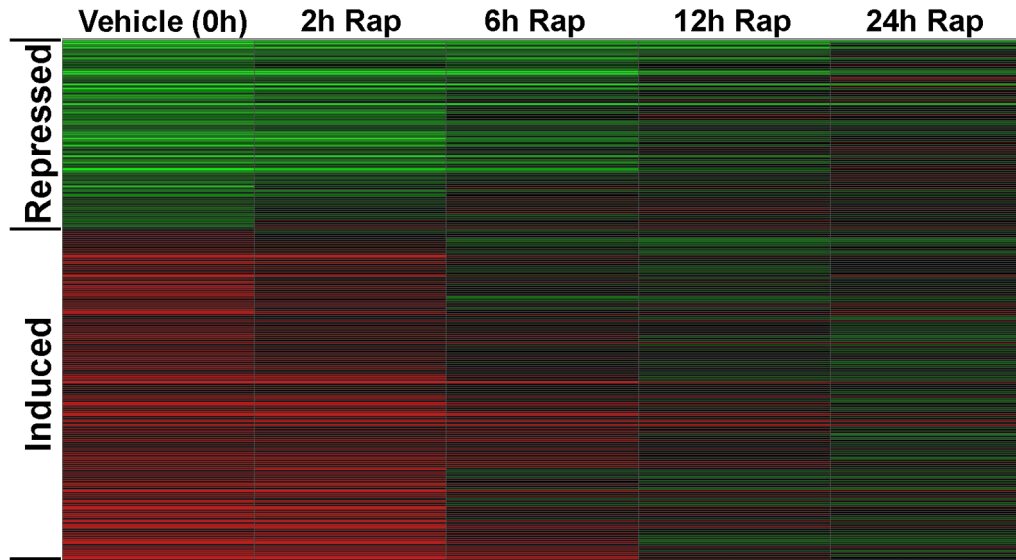
Figure 2-2. Expression pattern of mTORC1-regulated transcripts in *Tsc1* null cells.
Heat map of the stringent 239 probes, representing 209 genes, found to be regulated by mTORC1 signaling in this study, showing their expression levels and response to a rapamycin time course in *Tsc1*$^{-/-}$ cells. Expression levels shown are the $\log_2$ averages obtained from independent replicates per time point. The brightness of green and red represents the degree to which expression is respectively lower or higher in the *Tsc1*$_{-/-}$ cells relative to vehicle treated wild-type cells. The list of genes and normalized $\log_2$ expression levels are available online. **(AIL, PR)**

Table 2-1: Gene-set enrichment analysis of mTORC1-regulated genes[a]

Gene Set (MAP)	P-value
mTORC1 Induced:	
Neurodisease – Parkin disorder under Parkinson disease	2.36E-09
Pentose phosphate pathway	**6.64E-08**
Transcription – Ligand-dependent transcription of retinoid-target genes	1.92E-07
Immune response – Antigen presentation by MHC class I	6.15E-07
Unsaturated fatty acid biosynthesis	**4.89E-06**
Apoptosis and survival – Regulation by mitochondrial proteins	8.09E-05
Glycolysis and gluconeogenesis	**1.36E-04**
Galactose metabolism	2.00E-04
n-3/n-6 Polyunsaturated fatty acid biosynthesis	**2.40E-04**
Glycine, serine, cysteine, and threonine metabolism	3.98E-04
ATP/ITP metabolism	9.86E-04
Aminocyl-tRNA biosynthesis in cytoplasm	1.07E-03
Signal transduction – AKT signaling	1.10E-03
Apoptosis and survival – Endoplasmic reticulum stress response pathway	1.16E-03
Regulation of degradation of wt-CFTR	1.43E-03
Development – PACAP signaling in neural cells	2.69E-03
Cholesterol biosynthesis	**3.01E-03**
Signal transduction – PTEN pathway	6.42E-03
Cell Cycle – Role of Nek in cell cycle regulation	6.56E-03
Regulation of lipid metabolism – Insulin regulation of fatty acid metabolism	**6.84E-03**
mTORC1 Repressed:	
Apoptosis and survival - Anti-apoptotic TNFs/NF-kB/IAP pathway	3.11E-03
Apoptosis and survival - Lymphotoxin-beta receptor signaling	6.94E-03
Transcription - Role of heterochromatin protein1 family in transcriptional silencing	9.56E-03
Cardiac Hypertrophy - NF-AT signaling in Cardiac Hypertrophy	1.15E-02
Cell adhesion - Plasmin signaling	1.16E-02
Development - VEGF signaling and activation	1.51E-02
Cell cycle - Role of Nek in cell cycle regulation	1.56E-02
Cytoskeleton remodeling - Cytoskeleton remodeling	1.63E-02
Translation - Regulation activity of EIF4F	2.21E-02
Immune response - CD40 signaling	2.40E-02
Development - Role of HDAC and CaMK in control of skeletal myogenesis	2.46E-02
Translation - (L)-selenoaminoacids incorporation in proteins during translation	2.68E-02
Development - Cross-talk between VEGF and Angiopoietin 1 signaling pathways	2.75E-02
Immune response - MIF-mediated glucocorticoid regulation	2.81E-02
G-protein signaling - K-RAS regulation pathway	2.94E-02
Cytoskeleton remodeling - TGF, WNT and cytoskeletal remodeling	3.00E-02
Immune response - IL-10 signaling pathway	3.14E-02
Regulation of metabolism - Triiodothyronine and Thyroxine signaling	3.21E-02
Immune response - IL-6 signaling pathway	3.98E-02
Cooperation between Hedgehog, IGF-2 and HGF pathways in medulloblastoma	4.66E-02

[a]GSEA was performed using MetaCore on genes that were up or down regulated and responsive to rapamycin in both *Tsc1* and *Tsc2* null cells at a *P*-value<0.05. The top 20 non-redundant gene sets are shown for each.

(PR)
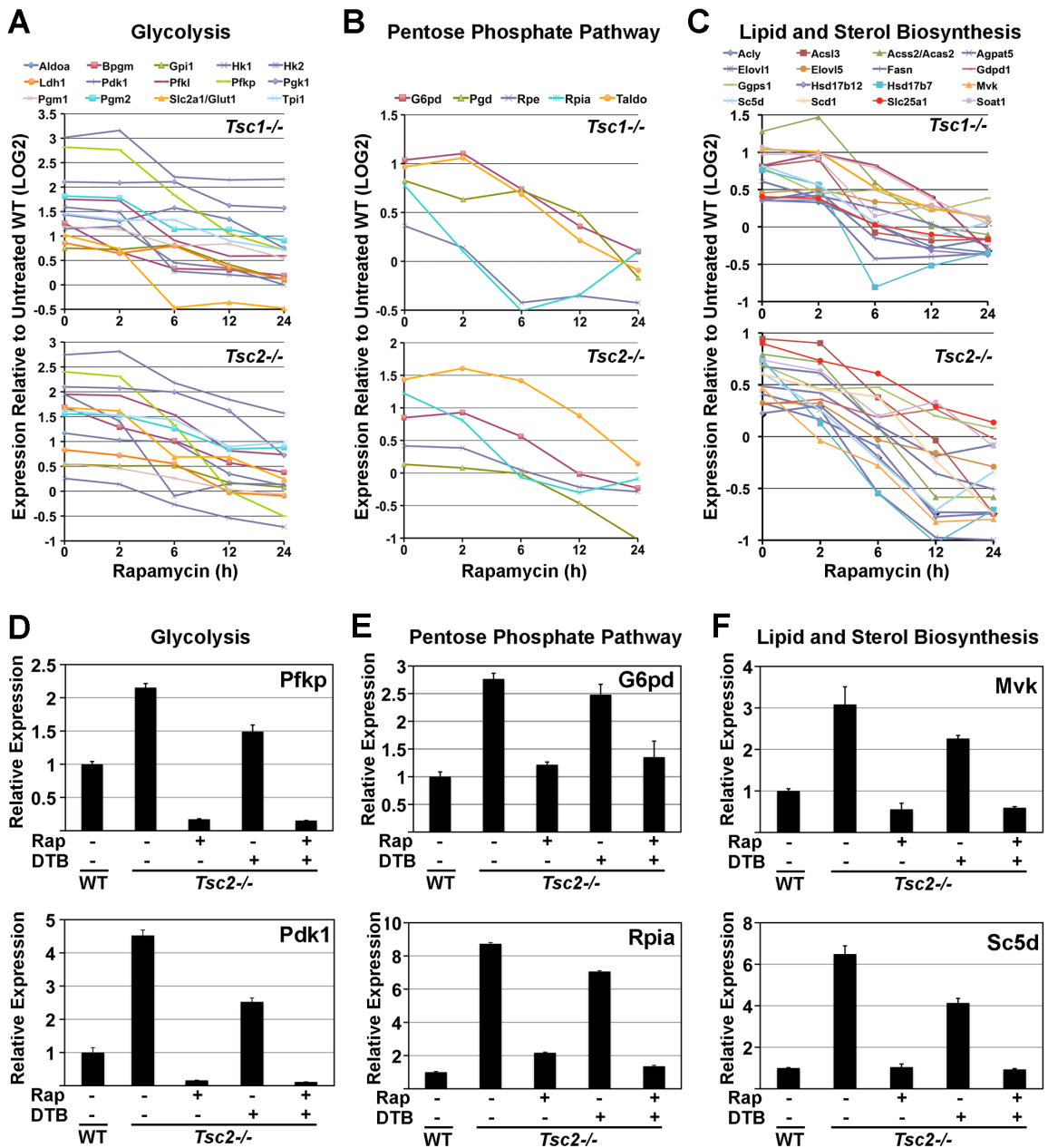
Figure 2-3. Transcriptional induction of metabolic genes downstream of mTORC1 activation.

A-C) mTORC1 activation leads to the induction of genes encoding the enzymes of glycolysis (A), the pentose phosphate pathway (B), and lipid and sterol biosynthesis (C) in $Tsc1^{-/-}$ (upper graphs) and $Tsc2^{-/-}$ (lower graphs) cells. The $\log_2$ expression levels shown are the average obtained from independent replicates per time point of rapamycin

Figure 2-3 continued

treatment normalized to the expression levels in vehicle-treated wild-type cells. **(KD)**

D-F) Confirmation of mTORC1-induced metabolic genes. The expression levels of

representative genes from (D) glycolysis, (E) the pentose phosphate pathway, and (F)

lipid and sterol biosynthesis was measured by qRT-PCR. MEFs were serum starved for

18 h in the presence of vehicle (-) or 20-nM rapamycin (+) and, where indicated, were

subjected to a proliferation arrest via double thymidine block (DTB). Expression levels

are presented as mean±SD relative to vehicle-treated $Tsc2^{+/+}$ cells and are

representative of at least three independent experiments. (See data in Figure 2-4) **(JLY)**

A Tsc2-/- MEFs reconstituted with wild-type TSC2 or empty vector:
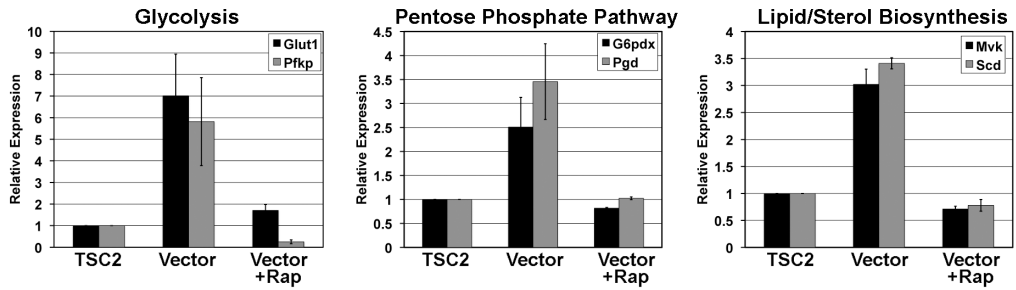
B HeLa cells with stable shRNA-mediated knockdown of TSC2:
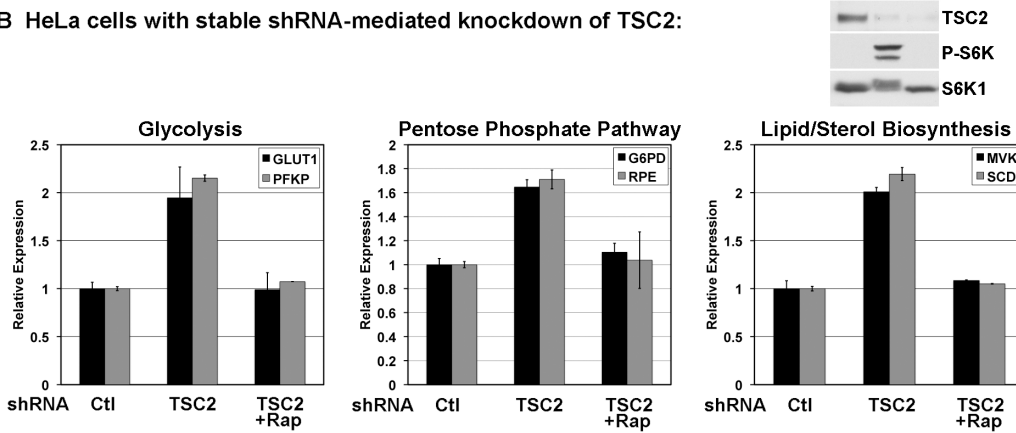
C Rheb overexpression in HEK-293 cells:

D

E

Figure 2-4. Confirmation that mTORC1 regulates metabolic gene expression.

Figure 2-4 continued

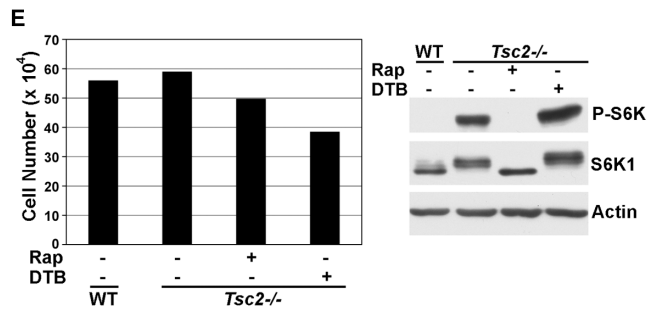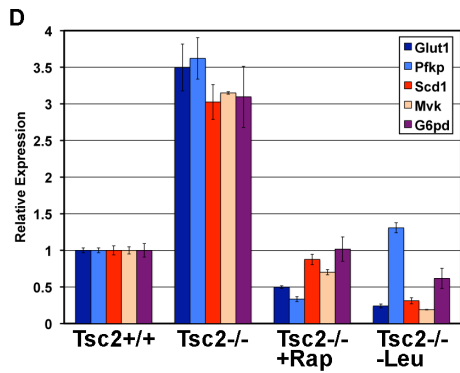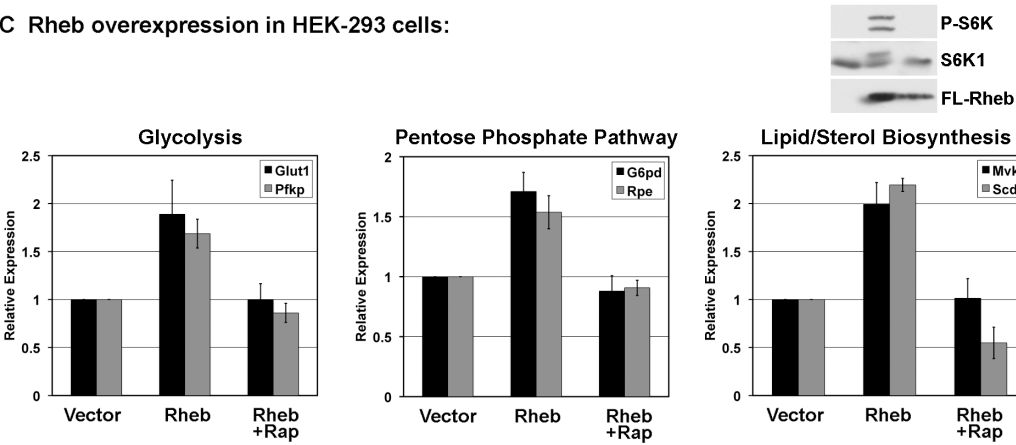A) Confirmation of mTORC1-induced metabolic genes in *Tsc2*-deficient cells

reconstituted with TSC2 or empty vector. *Tsc2*$^{-/-}$ MEFs stably reconstituted human

TSC2 or empty vector were serum starved for 16 h in the presence of vehicle or 20 nM

rapamycin (Rap). The expression levels of representative genes from the three

metabolic pathways, including glycolysis (*Glut1* and *Pfkp*, left), the pentose phosphate

pathway (*G6pd* and *Pgd*, middle), and lipid and sterol biosynthesis (*Scd1* and *Mvk*, right)

were measured by qRT-PCR. Expression levels are presented as mean±SD relative to

vehicle-treated TSC2-reconstituted cells over three independent experiments. **(KD)**

B) Confirmation of mTORC1-induced metabolic genes in human epithelial cells with

stable knockdown of TSC2. HeLa cells stably expressing shRNAs targeting TSC2 or

firefly luciferase (Ctl) treated as in (A). An immunoblot control is provided. The

expression levels of representative human genes from the three metabolic pathways,

including glycolysis (*GLUT1* and *PFKP*, left), the pentose phosphate pathway (*G6PD*

and *RPE*, middle), and lipid and sterol biosynthesis (*SCD1* and *MVK*, right) were

measured by qRT-PCR. Expression levels are presented as mean±SD relative to

untreated cells expressing control shRNAs and are representative of three independent

experiments. **(SM)**

C) Confirmation of mTORC1-induced metabolic genes in human epithelial cells

overexpressing Rheb. HEK-293 cells were transiently transfected with FLAG-Rheb or

empty vector and serum starved for 16 h in the presence or absence of rapamycin (20

nM). An immunoblot control is provided. Representative metabolic genes were

analyzed as in (B). Expression levels are presented as mean±SEM relative to untreated

vector-transfected cells over three independent experiments. **(KD)**

D) Like rapamycin, Leucine starvation blocks the enhanced expression of metabolic

genes in *Tsc2*$^{-/-}$ MEFs. Cells were serum-starved overnight in DMEM or DMEM lacking

Figure 2-4 continued

Leucine (-Leu) in the presence of vehicle or rapamycin (20 nM, Rap). Expression levels

are presented as mean±SD relative to $Tsc2^{+/+}$ cells and are representative of two

independent experiments. **(KD)**

E) Comparison of the effects of rapamycin and the double thymidine block (DTB) on the

proliferation of $Tsc2^{-/-}$ MEFs. $2x10^5$ cells were plated and upon attachment, thymidine

(2mM) or vehicle (PBS) was added to the normal growth medium for 20 h. Cells were

restored to their normal growth medium for 12 h prior to a second treatment with

thymidine or vehicle in serum-free medium in the presence or absence of rapamycin (20

nM) for 18 h. Viable cell counts per well are shown at the end of the experiment, when

cells were harvested for expression analysis. Lysates were prepared in parallel to

determine effects on mTORC1 signaling (P-S6K1-T389 in the accompanying blot). **(JLY)**

pathway, and lipid/sterol biosynthesis and rapamycin reversed this effect. Finally, consistent with these genes being downstream of mTORC1, withdrawal of the essential amino acid leucine from $Tsc2^{-/-}$ cells led to a repression of these metabolic genes similar to that seen with rapamycin (Figure 2-4D).

Due to sustained mTORC1 signaling, cells lacking the TSC1-TSC2 complex can proliferate in the absence of growth factors ([17]; see below). This raises the possibility that the differences in metabolic gene expression between wild-type and TSC-deficient cells are due to differences in proliferation. This was addressed by arresting the proliferation of $Tsc2^{-/-}$ cells through a standard double thymidine block (DTB). The DTB had a more pronounced effect on proliferation than rapamycin in these cells, but did not inhibit mTORC1 signaling (Figure 2-4E). While the DTB-mediated arrest of $Tsc2^{-/-}$ cells led to a modest decrease in the expression of representative metabolic genes, their expression remained significantly higher than in wild-type cells and fully sensitive to rapamycin (Figure 2-3D-F). Therefore, the mTORC1-induced expression of these metabolic genes is independent of cell proliferation.

mTORC1 activation is sufficient to induce specific metabolic processes

As depicted in Figure 2-3A, mTORC1 signaling activates the expression of genes encoding nearly every step of glycolysis and the pentose phosphate pathway, as well as critical enzymes in the *de novo* synthesis of sterols, isoprenoids, and fatty acids. To investigate whether these transcriptional changes are also reflected by changes in cellular metabolism, we measured effects on both specific metabolic processes and global metabolites. Consistent with the gene expression profile, $Tsc2^{-/-}$ cells exhibit a rapamycin-sensitive increase in glucose uptake (Figure 2-5B), lactate secretion (Figure 2-5C), and *de novo* lipid biosynthesis (Figure 2-5D). To obtain a more global and unbiased analysis of mTORC1-mediated changes in intracellular metabolites, a liquid
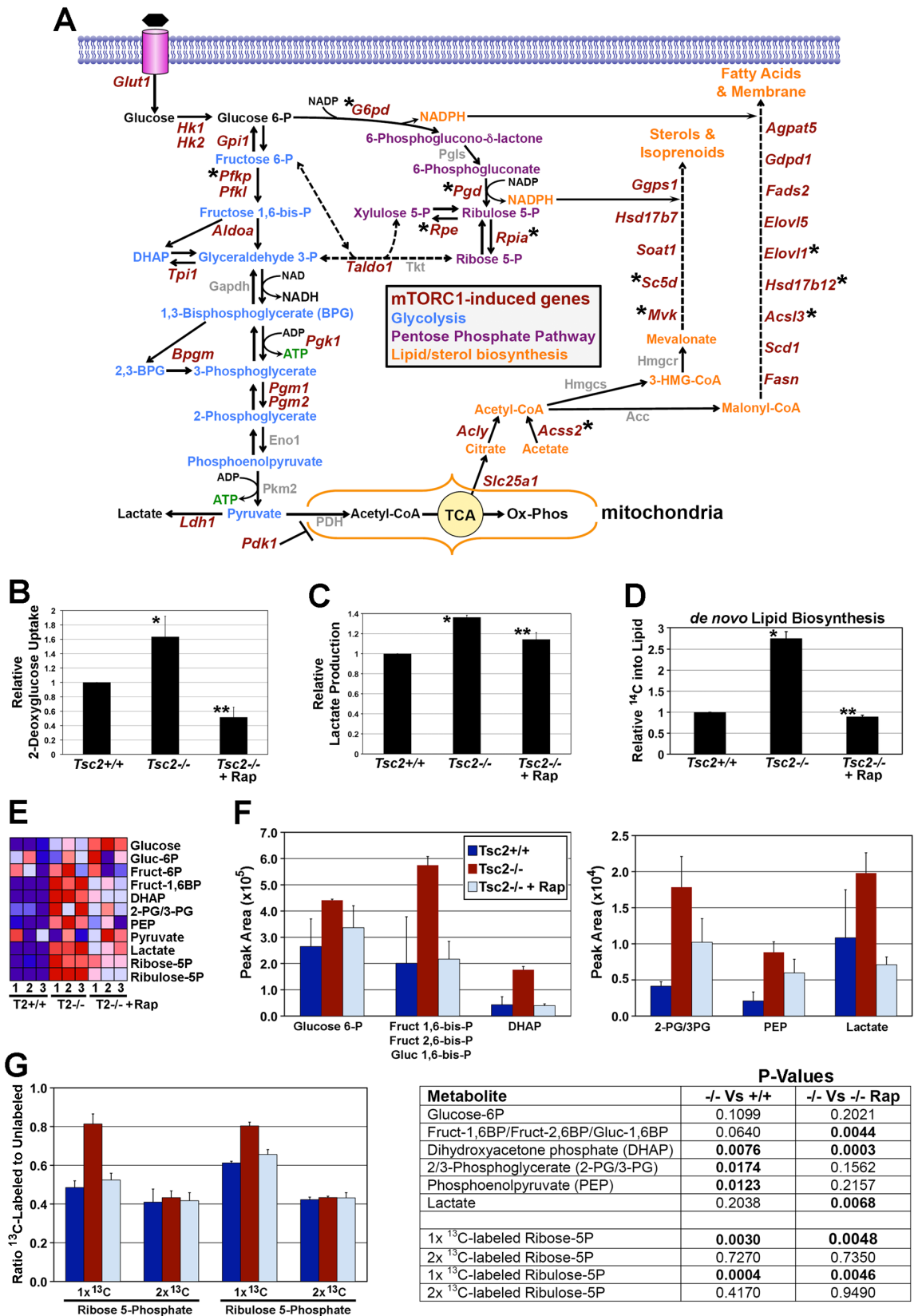
Figure 2-5. Alterations in cellular metabolism induced by mTORC1 activation.

Figure 2-5 continued

A) Placement of the mTORC1-induced metabolic genes within their metabolic pathways. Genes found to be regulated by mTORC1 are shown in red, with those in the most stringent set indicated (*).

B) mTORC1 signaling stimulates glucose uptake. MEFs were serum starved for 16 hours in the presence of vehicle or rapamycin (20 nM). Glucose uptake was measured as the incorporation of 2-deoxy-D-[^{3}H]-glucose over 4 minutes and normalized to cell number. Levels are presented as mean±SD relative to *Tsc2$^{+/+}$* cells from four independent experiments. *p<0.002 versus *Tsc2$^{+/+}$*; **p<0.009 versus *Tsc2$^{-/-}$*. **(KD)**

C) mTORC1 signaling increases lactate production. Cells were grown as in (B), and lactate secretion into the media was measured over the final hour. Lactate concentrations normalized to cell number are presented as mean±SD relative to *Tsc2$^{+/+}$* cells from three independent experiments. *p<0.00001 versus *Tsc2$^{+/+}$*; **p<0.006 versus *Tsc2$^{-/-}$*. **(JLY)**

D) mTORC1 signaling stimulates *de novo* lipid biosynthesis. MEFs were serum starved for 24 h in the presence of vehicle or rapamycin (20 nM) and were incubated with D-[6-^{14}C]-glucose for the final 4 h. ^{14}C incorporation into the lipid fraction was measured and is presented as mean±SD relative to *Tsc2$^{+/+}$* cells. These data are representative of three independent experiments. *p<0.006 versus *Tsc2$^{+/+}$*; **p<0.004 versus *Tsc2$^{-/-}$*. **(JLY)**

E) Metabolomic profiling demonstrates that mTORC1 activation increases metabolites of glycolysis and the pentose phosphate pathway. MEFs were grown as in (B) and metabolites were extracted and profiled by LC-MS. Relative levels of specific metabolites, normalized to cell number, from three independent samples for each cell line and treatment are shown in the heat map. Metabolites showing a pattern consistent with mTORC1 regulation are indicated (*). The complete metabolomic profile is provided as supplemental Figure 2-6. **(KD, ALS, CBC)**

Figure 2-5 continued

F) mTORC1 signaling increases flux through glycolysis. MEFs were grown as in (B) and incubated with [1,2-^{13}C]-glucose for 15 min prior to metabolite extraction and LC-MS analysis. Levels of dually ^{13}C-labeled glycolytic intermediates, normalized to cell number, are presented as mean±SD over three independent samples. **(KD, ALS, CBC)**

G) mTORC1 signaling increases flux through the oxidative branch of the pentose phosphate pathway. The ratio of singly (1x) and doubly (2x) ^{13}C-labeled to unlabeled (^{12}C) pentose phosphate pathway metabolites were measured by LC-MS in the samples from (F). P-values for pair-wise comparisons in (F) and (G) are listed in the accompanying table. **(KD, ALS, CBC)**

chromatography mass spectrometry (LC-MS)-based metabolomics approach was

employed. As with our genomic study, we compared littermate-derived wild-type and

$Tsc2^{-/-}$ MEFs under growth factor-free conditions, where mTORC1 signaling is off in wild-

type cells but fully active and rapamycin sensitive in the $Tsc2$ null cells. Only 21 of the

119 metabolites measured showed a pattern consistent with mTORC1-induced changes

(i.e., elevated in $Tsc2^{-/-}$ cells relative to $Tsc2^{+/+}$ and decreased by rapamycin; Figure 2-6).

Of these, only the intermediates of glycolysis and the pentose phosphate pathway

showed a pathway-specific pattern of increase by mTORC1 signaling (Figure 2-5E).

To determine whether the steady state increase in these intermediates reflects

an increase in flux through these pathways, we measured metabolite levels following a

15 min pulse of [1,2-^{13}C]-glucose. Indeed, we found increased ^{13}C-labeling of glycolytic

and pentose phosphate pathway intermediates in $Tsc2^{-/-}$ cells, which was blocked by

rapamycin treatment (Figure 2-5F and G). The use of doubly labeled [1,2-^{13}C]-glucose

allowed us to determine whether the increase in ribulose 5-phosphate and ribose 5-

phosphate was the result of increased flux through the oxidative (glucose 6-phosphate

dehydrogenase (G6PD)-mediated) or non-oxidative branches of the pentose phosphate

pathway. If ribulose 5-phosphate and ribose 5-phosphate are singly labeled, they are

produced through the oxidative arm, as phosphogluconate dehydrogenase (PGD)

catalyzes decarboxylation and loss of the 1 carbon as CO_2, whereas doubly labeled

intermediates could only come from the non-oxidative branch. Consistent with the

mTORC1-dependent increase in expression of G6PD and PGD, there was a rapamycin-

sensitive increase in singly labeled ribose and ribulose in the $Tsc2^{-/-}$ cells, while there

was no difference in levels of doubly labeled pentose phosphate pathway intermediates

(Figure 2-5G). These data demonstrate that the mTORC1-induced expression of genes

encoding the enzymes of glycolysis and the oxidative arm of the pentose phosphate

pathway is accompanied by increased flux through these pathways.
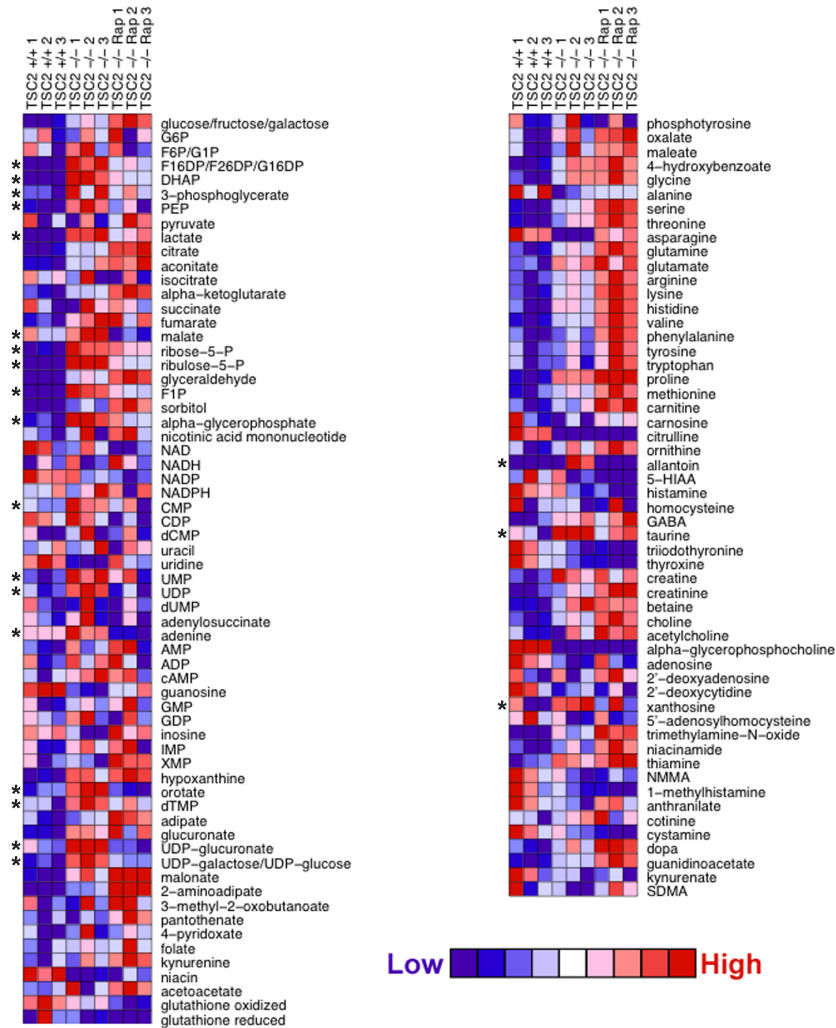
Figure 2-6. mTORC1 regulates specific intracellular metabolites.

Metabolomic profiling of wild-type and *Tsc2*-deficient MEFs to identify mTORC1-regulated metabolites. Littermate-derived *Tsc2*$^{+/+}$ and *Tsc2*$^{-/-}$ MEFs were serum starved for 16 h in the presence of vehicle or rapamycin (20 nM). Small metabolites were extracted and profiled by liquid chromatography mass spectrometry (LC-MS). Relative levels of specific metabolites, normalized to cell number, from three independent samples for each cell line and treatment are shown in the heat map, with metabolites grouped according to metabolic pathways. Metabolites showing a pattern consistent with regulation by mTORC1 signaling (i.e., increased in *Tsc2*$^{-/-}$ relative to *Tsc2*$^{+/+}$ and rapamycin sensitive) are indicated (*). **(KD, ALS, CBC)**

Identification of enriched transcription factor-binding elements in mTORC1-regulated genes

To identify candidate transcription factors downstream of mTORC1, we used a previously described unbiased bioinformatic approach (MotifADE; [18,19]) to detect transcription factor-binding motifs enriched in the promoters of mTORC1-regulated genes from the expression array study. This approach identifies over-represented *cis* regulatory elements present in the promoters of specific gene sets. An analysis of all genes sensitive to rapamycin at 24 h revealed that binding motifs for only four transcription factors are significantly enriched (q-value>0.01) in the data from both *Tsc1*^{-/-} and *Tsc2*^{-/-} cells (Table 2-2). Interestingly, two of these factors, sterol regulatory element-binding protein (SREBP) and c-Myc are well known to regulate specific aspects of cellular metabolism. C-Myc has been estimated to regulate up to 15% of all genes, including the genes of glycolysis [20]. However, the c-Myc protein is very unstable and following 24 h of serum deprivation, as performed in our gene expression analysis, it is not detectable in the TSC-deficient cells (e.g., Figure 2-7A). Importantly, the transcription factor hypoxia-inducible factor (HIF1) stimulates the same genes of glycolysis and, like c-Myc, is a basic helix loop helix (bHLH) transcription factor that recognizes an overlapping promoter-binding element (Table 2-2; [21, 22]).

HIF1α is responsible for the glycolytic response downstream of mTORC1

Given that known targets of HIF1 involved in glycolysis are elevated in an mTORC1-dependent manner in the TSC-deficient cells, we analyzed 26 previously characterized HIF1 targets in our expression array data. These genes all demonstrated a pattern of induction by mTORC1, as they were elevated in both *Tsc1* and *Tsc2* null cells and rapamycin sensitive (Figure 2-8A). These genes included those encoding the enzymes of glycolysis as well as non-metabolic targets, several of which were in our

Table 2-2. Enrichment of transcription factor binding elements in the promoters of mTORC1-induced genes[a].

Transcription Factor	Binding Motif	Rap-Sensitive Probes (Total)[c]	p-value[d]	q-value[e]
SREBP	VNNVTCACCCYA	33 (82)	2.41E-07	1.28E-05
c-Myc (**HIF1**)[b]	RAC**CACGTG**CTC	385 (1164)	4.52E-06	1.45E-04
HNF4alpha	VTGAACTTTGMMB	853 (2084)	2.17E-05	4.34E-04
ATF4	CVTGACGYMABG	18 (30)	5.57E-04	6.36E-03

[a]Over-represented transcription factor-binding motifs in all rapamycin-sensitive genes from both *Tsc1*^{-/-} and *Tsc2*^{-/-} MEFs identified using a modified version of the MotifADE method (Mootha et al. 2004; Ma et al. 2008). Only these 4 motifs were in enriched in both cell lines with a q-value<0.01. Numbers for the *Tsc2* null cells are provided.

[b]The HIF1-binding hypoxia response element (bold) overlaps with this motif.

[c]Numbers are based on 39,000 gene probes analyzed in triplicate with Affymetrix microarrays, comparing vehicle-treated versus rapamycin-treated (24 h) *Tsc2*^{-/-} MEFs.

[d]Two-tailed Mann-Whitney rank sum p-value.

[e]Multiple testing corrected false discover rate (FDR) q-value.

(PR)
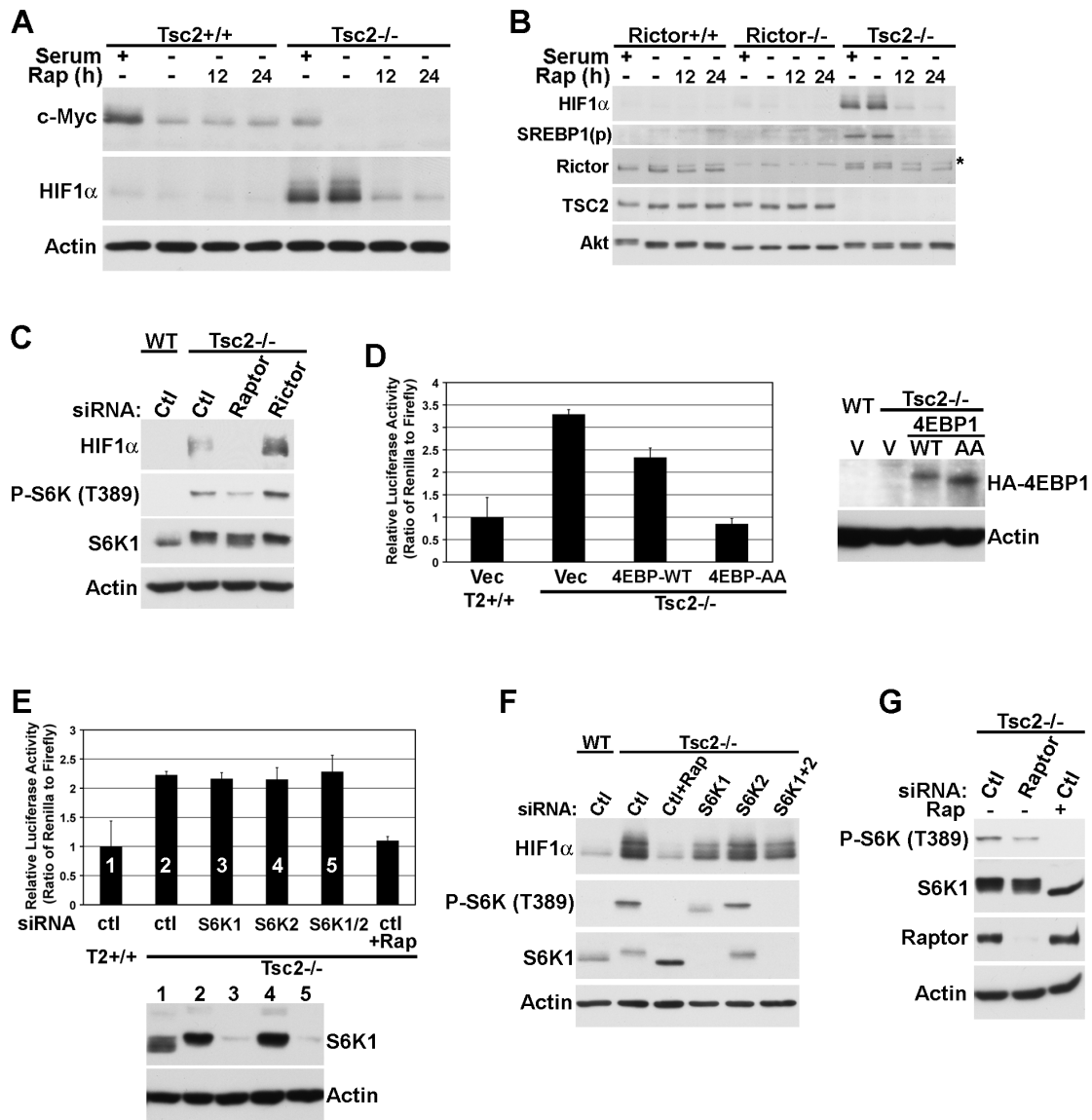
Figure 2-7. Alternative mechanisms involving C-Myc and mTORC2 are not involved and 4EBP is responsible for increased Hif1α levels.

A) C-myc is not expressed in *Tsc2*^{-/-} cells under the prolonged serum-free growth conditions used for expression analyses in this study. MEF lines were serum starved for 24 h in the presence of vehicle (-) or 20-nM rapamycin (12 or 24 h) and, where indicated, were stimulated with 10% serum for the final 1 h. **(JLY)**

Figure 2-7 continued

B) Levels of Hif1α and processed SREBP1 are not affected by the status of mTORC2. Littermate-derived *Rictor*$^{+/+}$ and *Rictor*$^{-/-}$ MEFs, along with *Tsc2-/-* MEFs, were treated as in (A). **(JLY)**

C) The elevated level of HIF1α in *Tsc2*$^{-/-}$ MEFs is dependent on mTORC1 and not mTORC2. MEFs were transfected with control non-targeting siRNAs (ctl) or siRNAs targeting Raptor or Rictor for 48 h followed by serum starvation for 24 hours. **(SM)**

D) The mTORC1-dependent induction of translation from the 5'-UTR of HIF1α is more strongly inhibited by the active phosphorylation-site mutant of 4E-BP1 relative to wild-type 4E-BP1. The bicistronic reporter encoding *Renilla* luciferase under translational control of the HIF1α-5'-UTR and firefly luciferase under control of a polio-virus IRES was cotransfected into either *Tsc2*$^{+/+}$ or *Tsc2*$^{-/-}$ MEFs with empty vector (Vec), 4E-BP1 (4EBP-WT), or mutant 4E-BP1 lacking two of the mTORC1-regulated phosphorylation sites (T37A/T46A; 4EBP-AA). 24 h post-transfection, cells were serum starved for 16 h and the ratio of *Renilla* to firefly luciferase was measured. The ratios are presented as mean±SD relative to *Tsc2*$^{+/+}$ cells and are representative of two independent experiments. The accompanying immunoblot shows the relative protein levels of exogenous wild-type and mutant 4E-BP1 expressed in this experiment. **(SM)**

E) The mTORC1-dependent induction of translation from the 5'-UTR of HIF1α is not affected by S6K1 or S6K2. *Tsc2*$^{+/+}$ and *Tsc2*$^{-/-}$ MEFs were transfected with control non-targeting siRNAs (ctl) or siRNAs targeting S6K1 and/or S6K2. 24 h post-transfection, the cells were transfected with the bicistronic reporter described in (D). 24 h later, the cells were serum starved for 16 h in the presence or absence of rapamycin (Rap, 20 nM), and the ratio of *Renilla* to firefly luciferase was measured. The ratios are presented

Figure 2-7 continued

as mean±SD relative to *Tsc2$^{+/+}$* cells. An immunoblot is provided showing the sustained effects of the siRNAs at the end of this experiment. **(SM)**

F) S6K1 has modest effects on Hif1α protein levels. *Tsc2$^{+/+}$* and *Tsc2$^{-/-}$* MEFs were transfected with siRNAs targeting the indicated transcripts or control non-targeting siRNAs (ctl). 24 h post-transfection, cells were serum starved for 18 h in the presence of vehicle or rapamycin (20 nM), where indicated. **(JLY)**

G) Rapamycin is more potent than Raptor siRNAs at inhibiting mTORC1 signaling. *Tsc2$^{-/-}$* MEFs were transfected with control non-targeting siRNAs (ctl) or siRNAs targeting Raptor. 48 h post-transfection, cells were serum starved for 24 h in the presence or absence of rapamycin (Rap, 20 nM). **(SM)**
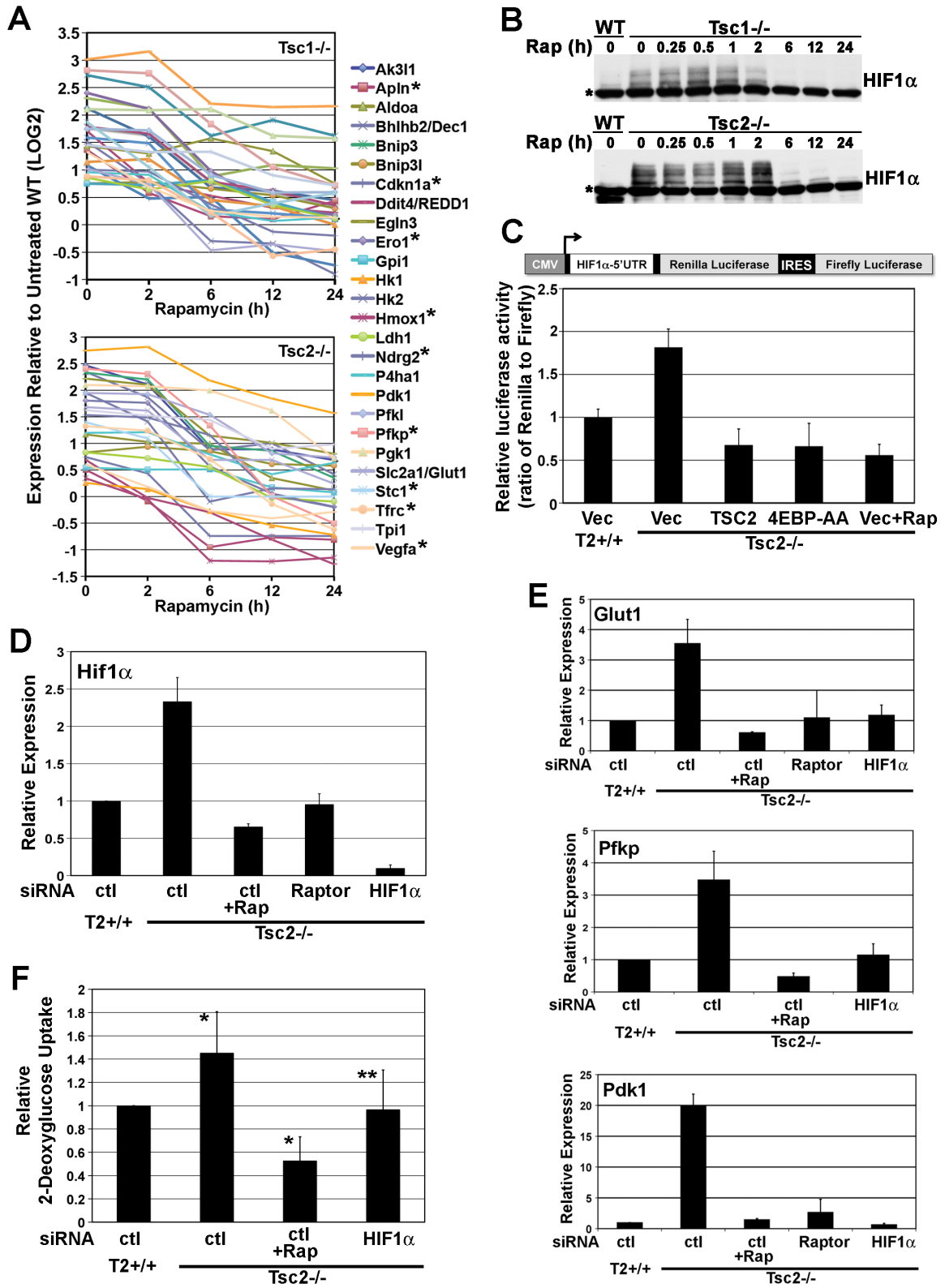
Figure 2-8. HIF1α and its target genes are upregulated by mTORC1 signaling.

Figure 2-8 continued

A) HIF1 target genes are elevated and rapamycin sensitive in *Tsc1* (upper graph) and *Tsc2* (lower graph) null cells. The $\log_2$ expression levels shown are the average obtained from independent replicates per time point of rapamycin treatment normalized to the expression levels in vehicle-treated wild-type cells, with those in the most stringent set indicated (*). **(KD)**

B) HIF1α protein levels are shown in wild-type and either *Tsc1* or *Tsc2* null MEFs grown in serum-free media and subjected to a time course of rapamycin (20 nM). *non-specific band. (See also Figures 2-7A-C) **(AIL)**

C) Induction of translation from the 5'-UTR of HIF1α is regulated by 4E-BP1. The bicistronic reporter was cotransfected with empty vector (Vec), TSC2, or 4E-BP1-AA (T37A/T46A). 24 h post-transfection, cells were serum starved for 16 h in the presence or absence of rapamycin (Rap, 20 nM), and the ratio of *Renilla* to firefly luciferase was measured. The ratios are presented as mean±SD relative to $Tsc2^{+/+}$ cells and are representative of three independent experiments. (See also Figures 2-7D-F) **(SM)**

D, E) mTORC1-dependent increase in the expression *Hif1α* (D) and its glycolytic gene targets (E). MEFs were transfected with siRNAs targeting the indicated transcripts or control non-targeting siRNAs (ctl). 32 h post-transfection, the cells were serum starved for 16 hours in the presence or absence of rapamycin (Rap, 20 nM). Transcript levels, measured by qRT-PCR, are presented as the mean±SD relative to levels in $Tsc2^{+/+}$ (Ctl) cells over three independent experiments. (See also Figure 2-7G) **(KD)**

F) The stimulation of glucose uptake downstream of mTORC1 is dependent on HIF1α. MEFs were transfected with siRNAs and treated as in (D). Glucose uptake was measured as the incorporation of 2-deoxy-D-[^{3}H]-glucose over 4 min and normalized to cell number. Levels are presented as mean±SD relative to $Tsc2^{+/+}$ (Ctl) cells over six

Figure 2-8 continued

independent experiments. *p<0.003 for $Tsc2^{+/+}$ versus $Tsc2^{-/-}$ and $Tsc2^{-/-}$ versus

rapamycin-treated $Tsc2^{-/-}$; **p<0.03 for $Tsc2^{-/-}$ versus $Tsc2^{-/-}$ with $Hif1\alpha$ knockdown. **(KD)**

most stringent dataset. The HIF1 transcription factor is a heterodimer comprised of the

constitutively expressed HIF1β/ARNT subunit complexed with either HIF1α or

HIF2α/EPAS1 [21, 22]. The HIFα subunit appears to dictate the target specificity of the

HIF1 heterodimer [23], and TSC-deficient cells display mTORC1-dependent

transcriptional upregulation of targets specific to HIF1α (e.g., glycolysis genes), as well

as those shared between HIF1α and HIF2α (e.g., VEGF).

As we are focused here on the metabolic genes, we examined the mechanism

leading to upregulation of the HIF1α subunit, which activates the genes of glycolysis [23,

24]. Consistent with the global upregulation of HIF1α targets and the findings from a

previous study [25], both $Tsc1^{-/-}$ and $Tsc2^{-/-}$ cells have elevated levels of HIF1α protein

relative to their wild-type counterparts (Figure 2-8B). Similar to its transcriptional targets,

this increase is blocked following 2 to 6 h of rapamycin treatment. The upregulation of

HIF1α is specific to mTORC1 and not affected by the status of mTORC2 in these cells.

Unlike $Tsc2^{-/-}$ MEFs, $Rictor^{-/-}$ MEFs do not show elevated levels of HIF1α (Figure 2-7B),

and the increased HIF1α in $Tsc2^{-/-}$ cells is sensitive to siRNAs targeting Raptor but not

Rictor (Figure 2-7C). Through studies using rapamycin, mTORC1 signaling has been

implicated in the activation of HIF1 (e.g., [26, 27]), in part through selective control of

translation from the 5'-untranslated region (UTR) of the HIF1α mRNA [28, 29]. To test

whether mTORC1 activation alone was sufficient to stimulate translation from the HIF1α

5'-UTR, we utilized a bicistronic reporter in which the translation of $Renilla$ luciferase is

under control of the HIF1α 5'-UTR and firefly luciferase is translated from an internal

ribosomal entry sequence (IRES; Figure 2-8C). $Tsc2^{-/-}$ MEFs showed enhanced

translation from the HIF1α 5'-UTR, and this was rescued by expression of human TSC2

or rapamycin treatment. Expression of a dominantly active 4E-BP1 mutant lacking two

mTORC1 inhibitory phosphorylation sites (4E-BP1-T37A/T46A) blocked this selective

translation (Figure 2-8C), whereas expression of wild-type 4E-BP1 resulted in a partial

decrease (Figure 2-7D). We found no effect of siRNAs targeting S6K1 and S6K2 on

translation from the HIF1α 5'-UTR (Figure 2-7E), but S6K1 knockdown led to a modest

decrease in HIF1α protein levels (Figure 2-7F). These data suggest that mTORC1

activation is sufficient to stimulate an increase in HIF1α protein levels, at least in part,

through mTORC1-mediated inhibition of 4E-BP1 and subsequent activation of 5'-cap-

dependent translation. However, we cannot rule out further contributing effects from

gene expression, as both *Hif1α* (Figure 2-8D) and *Hif2α* (data not shown) mRNA levels

are increased in an mTORC1-dependent manner (i.e., sensitive to rapamycin or siRNAs

targeting Raptor) in *Tsc2*-deficient cells.

    To determine whether HIF1α is the transcription factor downstream of mTORC1

in the control of glycolytic genes, the expression of representative genes was analyzed

following the introduction of siRNAs targeting either Raptor or HIF1α (Figure 2-8E).

Indeed, HIF1α knockdown reduced the mRNA levels of *Glut1*, *Pfkp*, and *Pdk1* in *Tsc2$^{-/-}$*

cells to wild-type levels, similar to Raptor siRNAs or rapamycin treatment. In this

experiment and those described below, transient knockdown of Raptor generally elicits a

weaker inhibitory effect than rapamycin, and this is reflected in an incomplete block of

mTORC1 signaling by Raptor siRNAs in the *Tsc2$^{-/-}$* cells (Figure 2-7G). Consistent with

the increase in HIF1α and its targets being responsible for the mTORC1-dependent

increase in glycolysis observed, siRNA-mediated knockdown of HIF1α in *Tsc2$^{-/-}$* cells

significantly blocked the increase in glucose uptake (Figure 2-8F).

SREBP is responsible for increased lipid biosynthesis, the pentose phosphate pathway, and cell proliferation downstream of mTORC1

The DNA-binding element recognized by SREBP was found to be the most highly enriched motif in the promoters of rapamcyin-sensitive genes in our expression array study (Table 2-2). Importantly, SREBP1 and SREBP2 are master transcriptional regulators of genes involved in *de novo* lipid and sterol biosynthesis genes [30]. Full-length SREBPs reside as inactive, transmembrane precursors in the endoplasmic reticulum and are activated by trafficking to the Golgi where they are processed by proteases. The active processed form then translocates to the nucleus to turn on its target genes. Interestingly, a recent study found that overexpression of an activated version of Akt leads to a rapamycin-sensitive increase in the processed form of SREBP1 [31]. To gain insights into how mTORC1 activation might increase the transcription of a large number of known SREBP targets, we compared the protein levels of full length and processed SREBP1 in littermate-derived wild-type and either $Tsc1^{-/-}$ or $Tsc2^{-/-}$ cells. While modest increases in the levels of full length SREBP1 could be detected, larger differences were seen in the processed active form of SREBP1, which were elevated in the TSC-deficient lines relative to their wild-type counterparts (Figure 2-9A). This is reflected by an increase in the ratio of processed to full length SREBP1 in these cells that is sensitive to rapamycin. The increased levels of processed SREBP1 are specific to mTORC1 and not affected by the status of mTORC2 in these cells. Unlike $Tsc2^{-/-}$ MEFs, $Rictor^{-/-}$ MEFs do not show elevated levels of processed SREBP1 (Figure 2-7B), and the increase in $Tsc2^{-/-}$ cells is sensitive to siRNAs targeting Raptor but not Rictor (Figure 2-9B). However, as with $Hif1\alpha$ and $Hif2\alpha$, rapamycin-sensitive increases in $Srebp1$ and $Srebp2$ transcript levels are detected in $Tsc2$-deficient cells (Figures 2-10A and B) or HEK-293 cells overexpressing Rheb (Figures 2-10C and D). Interestingly, siRNAs

Figure 2-9. mTORC1 signaling activates SREBP1 to induce *de novo* lipid biosynthesis and growth factor-independent proliferation.
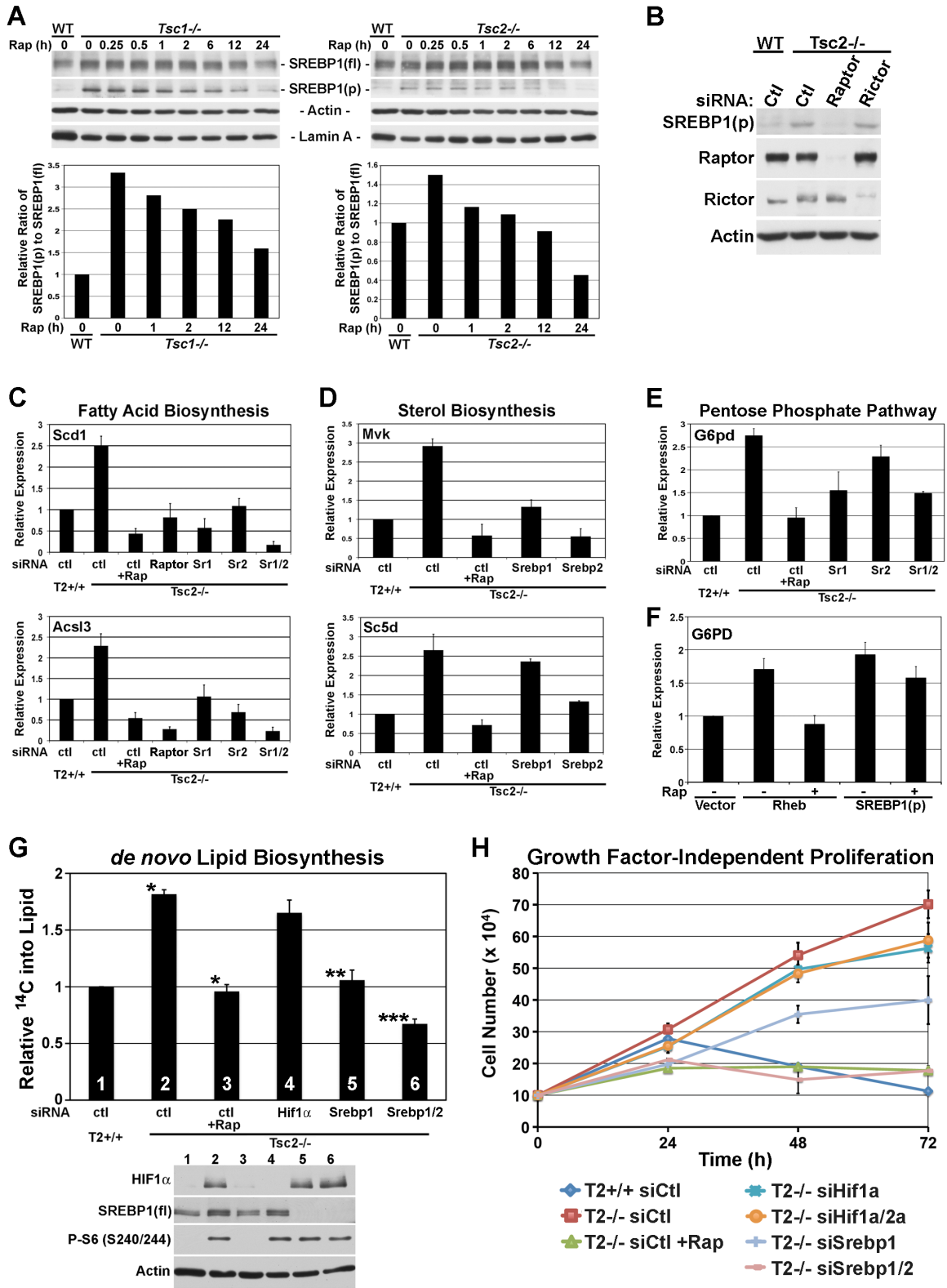
Figure 2-9 continued

A) Levels of full length (fl) and processed (p) SREBP1 are shown from littermate-derived pairs of wild-type and either *Tsc1* or *Tsc2* null MEFs grown in serum-free media and subjected to a time course of rapamycin (20 nM). (Below) The ratio of processed to full length SREBP1 at the indicated time points was quantified and plotted relative to untreated wild-type cells. **(JLY)**

B) MEFs were transfected with control non-targeting siRNAs (ctl) or siRNAs targeting *Raptor* or *Rictor*, and 48 h post-transfection, cells were serum starved for 24 hours. **(SM)**

C, D, E) The mTORC1-induced expression of genes involved in fatty acid (C) and sterol (D) biosynthesis and the pentose phosphate pathway (E) is dependent on SREBP. MEFs were transfected with control non-targeting siRNAs (ctl) or siRNAs targeting *Raptor*, *Srebp1* (Sr1), *Srebp2* (Sr2), or both (Sr1/2). 32 h post-transfection, cells were serum starved for 16 h in the presence or absence of rapamycin (Rap, 20 nM). The expression levels of representative genes were measured by qRT-PCR and are presented as the mean±SD relative to levels in *Tsc2*$^{+/+}$ cells over three independent experiments. (See also Figures 2-10A and B) **(KD)**

F) Overexpression of Rheb or the processed form of SREBP1a induces *G6PD* expression. HEK-293 cells were transiently transfected with empty vector (Vec), FLAG-RHEB, or FLAG-processed SREBP1a. 24 h post-transfection, cells were serum starved for 16 h in the presence of vehicle or rapamycin (20 nM). *G6PD* mRNA levels, measured by qRT-PCR, are presented as the mean±SD relative to levels in vector-transfected cells over three independent experiments. (See also Figures 2-10C and D) **(KD)**

G) The stimulation of *de novo* lipid biosynthesis downstream of mTORC1 is dependent on SREBP. MEFs were transfected with siRNAs targeting the indicated transcripts or control non-targeting siRNAs (ctl). 24 h post-transfection, cells were serum starved for

Figure 2-9 continued

24 h in the presence of vehicle or rapamycin (20 nM) and were incubated with D-[6-^{14}C]-

glucose for the final 4 h. ^{14}C incorporation into the lipid fraction was measured and is

presented as mean±SD relative to $Tsc2^{+/+}$ (Ctl) cells. These data are representative of

three independent experiments. *p<0.004 for $Tsc2^{+/+}$ versus $Tsc2^{-/-}$ and $Tsc2^{-/-}$ versus

rapamycin-treated $Tsc2^{-/-}$; **p<0.008 versus $Tsc2^{-/-}$ (ctl); ***p<0.002 versus $Tsc2^{-/-}$ (ctl).

A control immunoblot is provided with numbering matching the samples from the graph.

(See also Figure 2-10E) **(JLY)**

H) The mTORC1-driven proliferation of $Tsc2$ null cells in the absence of growth factors is

dependent on SREBP. $Tsc2^{+/+}$ (T2+/+) and $Tsc2^{-/-}$ (T2-/-) MEFs were transfected with

siRNAs targeting indicated genes or non-targeting control siRNAs (siCtl). 24 h post-

transfection, 1X10^5 cells per well were re-seeded and grown in serum-free medium in

the presence of vehicle or rapamycin (20 nM, Rap), with daily medium changes.

Triplicate samples were counted every 24 h, and the mean cell numbers ±SD for a

representative experiment are shown. (See also Figure 2-10F) **(KD)**
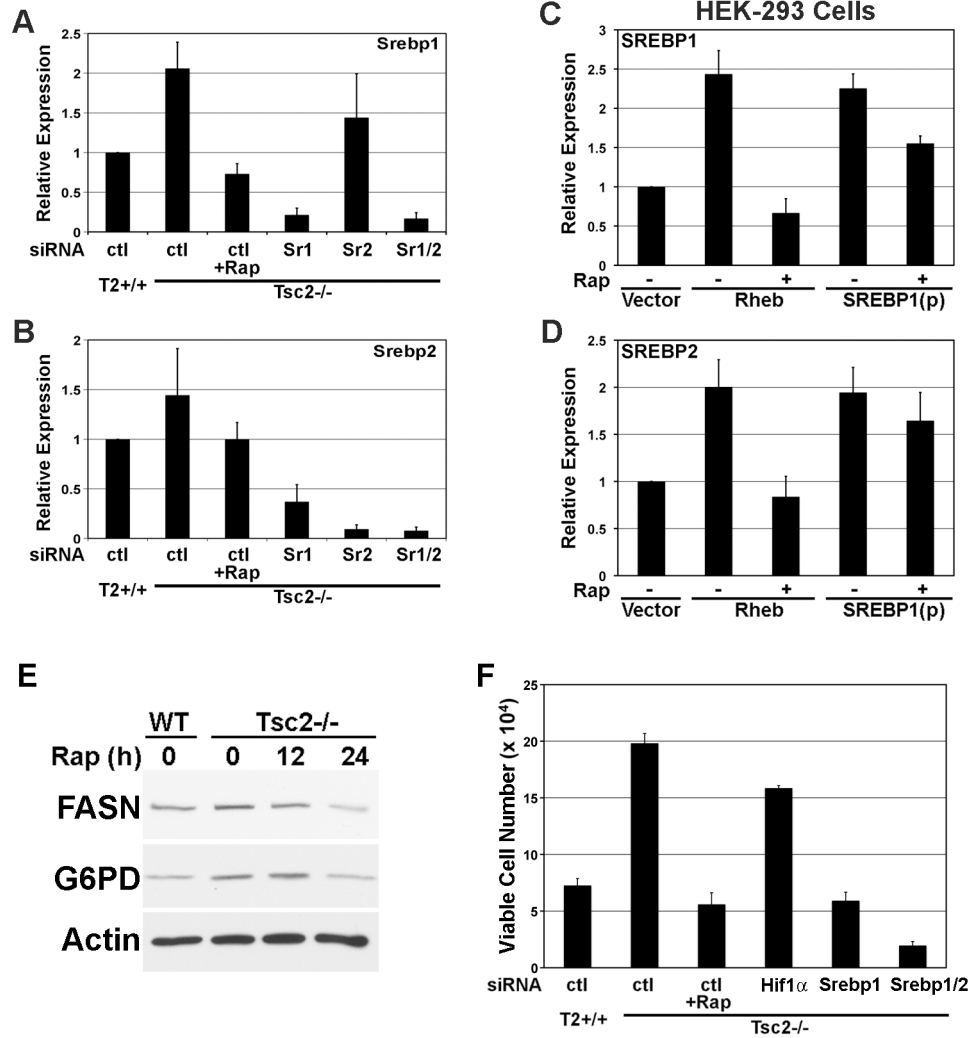
Figure 2-10. SREBP regulates its own expression downstream of mTORC1.

A, B) mTORC1-dependent up-regulation of *Srebp1* and *Srebp2* transcript levels in *Tsc2⁻/⁻* cells. *Tsc2^{+/+}* and *Tsc2^{-/-}* MEFs were transfected with siRNAs targeting *Srebp1* (Sr1), *Srebp2* (Sr2), or both (Sr1/2) or control non-targeting siRNAs (ctl). 32 h post-transfection, the cells were serum starved for 16 hours in the presence or absence of rapamycin (Rap, 20 nM). The mRNA levels of *Srebp1* (A) and *Srebp2* (B), measured by qRT-PCR, are presented as the mean±SD relative to levels in *Tsc2^{+/+}* cells treated with control siRNAs over three independent experiments. **(KD)**

Figure 2-10 continued

C, D) Induction of *SREBP1* and *SREBP2* expression by Rheb and the processed form of

SREBP1. HEK-293 cells were transiently transfected with empty vector (Vec), FLAG-

RHEB, or FLAG-processed SREBP1a. 24 h post-transfection, cells were serum starved

for 16 h in the presence of vehicle or rapamycin (20 nM), as indicated. *SREBP1* (C) and

SREBP2 (D) mRNA levels were measured by qRT-PCR and are presented as the

mean±SEM relative to levels in vector-transfected cells over three independent

experiments. **(KD)**

E) mTORC1-dependent changes in the levels of enzymes encoded by SREBP-target

genes. Protein levels of two SREBP targets are shown in $Tsc2^{+/+}$ and $Tsc2^{-/-}$ MEFs

serum starved for 24 h in the presence of vehicle or rapmacyin (20nM) for 12 or 24 h, as

indicated. **(JLY)**

F) The effects of SREBP knockdown on $Tsc2^{-/-}$ viable cell counts following 48 h serum

starvation. $Tsc2^{+/+}$ (T2+/+) and $Tsc2^{-/-}$ MEFs were transfected with siRNAs targeting

Hif1α, Srebp1, *Srebp1* and *Srebp2*, or non-targeting control siRNAs (siCtl), as indicated.

24 h post-transfection, 5×10^4 cells per well were re-seeded and grown in serum-free

medium in the presence of vehicle (DMSO) or rapamycin (20 nM, Rap), with daily

medium changes. Viable cell counts (via trypan blue exclusion) were measured for

triplicate samples at 48 h. The mean viable cell numbers ±SD are shown and are

representative of three independent experiments. **(KD)**

specific to *Srebp1* strongly down-regulate the transcript levels of *Srebp2*. These data suggest that the mTORC1-dependent increase in *Srebp1* and *Srebp2* transcript levels are due to their transcriptional activation by processed SREBP1. In support of this idea, we found that overexpressing the processed form of SREBP1 in HEK-293 cells can increase the endogenous transcript levels of both *SREBP1* and *SREBP2* (Figure 2-10C and D). Furthermore, unlike Rheb overexpression, this effect is resistant to rapamycin, indicating that the processed form of SREBP1 acts downstream of mTORC1.

To confirm that the mTORC1-driven expression of fatty acid and sterol biosynthesis genes is dependent on the SREBP transcription factors, the expression of representative gene were analyzed following siRNA-mediated knockdown of *Srebp1* and/or *Srebp2*. Similar to Raptor knockdown, siRNAs targeting one or both of these transcription factors blocked the expression of genes encoding enzymes involved in *de novo* fatty acid biosynthesis (e.g., *Scd1* and *Acsl3*, Figure 2-9C). Knockdown of either *Srebp1* or *Srebp2* also blocked the expression of genes involved in sterol and isoprenoid biosynthesis (e.g., *Mvk* and *Sc5d*, Figure 2-9D), with SREBP2 playing a more dominant role in the regulation of these genes. Therefore, the SREBP1 and SREBP2 transcription factors are required for the mTORC1-induced expression of fatty acid and sterol biosynthesis genes.

The unbiased genomic and metabolomic profiling described above revealed that mTORC1 signaling stimulates the oxidative pentose phosphate pathway. To gain insight into the regulation of this pathway by mTORC1, we used siRNAs targeting a number of candidate transcription factors and measured effects on the mRNA levels of *G6pd*, encoding the rate-limiting enzyme in the oxidative phase of the pentose phosphate pathway. Interestingly, we found that siRNA-mediated knockdown of SREBP1 decreased the rapamycin-sensitive expression of *G6pd* in *Tsc2*-deficient cells (Figure 2-9E). Furthermore, overexpression of the processed form of SREBP1 could induce *G6PD*

expression in HEK-293 cells (Figure 2-9F). Unlike Rheb overexpression, the effects of

SREBP1 on *G6PD* transcript levels were largely resistant to rapamycin, suggesting that

the processed form of SREBP1 is downstream of mTORC1 for the regulation of this

gene.

We next determined the role of SREBP in mTORC1-dependent cellular

processes. The transcriptional activation of SREBP targets encoding the key enzymes of

fatty acid biosynthesis (FASN) and the pentose phosphate pathway (G6PD) leads to a

rapamycin-sensitive increase in the level of these enzymes in $Tsc2^{-/-}$ cells (Figure 2-

10E). Importantly, we found that the mTORC1-dependent increase in *de novo* lipid

biosynthesis observed in $Tsc2^{-/-}$ cells was dependent on SREBP, but not HIF1α, with

Srebp1 knockdowns reducing the levels to that of wild-type cells and *Srebp1/2* double

knockdowns reducing it further (Figure 2-9G). Unlike rapamycin, knockdown of neither

HIF1α nor SREBP1 and 2 affected mTORC1 signaling. Interestingly, the growth factor-

independent, mTORC1-dependent proliferation of the $Tsc2^{-/-}$ cells was blocked by

siRNAs targeting both *Srebp1* and *Srebp2*, displaying similar effects to that of rapamycin

(Figures 2-9H and 2-10F). Knocking down *Srebp1* alone decreased proliferation to a

lesser extent, whereas knocking down *Hif1α* alone or in combination with *Hif2α* had only

marginal effects on this phenotype. These findings indicate that the SREBP-dependent

activation of a lipogenic program is required for mTORC1-driven cell proliferation.

mTORC1 activates SREBP1 through S6K1

Once processed and released from the Golgi, the active form of SREBP1 is

susceptible to proteasomal degradation [30]. To gain insight into how mTORC1 signaling

leads to elevated levels of processed SREBP1, we examined the stability of this active

form. Following cyclohexamide treatment, the processed form of SREBP1 was degraded

with similar kinetics in the presence or absence of TSC2 (Figure 2-11). This suggests
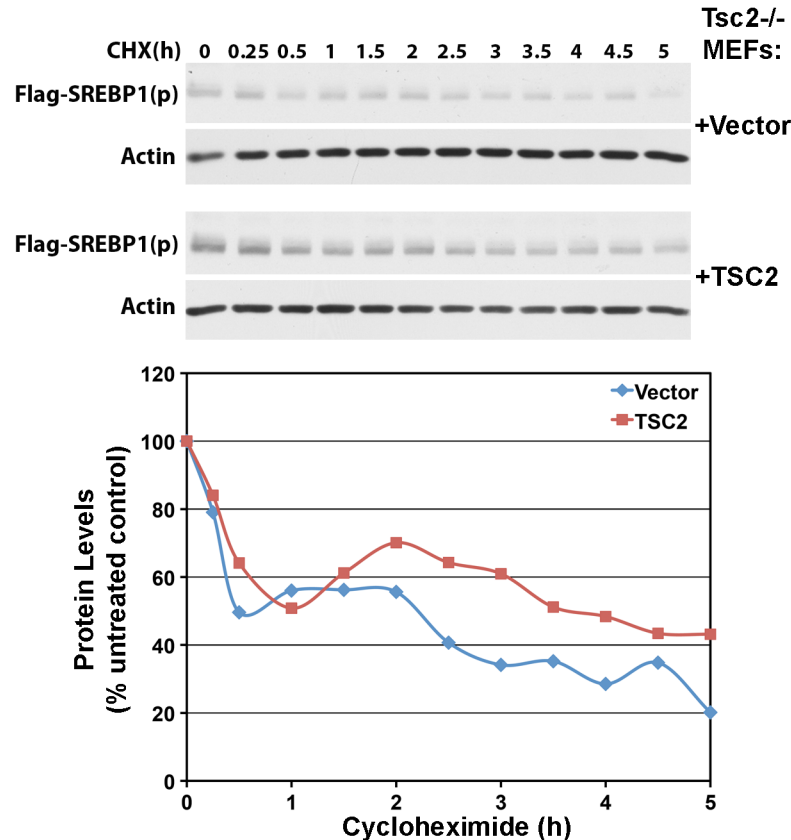
Figure 2-11. mTORC1 does not regulate the stability of processed SREBP.

The processed form of SREBP1 displays similar stability in the presence or absence of

TSC2. Tsc2-/- cells transfected with FLAG-processed SREBP1a were co-transfected

with either empty vector or FLAG-TSC2. Cells were serum starved for a total of 24 h and

treated with either vehicle or cycloheximide (CHX, 50μM) for the indicated time points

before harvesting. Immunoblots for FLAG-processed SREBP1a were normalized to the

actin loading control and their untreated control using densitometry. Graphs show the

percentage of protein relative to control remaining after various durations of CHX for

vector- or TSC2-expressing cells. **(JLY)**

that the mTORC1-dependent accumulation of processed SREBP1 in $Tsc1^{-/-}$ and $Tsc2^{-/-}$ cells is not due to increased protein stability. To further examine potential differences in SREBP1 degradation, we tested the effects of a proteasome inhibitor (ALLN) on this regulation. While ALLN treatment substantially increased the overall levels of processed SREBP1, this active form remained higher in the $Tsc2$-/- cells and, compared to untreated cells, was equally sensitive to rapamycin (Figure 2-12A). Finally, as GSK3-mediated phosphorylation of SREBP1 has been found to target it for degradation [32], we examined a potential role for GSK3. Efficient knockdown of GSK3α and β did not alter the levels or rapamycin sensitivity of processed SREBP1 in $Tsc2^{-/-}$ cells (Figure 2-12B). Collectively, these data suggest that mTORC1 signaling exerts a regulatory input into the processing step of SREBP1.

In order to identify the mTORC1-proximal signaling component responsible for the regulation of SREBP1 processing, we tested the effects of siRNAs targeting S6K1 and S6K2. Interestingly, knockdown of S6K1 or both S6K1 and 2 lead to a substantial decrease in the levels of processed SREBP1 in $Tsc2^{-/-}$ cells, even in the presence of the proteasome inhibitor (Figure 2-12B). The inhibitory effects of S6K1 knockdown on the levels of active SREBP1 is also reflected by a decrease in the expression levels of several of its transcriptional targets, including both lipid biosynthesis and pentose phosphate pathway genes (2-12C). Finally, loss of S6K1 leads to a partial but significant attenuation of the enhanced lipid biosynthesis phenotype of $Tsc2^{-/-}$ cells (2-12D). Therefore, S6K1 is the major downstream target of mTORC1 stimulating the activation of SREBP1.
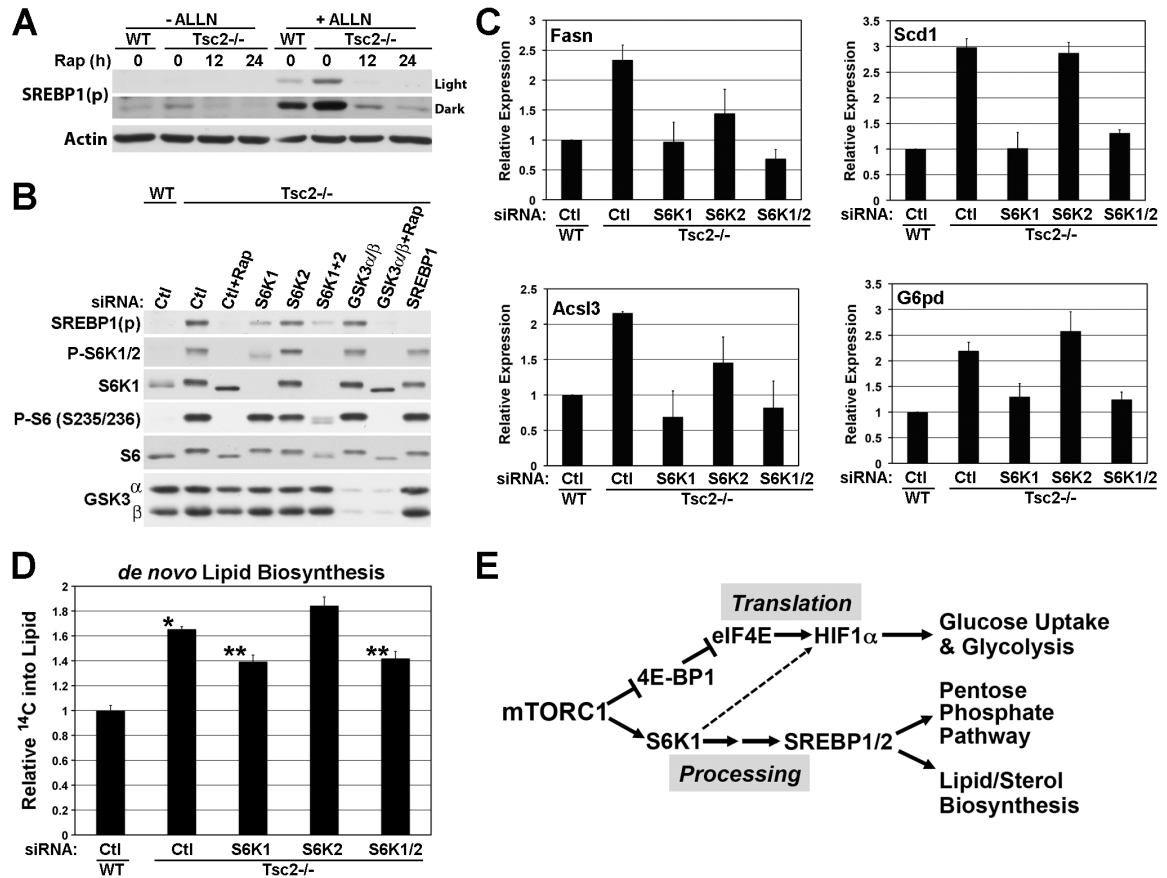
Figure 2-12. mTORC1 regulates SREBP1 through S6K1 but independent of GSK3 and effects on proteasomal degradation.

A) The inhibitory effects of rapamycin on processed SREBP1 (SREBP1(p)) are independent of proteasomal degradation. MEFs were serum starved for 24 h in the presence of vehicle or 20-nM rapamcyin (12 or 24 h) and, where indicated, were treated with ALLN (25 μg/mL) for the final 1 h. Light and dark exposures of the same blot of SREBP1(p) are shown. **(JLY)**

B) Involvement of S6K1, but not GSK3, in the mTORC1-dependent effects on SREBP1. MEFs were transfected with siRNAs targeting the indicated transcripts or control non-targeting siRNAs (ctl). 24 h post-transfection, cells were treated as in (A) with ALLN. **(JLY)**

Figure 2-12 continued

C) S6K1 regulates expression of SREBP1 target genes. MEFs were transfected with the indicated siRNAs, and 32 h post-transfection, cells were serum starved for 16 h in the presence or absence of rapamycin (Rap, 20 nM). Transcript levels were measured by qRT-PCR and are presented as the mean±SD relative to levels in $Tsc2^{+/+}$ (Ctl) cells over three independent experiments. **(JLY)**

D) S6K1 contributes to stimulation of *de novo* lipid biosynthesis downstream of mTORC1. Cells were transfected with the indicated siRNAs and serum starved for 24 h. For the final 4 h, cells were labeled with D-[6-^{14}C]-glucose. ^{14}C incorporation into the lipid fraction was measured and is presented as mean±SD relative to $Tsc2^{+/+}$ (Ctl) cells. *$p<0.003$ versus WT; **$p<0.03$ versus $Tsc2^{-/-}$ (ctl). **(JLY)**

E) Model of the control of specific metabolic pathways downstream of mTORC1. See text for details.

DISCUSSION

The cell lines and conditions chosen for this study were designed to isolate mTORC1 signaling from mTORC2, upstream branching pathways, parallel pathways, and feedback mechanisms that all accompany mTORC1 activation downstream of growth factors. While studies using rapamycin alone can reveal functions for which mTORC1 is necessary, combining rapamycin with an mTORC1 gain-of-function approach can identify those processes and pathways for which mTORC1 activity is both necessary and sufficient. Previous studies have profiled the effects of rapamycin on gene expression in lymphocytes [33, 34], and these studies have identified individual genes of glycolysis and lipid biosynthesis that were also classified as mTORC1-regulated transcripts in our study. Our study demonstrates that the genes of glycolysis, the pentose phosphate pathway, and sterol and lipid biosynthesis are amongst the most prominently induced by mTORC1. Interestingly, the set of mTORC1-regulated transcripts indentified in this study has substantial overlap with gene sets from two independent studies that have profiled transcriptional changes induced by forced expression of membrane-targeted Akt (myr)-Akt, which is constitutively active and potently affects many downstream pathways, including the TSC-mTORC1 pathway [35, 36]. One of these studies concluded that myr-Akt induces most of the genes of glycolysis through increased HIF1α [35], while the other found that myr-Akt induces many genes involved in lipid and cholesterol biosynthesis through increased SREBP1 and SREBP2 [36]. We find that mTORC1 signaling alone is sufficient to activate these transcription factors and their many downstream targets.

Perhaps the most striking finding from our unbiased analyses of mTORC1-regulated transcripts is the specificity of the effects of mTORC1 activation on HIF1 and SREBP, relative to other transcription factors. However, the mechanism by which

mTORC1 activates these two sets of transcription factors appears to be quite different

(see model in Figure 2-12E). Our data support previous studies using rapamycin alone,

which have concluded that mTORC1 signaling increases HIF1α protein levels by

promoting mRNA translation from its 5'UTR [28; 29], and we find that this induction

requires the inhibitory phosphorylation of 4E-BP1. However, we also find an mTORC1-

dependent increase in *Hif1α* and *Hif2α/Epas1* transcript levels, indicating either

autoregulation of *Hifα* transcripts or additional mTORC1-dependent inputs into their

regulation. Our data regarding the mTORC1-driven activation of SREBP1, on the other

hand, suggests that transcriptional and translational control have only minor effects and

that the induction involves a specific increase in the processed active form of SREBP1.

This finding is consistent with that of a recent study on cells overexpressing myr-Akt [31].

While we find a modest, but reproducible, increase in the full-length inactive form of

SREBP1 in TSC-deficient cells, this appears to reflect transcriptional autoregulation.

Importantly, mTORC1 signaling does not alter the stability of active SREBP1, suggesting

that this regulation is at the level of SREBP1 processing. This is also supported by our

finding that exogenous expression of the processed form of SREBP1 renders its gene

targets resistant to rapamycin. Our data indicate that S6K1 is required for the mTORC1-

driven increase in processed SREBP1 and downstream activation of its transcriptional

targets. Therefore, S6K1 promotes the processing of SREBP1 through an, as yet,

unknown molecular mechanism.

In addition to enhancing the *de novo* synthesis of lipids through SREBP-

dependent induction of the relevant enzymes, our studies demonstrate that mTORC1

activity is sufficient to increase metabolic flux through both glycolysis and the oxidative

arm of the pentose phosphate pathway. Consistent with previous studies [23, 24], we

find that HIF1α, but not HIF2α, regulates glucose uptake and glycolysis downstream of

mTORC1. Interestingly, knockdown of SREBP1 led to an attenuation of the mTORC1-dependent increase in the expression of *G6pd*, which encodes the rate-limiting enzyme in the oxidative phase of the pentose phosphate pathway. The promoter regions of both the rodent and human genes encoding G6PD contain predicted sterol regulatory elements, and SREBP1 has been shown to be capable of driving transcription from the rat version of this promoter [37]. Furthermore, data from *Srebp1* transgenic and knockout mice indicate that SREBP1c is involved in the induction of *G6pd* expression in liver [38, 39, 40]. Therefore, mTORC1 signaling increases flux through the oxidative pentose phosphate pathway, at least in part, through activation of SREBP1. A large amount of NADPH is needed for reducing power during *de novo* lipid biosynthesis, perhaps explaining the regulation of *G6PD* by SREBP1. In addition, it is likely that this connection between mTORC1 and the pentose phosphate pathway, leading to the production of NADPH needed for many biosynthetic processes and ribose needed for the synthesis of nucleotides, contributes to the promotion of anabolic cell growth and proliferation downstream of mTORC1. To this end, knocking down the expression of SREBP1 and SREBP2 has the same effect as rapamycin for blocking the proliferation of *Tsc2*^{-/-} cells, suggesting an essential role for lipid biosynthesis and, perhaps, the pentose phosphate pathway.

mTORC1 activation rarely occurs in isolation, but rather cooperates with many other signaling events to alter cell physiology. There is a growing appreciation that cell intrinsic alterations in nutrient and energy metabolism underlie multiple disease states, including cancer, diabetes, and neurological disorders. mTORC1 has been implicated in all of these pathological conditions and is a key component in a signaling network that regulates metabolism. Together with recent genetic approaches to understand the role of mTORC1 in integrated physiology [41, 42], we are gaining important insights into the

contributions of mTORC1 to the metabolic reprogramming of cells in response to the

physiological or pathological activation of upstream signaling pathways.

MATERIALS AND METHODS

Cell culture, constructs, and RNAi

Cell lines were maintained in Dulbecco's Modified Eagle Medium (DMEM) with

4.5 g/L glucose containing 10% fetal bovine serum (FBS) prior to the described

experiments in serum-free DMEM. Immortalized littermate-derived pairs of wild-type and

null *Tsc1* (3T3 immortalized) and *Tsc2* ($p53^{-/-}$) MEFs were provided by Dr. D.J.

Kwiatkowski [14, 16]. The stable pools of $Tsc2^{-/-}$ MEFs reconstituted with human *TSC2*

or empty vector were described previously [17]. Previously described pcDNA3-based

constructs encoding FLAG-tagged versions of the processed nuclear form of SREBP1a

(gift of Dr. T. Osborne [43]) and Rheb [15] were transfected into HEK293 cells using

Lipofectamine 2000 (Invitrogen), according to the manufacturer's protocol. The HA-4E-

BP1 constructs and HIF1α-5'UTR bicistronic reporter were gifts of Dr. J. Blenis, and the

corresponding methods were described previously [44]. HeLa cells stably expressing

shRNAs targeting firefly luciferase or *TSC2* were described elsewhere [11]. All siRNA-

mediated knockdown experiments were carried out with ON-TARGETplus or siGENOME

SMARTpool siRNAs (40 nM; Dharmacon). Cells were transfected using Lipofectamine

RNAiMAX (Invitrogen), according to the manufacturer's protocol for reverse transfection.

Gene expression array and bioinformatic analyses

MEFs were grown to 70% confluence in 10 cm plates and were serum starved

for 24 h in the presence of vehicle (DMSO) for 24 h or rapamycin (20 nM) for 2, 6, 12, or

24 h. All vehicle-treated samples (0 h time points) were plated in triplicate and all

rapamycin time course samples were plated in duplicate. For each replicate, expression analysis was performed by hybridization to an Affymetrix Mouse 430_2 oligonucleotide microarray chip. The complete microarray data set is available at www.ncbi.nlm.nih.gov/geo (accession number GSE21755). Detailed protocols describing this analysis and the subsequent bioinformatic approaches, including GSEA and MotifAde, are provided with the supplemental materials.

Metabolomic profiling

To measure the intracellular levels of metabolites, extracts were prepared and then analyzed using LC-MS. Triplicate 10-cm plates (~70% confluent) were incubated in serum-free medium for 16 h, with a medium change 2 h prior to extraction. For the flux studies, cells were washed once with glucose-free DMEM and then incubated in DMEM containing a 10-mM 1:1 mixture of D-[1,2-^{13}C]-glucose and unlabeled D-glucose for 15 min. Metabolites were extracted on dry ice with 5-mL 80% methanol (-80°C). The extract was dried down under nitrogen and resuspended in 80 μL water just prior to the LC-MS run.

LC-MS data were acquired using a 4000 QTRAP triple quadrupole mass spectrometer (Applied Biosystems/Sciex) equipped with an HTS PAL autosampler (Leap Technologies) and an Agilent 1200 Series binary HPLC pump. Water-soluble metabolites were profiled using hydrophobic interaction chromatography (HILIC) with MS operation in the positive ion mode and ion pairing chromatography (IPC) with MS operation in the negative ion mode. Amino acids, biogenic amines and other positively charged polar metabolites were separated using an Atlantis HILIC column (150 x 2.1 mm; Waters) eluted with a 10-min linear gradient, initiated with 100% mobile phase B (acetonitrile with 0.1% formic acid, v/v) and concluded with 60% mobile phase A (10 mM ammonium formate and 0.1% formic acid, v/v). Central metabolites, purines,

pyrimidines, and other negatively charged polar compounds were analyzed using a

modified version of the IPC method. The mobile phases used in this method were 10

mM tributylamine/15 mM acetic acid (mobile phase A) and methanol (mobile phase B),

and the stationary phase was an Atlantis T3 column (150 x 2.1mm; Waters). The column

was eluted at a flow rate of 300 mL/min using the following program: 100% mobile phase

A at initiation, 100% A at 4.0 min, 2% A at 34 min, 2% mobile phase A at 39 min, 100%

mobile phase A at 39.5 min, and 100% mobile phase A at 55 min. Multiple reaction

monitoring (MRM) was used to acquire targeted MS data for specific metabolites (HILIC:

53 metabolites measurable of 88 targeted; IPC: 68 metabolites of 148 targeted).

Declustering potentials and collision energies were optimized for each metabolite by

infusion of reference standards prior to sample analyses. The scheduled MRM algorithm

in the Analyst 1.5 software (Applied Biosystems/Sciex) was used to automatically set

dwell times for each transition. MultiQuant software (Version 1.1; Applied

Biosystems/Sciex) was used for automated peak integration and metabolite peaks were

manually reviewed for quality of integration and compared against a known standard to

confirm identity. For ^{13}C tracer studies, LC-MS sample preparation and analyses were

carried out as described above with minor modification to the mass spectrometer data

acquisition method to include specific MRM settings for M+1 and M+2 isotopes.

Measurements of glucose uptake, lactate production, and *de novo* lipid

biosynthesis

Glucose uptake was measured as the incorporation of radiolabeled 2-

deoxyglucose, based on a previously described method [45]. Briefly, cells were grown in

12-well plates and serum-starved in the presence of vehicle (DMSO) or rapamycin for 16

h. The cells were then washed twice with KRH buffer (20 mM HEPES, pH 7.4, 136 mM

NaCl, 4.7 mM KCl, 1.25 mM $MgSO_4$, 1.25 mM $CaCl_2$) containing 0.1% bovine serum

albumin (BSA) and incubated for 15 min in 0.45 ml KHR/BSA, followed by addition of 0.1

mM cold 2-deoxy-D-glucose and 0.5 μCi 2-deoxy-D-[^{3}H] glucose (American

Radiolabeled Chemicals) for 4 min. Following the 4 min incubation, cells were placed on

ice, washed twice with ice-cold PBS, and lysed in 0.5 ml of 0.05% SDS. 0.4 ml lysate

was counted in 5 ml of scintillation fluid using a Beckman LS6500 scintillation counter.

Rates of non-specific glucose uptake were determined in samples pre-treated for 10 min

with cytochalasin B (10 mM, Sigma) and were subtracted from the total uptake. The

specific glucose uptake was normalized to cell number obtained from parallel wells.

Each cell line and condition was assayed in triplicate.

For measurements of lactate secretion, cells were plated (four replicates per

condition) at subconfluent density (4×10^4 cells/well) in 12 well dishes, and after 24 h,

cells were switched to serum-free medium containing DMSO or rapamycin (20 nM) for

16 h. For the final hour, cells were incubated in fresh serum free medium with DMSO or

rapamycin, and lactate secreted into the medium over this time was measured, in

triplicate for each sample, using the fluorescence mode of a Lactate Assay Kit (Biovision

Inc.). Fluorescent readings were averaged for each sample replicate, which were then

averaged for each condition replicate, and were normalized to cell number obtained from

parallel wells.

Following a 20 h incubation in serum-free medium, *de novo* lipogenesis was

measured by changing to fresh serum-free, low-glucose medium containing 4 μCi/mL D-

[6-^{14}C]-glucose (Amersham) for 4 h prior to lipid extraction. Cells were incubated with

vehicle (DMSO) or rapamycin (20 nM) for the duration of the 24 h incubation. As a

background control, one sample was labeled for just 1 min prior to extraction. Cells were

washed twice with D-PBS before lysing in 0.5% Triton X-100. The lipid fraction was

extracted by sequential addition of chloroform and methanol (2:1 v/v) with vortexing.

After washing with water, phase separation was achieved by low-speed centrifugation

(1000 rpm, 15 min), and ^{14}C incorporation into the lower lipid-containing phase was

counted in 3 ml scintillation fluid using a Beckman LS6500 scintillation counter. Each cell

line and condition was assayed in duplicate, and after subtracting background values,

average readings were normalized to cell counts from parallel plates. For all of these

metabolic assays, a two-tailed Student's t-test was used to determine the statistical

significance of the relative differences measured.

Cell Lines

The littermate-derived pair of immortalized ($p53^{-/-}$) $Rictor^{+/+}$ and $Rictor^{-/-}$ MEFs

were provided by Drs. D.A. Guertin (University of Massachusetts Medical School,

Worcester, MA) and D.M. Sabatini (Massachusetts Institute of Technology).

Immunoblotting

Cell lysates and immunoblots were prepared as described previously (Manning

et al., 2002). Antibodies used include those recognizing mouse SREBP1 (C20 from

Santa Cruz) and Hif1α (Figure 4B, gift of Dr. M.C. Simon; all other blots, Cayman

Chemicals), G6PD and Rictor (Bethyl Laboratories), and β-actin (Sigma). All other

antibodies were from Cell Signaling Technologies. Image J Software was used to

quantify band intensities.

mRNA expression analysis

For gene expression analyses, RNA was isolated using the RNeasy Mini Kit

(Qiagen). cDNAs were generated using the Superscript III First Strand Synthesis System

for RT-PCR kit (Invitrogen), and SYBR green-based quantitative RT-PCR was

performed using an Applied Biosystems 7300 Real Time PCR System. Samples for

each experimental condition were run in triplicate and were normalized to either Rplp0

(m36b4) or β-actin mRNA to determine relative expression levels. Primer sets used in this study are provided in supplemental Table 2-3. For expression analysis following a standard double thymidine block, cells were plated in triplicate at a density of $2x10^5$ per well in six well dishes. After attachment, thymidine (2 mM in PBS) or an equal volume of PBS was added for 20 h. Cells were then washed and restored to their normal growth medium for 12 h prior to a second treatment with thymidine or PBS alone in serum-free medium in the presence or absence of rapamycin (20 nM) for 18 h. Cell counts were taken to confirm the proliferation arrest, and RNA was isolated and analyzed by qRT-PCR, as above.

Gene expression array and bioinformatic analyses

  Tsc1 and *Tsc2* wild-type and null MEFs were grown to 70% confluence in 10 cm plates and were serum starved for 24 h in the presence of vehicle (DMSO) for 24 h or rapamycin (20 nM, Calbiochem) for 2, 6, 12, or 24 h. All vehicle-treated samples (0 h time points) were plated in triplicate and all rapamycin time course samples were plated in duplicate. For each replicate, RNA was isolated using an RNeasy Mini Kit (Qiagen), and 2.5 to 5 μg of RNA were used to synthesize double-stranded cDNA according to standard Affymetrix protocols (GeneChip One-Cycle Target Labelling). Linear amplification with T7-RNA polymerase and biotin labeling were performed by *in vitro* transcription, and the resulting biotin-labeled cRNA was fragmented and hybridized to the Affymetrix Mouse 430_2 oligonucleotide microarray chip for 16 h at 45°C. Following hybridization, the chip was washed, stained, and scanned on an Affymetrix GCS 3000 GeneArray Scanner. Gene expression visualizations were done in Spotfire DecisionSite and Spotfire DXP (TIBCO). The data generated from the scan were then analyzed using the MicroArray Suite software (MAS 5.0, Affymetrix).

Table 2-3: RT-PCR Primers

Primers for mouse transcripts

Gene	Forward Primer	Reverse primer
Acsl3	5'-ggggctggaacaattacaga-3'	5'- atagccaccttcctcccagt-3'
Epas1 (Hif2a)	5'-cctgcagcctcagtgtatca-3'	5'-gtgtggcttgaacagggatt-3'
G6pdx	5'-cctaccatctggtggctgtt-3'	5'-tggctttaaagaagggctca-3'
Hif1a	5'-tccatgtgaccatgaggaaa-3'	5'-cttccacgttgctgacttga-3'
Mvk	5'-gggacgatgtcttccttgaa-3'	5'-gaacttggtcagcctgcttc-3'
Pdk1	5'-ggcggctttgtgatttgtat-3'	5'-acctgaatcggggggataaac-3'
Pfkp	5'-aggagggcaaaggagtgttt-3'	5'-ttggcagaaatcttggttcc-3'
Pgd	5'-agacaggcagccactgagtt-3'	5'-aagttctgggtttcgctcaa-3'
Rpe	5'-gggcagaaattcatggaaga-3'	5'-ctggggtcatcactcctca-3'
Rpia	5'-agtgctgggaattggaagtg-3'	5'-ctctgggtgttgatccaggt-3'
Rplp0 (36b4)	5'-agatgcagcagatccgcat-3'	5'-gttcttgcccatcagcacc-3'
Sc5d	5'-ccaaatggctggattcatct-3'	5'-gtccacagggtgaaaagcat-3'
Scd1	5'-ctgacctgaaagccgagaag-3'	5'-gcgttgagcaccagagtgta-3'
Slc2a1 (Glut1)	5'-gctgtgcttatgggcttctc-3'	5'-agaggccacaagtctgcat-3'
Srebf1 (Srebp1)	5'-gatcaaagaggagccagtgc-3'	5'-tagatggtggctgctgagtg-3'
Srebf2 (Srebp2)	5'-ggatcctcccaaagaaggag-3'	5'-ttcctcagaacgccagactt-3'

Primers for human transcripts

Gene	Forward primer	Reverse Primer
ACSL3	5'-acacaagggcgcatatcttc-3'	5'-gtggtgtgacacaggaccag-3'
EPAS1	5'- ttgatgtggaaacggatgaa-3'	5'-ggaacctgctcttgctgttc-3'
G6PD	5'-aagaacgtgaagctccctga-3'	5'-aatataggggatgggcttgg-3'
HIF1A	5'-ccagatctcggcgaagtaaa-3'	5'-cctcacacgcaaatagctga-3'
MVK	5'-gctcaagttcccagagatcg-3'	5'-atggtgctggttcatgtcaa-3'
PDK1	5'-gaagcagttcctggacttcg-3'	5'-accaattgaacggatggtgt-3'
PFKP	5'-ctacaagcgacttgccatca-3'	5'-atcatagatggcgagcatcc-3'
PGD	5'-ggtgcacaacgggatagagt-3'	5'-ccatcggtgtcttggaactt-3'
RPE	5'-tggaaaggatctgggaagtg-3'	5'-ccttggggtcaagatccata-3'
RPIA	5'-ctggatcgacacccagagat-3'	5'-cgatcacgatgaagcgacta-3'
RPLP0	5'-agatgcagcagatccgcat-3'	5'-gttcttgcccatcagcacc-3'
SC5DL	5'-tatctcttccgcccatgttc-3'	5'-tggctcattcaccatttcaa-3'
SCD	5'-cccagctgtcaaagagaagg-3'	5'-caagaaagtggcaacgaaca-3'
SLC2A1/GLUT1	5'-cttcactgtcgtgtcgctgt-3'	5'-ccaggacccacttcaaagaa-3'
SREBF1	5'-tgcattttctgacacgcttc-3'	5'- ccaagctgtacaggctctcc-3'
SREBF2	5'-tggcttctctccctactcca-3'	5'-gagaggcacaggaaggtgag-3'
TSC2	5'-tgctcatcaacaggcagttc-3'	5'-gccatcaccttctcgatgat-3'

The raw data for microarray results were normalized using RMA from the R/Bioconductor package 'affy' [46-48]. The expression levels from rapamycin-treated (2, 6, 12, and 24 h) $Tsc1^{-/-}$ and $Tsc2^{-/-}$ cells were compared to their 0 h controls (vehicle treated), and the vehicle-treated wild-type levels were compared to levels from both the 0 h and 24 h rapamycin time points for $Tsc1^{-/-}$ and $Tsc2^{-/-}$ cells. Fold changes and p-values for array comparisons were calculated using the R/Bioconductor package 'Limma' [49]. Gene set enrichment analysis was performed on a set of 541 mTORC1-regulated probes (representing 464 genes) that met the four criteria detailed in the results section accompanying Figure 1, at a p-value cutoff of < 0.05. Enrichment and pathway analysis was done using the MetaCore application (GeneGo). MotifAde analysis was performed, as described previously [19], on all genes sensitive to rapamycin at 24 h in both $Tsc1^{-/-}$ and $Tsc2^{-/-}$ cells.

ACKNOWLEDGEMENTS

REFERENCES

1.   Menon, S., and Manning, B.D. (2009). Common corruption of the mTOR signaling network in human tumors. Oncogene *27, S43-S51*.

2.   Dann, S.G., Selvaraj, A., and Thomas, G. (2007). mTOR Complex1-S6K1 signaling: at the crossroads of obesity, diabetes and cancer. Trends in molecular medicine *13*, 252-259.

3.   Ehninger, D., de Vries, P.J., and Silva, A.J. (2009). From mTOR to cognition: molecular and cellular mechanisms of cognitive impairments in tuberous sclerosis. J Intellect Disabil Res *53*, 838-851.

4.   Guertin, D.A., and Sabatini, D.M. (2009). The pharmacology of mTOR inhibition. Science signaling *2*, pe24.

5.   Wullschleger, S., Loewith, R., and Hall, M.N. (2006). TOR signaling in growth and metabolism. Cell *124*, 471-484.

6.   Ma, X.M., and Blenis, J. (2009). Molecular mechanisms of mTOR-mediated translational control. Nat Rev Mol Cell Biol *10*, 307-318.

7.   Sarbassov, D.D., Ali, S.M., Sengupta, S., Sheen, J.H., Hsu, P.P., Bagley, A.F., Markhard, A.L., and Sabatini, D.M. (2006). Prolonged rapamycin treatment inhibits mTORC2 assembly and Akt/PKB. Mol Cell *22*, 159-168.

8.   Avruch, J., Hara, K., Lin, Y., Liu, M., Long, X., Ortiz-Vega, S., and Yonezawa, K. (2006). Insulin and amino-acid regulation of mTOR signaling and kinase activity through the Rheb GTPase. Oncogene *25*, 6361-6372.

9.   Huang, J., and Manning, B.D. (2008). The TSC1-TSC2 complex: a molecular switchboard controlling cell growth. Biochem J *412*.

10.   Crino, P.B., Nathanson, K.L., and Henske, E.P. (2006). The tuberous sclerosis complex. N Engl J Med *355*, 1345-1356.

11.   Huang, J., Dibble, C.C., Matsuzaki, M., and Manning, B.D. (2008). The TSC1-TSC2 complex is required for proper activation of mTOR complex 2. Mol Cell Biol *28*.

12.   Huang, J., Wu, S., Wu, C.L., and Manning, B.D. (2009). Signaling events downstream of mammalian target of rapamycin complex 2 are attenuated in cells and tumors deficient for the tuberous sclerosis complex tumor suppressors. Cancer Res *69*, 6107-6114.

13.   Jaeschke, A., Hartkamp, J., Saitoh, M., Roworth, W., Nobukuni, T., Hodges, A., Sampson, J., Thomas, G., and Lamb, R. (2002). Tuberous sclerosis complex tumor suppressor-mediated S6 kinase inhibition by phosphatidylinositide-3-OH kinase is mTOR independent. J. Cell Biol. *159*, 217-224.

14.   Kwiatkowski, D.J., Zhang, H., Bandura, J.L., Heiberger, K.M., Glogauer, M., el-Hashemite, N., and Onda, H. (2002). A mouse model of TSC1 reveals sex-dependent lethality from liver hemangiomas, and up-regulation of p70S6 kinase activity in TSC1 null cells. Hum. Mol. Genet *11*, 525-534.

15.   Tee, A.R., Manning, B.D., Roux, P.P., Cantely, L.C., and Blenis, J. (2003). Tuberous sclerosis complex gene products, tuberin and hamartin, control mTOR signaling by acting as a GTPase-activating protein complex toward Rheb. Curr. Biol. *13*, 1259-1268.

16.   Zhang, H., Cicchetti, G., Onda, H., Koon, H.B., Asrican, K., Bajraszewski, N., Vazquez, F., Carpenter, C.L., and Kwiatkowski, D.J. (2003). Loss of Tsc1/Tsc2 activates mTOR and disrupts PI3K-Akt signaling through downregulation of PDGFR. J Clin Invest *112*, 1223-1233.

17.   Zhang, H.H., Lipovsky, A.I., Dibble, C.C., Sahin, M., and Manning, B.D. (2006). S6K1 regulates GSK3 under conditions of mTOR-dependent feedback inhibition of Akt. Mol Cell *24*, 185-197.

18.   Mootha, V.K., Handschin, C., Arlow, D., Xie, X., St Pierre, J., Sihag, S., Yang, W., Altshuler, D., Puigserver, P., Patterson, N*., et al.* (2004). Erralpha and Gabpa/b specify PGC-1alpha-dependent oxidative phosphorylation gene expression that is altered in diabetic muscle. Proc Natl Acad Sci U S A *101*, 6570-6575.

19.   Ma, Q., Chirn, G.W., Szustakowski, J.D., Bakhtiarova, A., Kosinski, P.A., Kemp, D., and Nirmala, N. (2008). Uncovering mechanisms of transcriptional regulations by systematic mining of cis regulatory elements with gene expression profiles. BioData mining *1*, 4.

20.   Dang, C.V., O'Donnell, K.A., Zeller, K.I., Nguyen, T., Osthus, R.C., and Li, F. (2006). The c-Myc target gene network. Seminars in cancer biology *16*, 253-264.

21.   Gordan, J.D., Thompson, C.B., and Simon, M.C. (2007). HIF and c-Myc: sibling rivals for control of cancer cell metabolism and proliferation. Cancer cell *12*, 108-113.

22.   Semenza, G.L. (2003). Targeting HIF-1 for cancer therapy. Nature reviews *3*, 721-732.

23.   Hu, C.J., Wang, L.Y., Chodosh, L.A., Keith, B., and Simon, M.C. (2003). Differential roles of hypoxia-inducible factor 1alpha (HIF-1alpha) and HIF-2alpha in hypoxic gene regulation. Mol Cell Biol *23*, 9361-9374.

24.   Semenza, G.L., Roth, P.H., Fang, H.M., and Wang, G.L. (1994). Transcriptional regulation of genes encoding glycolytic enzymes by hypoxia-inducible factor 1. J Biol Chem *269*, 23757-23763.

25.   Brugarolas, J.B., Vazquez, F., Reddy, A., Sellers, W.R., and Kaelin, W.G., Jr. (2003). TSC2 regulates VEGF through mTOR-dependent and -independent pathways. Cancer Cell *4*, 147-158.

26.   Hudson, C.C., Liu, M., Chiang, G.G., Otterness, D.M., Loomis, D.C., Kaper, F., Giaccia, A.J., and Abraham, R.T. (2002). Regulation of hypoxia-inducible factor 1alpha expression and function by the mammalian target of rapamycin. Mol Cell Biol *22*, 7004-7014.

27.   Zhong, H., Chiles, K., Feldser, D., Laughner, E., Hanrahan, C., Georgescu, M.M., Simons, J.W., and Semenza, G.L. (2000). Modulation of hypoxia-inducible factor 1alpha expression by the epidermal growth factor/phosphatidylinositol 3-

kinase/PTEN/AKT/FRAP pathway in human prostate cancer cells: implications for tumor angiogenesis and therapeutics. Cancer Res *60*, 1541-1545.

28. Laughner, E., Taghavi, P., Chiles, K., Mahon, P.C., and Semenza, G.L. (2001). HER2 (neu) signaling increases the rate of hypoxia-inducible factor 1alpha (HIF-1alpha) synthesis: novel mechanism for HIF-1-mediated vascular endothelial growth factor expression. Mol Cell Biol *21*, 3995-4004.

29. Thomas, G.V., Tran, C., Mellinghoff, I.K., Welsbie, D.S., Chan, E., Fueger, B., Czernin, J., and Sawyers, C.L. (2006). Hypoxia-inducible factor determines sensitivity to inhibitors of mTOR in kidney cancer. Nat Med *12*, 122-127.

30. Espenshade, P.J., and Hughes, A.L. (2007). Regulation of sterol synthesis in eukaryotes. Annual review of genetics *41*, 401-427.

31. Porstmann, T., Santos, C.R., Griffiths, B., Cully, M., Wu, M., Leevers, S., Griffiths, J.R., Chung, Y.L., and Schulze, A. (2008). SREBP activity is regulated by mTORC1 and contributes to Akt-dependent cell growth. Cell Metab *8*, 224-236.

32. Sundqvist, A., Bengoechea-Alonso, M.T., Ye, X., Lukiyanchuk, V., Jin, J., Harper, J.W., and Ericsson, J. (2005). Control of lipid metabolism by phosphorylation-dependent degradation of the SREBP family of transcription factors by SCF(Fbw7). Cell Metab *1*, 379-391.

33. Grolleau, A., Bowman, J., Pradet-Balade, B., Puravs, E., Hanash, S., Garcia-Sanz, J.A., and Beretta, L. (2002). Global and specific translational control by rapamycin in T cells uncovered by microarrays and proteomics. J Biol Chem *277*, 22175-22184.

34. Peng, T., Golub, T.R., and Sabatini, D.M. (2002). The immunosuppressant rapamycin mimics a starvation-like signal distinct from amino acid and glucose deprivation. Mol Cell Biol *22*, 5575-5584.

35. Majumder, P.K., Febbo, P.G., Bikoff, R., Berger, R., Xue, Q., McMahon, L.M., Manola, J., Brugarolas, J., McDonnell, T.J., Golub, T.R.*, et al.* (2004). mTOR inhibition reverses Akt-dependent prostate intraepithelial neoplasia through regulation of apoptotic and HIF-1-dependent pathways. Nat Med *10*, 594-601.

36. Porstmann, T., Griffiths, B., Chung, Y.L., Delpuech, O., Griffiths, J.R., Downward, J., and Schulze, A. (2005). PKB/Akt induces transcription of enzymes involved in cholesterol and fatty acid biosynthesis via activation of SREBP. Oncogene *24*, 6465-6481.

37. Amemiya-Kudo, M., Shimano, H., Hasty, A.H., Yahagi, N., Yoshikawa, T., Matsuzaka, T., Okazaki, H., Tamura, Y., Iizuka, Y., Ohashi, K.*, et al.* (2002). Transcriptional activities of nuclear SREBP-1a, -1c, and -2 to different target promoters of lipogenic and cholesterogenic genes. Journal of lipid research *43*, 1220-1235.

38. Liang, G., Yang, J., Horton, J.D., Hammer, R.E., Goldstein, J.L., and Brown, M.S. (2002). Diminished hepatic response to fasting/refeeding and liver X receptor

agonists in mice with selective deficiency of sterol regulatory element-binding protein-1c. J Biol Chem *277*, 9520-9528.

39.   Shimano, H., Yahagi, N., Amemiya-Kudo, M., Hasty, A.H., Osuga, J., Tamura, Y., Shionoiri, F., Iizuka, Y., Ohashi, K., Harada, K.*, et al.* (1999). Sterol regulatory element-binding protein-1 as a key transcription factor for nutritional induction of lipogenic enzyme genes. J Biol Chem *274*, 35832-35839.

40.   Shimomura, I., Shimano, H., Korn, B.S., Bashmakov, Y., and Horton, J.D. (1998). Nuclear sterol regulatory element-binding proteins activate genes responsible for the entire program of unsaturated fatty acid biosynthesis in transgenic mouse liver. J Biol Chem *273*, 35299-35306.

41.   Bentzinger, C.F., Romanino, K., Cloetta, D., Lin, S., Mascarenhas, J.B., Oliveri, F., Xia, J., Casanova, E., Costa, C.F., Brink, M.*, et al.* (2008). Skeletal muscle-specific ablation of raptor, but not of rictor, causes metabolic changes and results in muscle dystrophy. Cell Metab *8*, 411-424.

42.   Polak, P., Cybulski, N., Feige, J.N., Auwerx, J., Ruegg, M.A., and Hall, M.N. (2008). Adipose-specific knockout of raptor results in lean mice with enhanced mitochondrial respiration. Cell Metab *8*, 399-410.

43.   Toth, J.I., Datta, S., Athanikar, J.N., Freedman, L.P., and Osborne, T.F. (2004). Selective coactivator interactions in gene activation by SREBP-1a and -1c. Mol Cell Biol *24*, 8288-8300.

44.   Choo, A.Y., Yoon, S.O., Kim, S.G., Roux, P.P., and Blenis, J. (2008). Rapamycin differentially inhibits S6Ks and 4E-BP1 to mediate cell-type-specific repression of mRNA translation. Proc Natl Acad Sci U S A *105*, 17414-17419.

46.   Erdman, C., and Emerson, J.W. (2008). A fast Bayesian change point analysis for the segmentation of microarray data. Bioinformatics (Oxford, England) *24*, 2143-2148.

47.   Gautier, L., Cope, L., Bolstad, B.M., and Irizarry, R.A. (2004). affy--analysis of Affymetrix GeneChip data at the probe level. Bioinformatics (Oxford, England) *20*, 307-315.

48.   Gentleman, R.C., Carey, V.J., Bates, D.M., Bolstad, B., Dettling, M., Dudoit, S., Ellis, B., Gautier, L., Ge, Y., Gentry, J.*, et al.* (2004). Bioconductor: open software development for computational biology and bioinformatics. Genome biology *5*, R80.

45.   Kozma, L., Baltensperger, K., Klarlund, J., Porras, A., Santos, E., and Czech, M.P. (1993). The ras signaling pathway mimics insulin action on glucose transporter translocation. Proc Natl Acad Sci U S A *90*, 4460-4464.

49.   Smyth, G.K., Michaud, J., and Scott, H.S. (2005). Use of within-array replicate spots for assessing differential expression in microarray experiments. Bioinformatics (Oxford, England) *21*, 2067-2075.

CHAPTER 3

mTORC1-Dependent and Independent Control of Hepatic SREBP1c

Adapted from:

Yecies, J.L.[1], Zhang, H.H.[1,3,5], Menon, S.[1,5], Liu, S.[1], Yecies, D.[1], Lipovsky, A.I.[1,4], Gorgun, C.[1], Kwiatkowski, D.J.[2], Hotamisligil, G.S.[1], Lee, C.H.[1], and Manning, B.D[1]. (2011). Akt stimulates hepatic SREBP1c and lipogenesis through parallel mTORC1-dependent and independent pathways. *Cell Metab* 14, 21-32.

[1]Department of Genetics and Complex Diseases, Harvard School of Public Health, Boston, MA 02115, USA

[2]Hematology Division, Department of Medicine, Brigham and Women's Hospital, Harvard Medical School, Boston MA 02115, USA

[3]Present Address: Joslin Diabetes Center, Boston, MA 02115, USA

[4]Present Address: Department of Genetics, Yale University School of Medicine, New Haven, CT 06520, USA

[5]These second authors contributed equally to this work.

JLY performed the experiments in Figures 3-1; 3-2; 3-3C, E, and F; 3-4D-F; 3-5F and G; 3-6; 3-7; 3-8; 3-9A-C; 3-10. SL isolated primary hepatocytes, SM injected mice and helped collect blood and harvest livers. HZ generated high-fat diet cohort and collected tissues. Author contributions are noted in figure legends.

SUMMARY

Through unknown mechanisms, insulin activates the sterol regulatory element-binding protein (SREBP1c) transcription factor to promote hepatic lipogenesis. We find that this induction is dependent on the mammalian target of rapamycin (mTOR) complex 1 (mTORC1). To further define the role of mTORC1 in the regulation of SREBP1c in the liver, we generated mice with liver-specific deletion of TSC1 (*LTsc1KO*), which results in insulin-independent activation of mTORC1. Surprisingly, the *LTsc1KO* mice are protected from age- and diet-induced hepatic steatosis and display hepatocyte-intrinsic defects in SREBP1c activation and *de novo* lipogenesis. These phenotypes result from attenuation of Akt signaling driven by mTORC1-dependent insulin resistance. Therefore, mTORC1 activation is not sufficient to stimulate hepatic SREBP1c in the absence of Akt signaling, revealing the existence of an additional downstream pathway also required for this induction. We provide evidence that this mTORC1-independent pathway involves Akt-mediated suppression of *Insig2a*, a liver-specific transcript encoding the SREBP1c inhibitor INSIG2.

BACKGROUND

The liver is a key organ in the systemic response to insulin, controlling both glucose and lipid metabolism. Hepatocytes respond to insulin by halting gluconeogenesis and increasing *de novo* lipid synthesis. Genetic mouse models have demonstrated that both of these responses to insulin occur, at least in part, downstream of the protein kinase Akt2 [1-3]. Akt2 mediates these effects primarily through the regulation of two downstream transcription factors, FOXO1 and SREBP1c, which control the expression of the metabolic enzymes underlying these processes. FOXO1 stimulates gluconeogenic gene expression in the liver and is directly phosphorylated and

inhibited by Akt [4]. While the mechanisms are less well characterized, Akt signaling appears to stimulate *de novo* lipid synthesis through the activation of SREBP isoforms (reviewed in [5]). SREBP1c is the dominant insulin-stimulated isoform in the liver responsible for inducing lipogenic gene expression and promoting fatty acid synthesis [6]. Akt activation appears to be both necessary and sufficient for the induction of hepatic SREBP1c and lipid accumulation [3, 7, 8]. An important feature of hepatic insulin signaling is that control of gluconeogenesis and lipogenesis is differentially affected under pathological conditions of insulin resistance associated with type 2 diabetes. Under such conditions, insulin fails to suppress glucose production by the liver, while the induction of hepatic lipogenesis is sustained, thereby contributing to both the hyperglycemic and hyperlipidemic states. Understanding this pathological phenomenon, referred to as selective insulin resistance [9], requires a deeper understanding of how insulin and Akt regulate hepatic lipid metabolism.

Recent cell-based studies have implicated the activation of mTOR complex 1 (mTORC1) downstream of Akt in the induction of SREBP isoforms (Chapter 2; [10, 11]). The primary mechanism by which Akt activates mTORC1 is through the phosphorylation and inhibition of the TSC2 protein within the TSC1-TSC2 complex (reviewed in [12]). This protein complex acts as a GTPase-activating protein (GAP) for a Ras-related small G protein called Rheb, thereby enhancing its conversion to the GDP-bound off state. GTP-bound Rheb stimulates mTORC1 kinase activity and downstream signaling. Therefore, Akt-mediated inhibition of the TSC1-TSC2 complex serves to activate Rheb and mTORC1. Importantly, increased activation of mTORC1, through the expression of an activated allele of Akt [10] or genetic disruption of the TSC1-TSC2 complex (Chapter 2; [11]), has been found to activate SREBP isoforms and promote an SREBP-dependent increase in *de novo* lipid synthesis. Furthermore, a recent study has shown that the ability of insulin to stimulate SREBP1c in rat hepatocytes requires mTORC1 [13].

SREBP1c regulation is quite complex [14, 15]. The protein is synthesized as an inactive precursor that resides in complex with SREBP cleavage-activating protein (SCAP) in the endoplasmic reticulum (ER) membrane, where it is sequestered through the interaction of SCAP with INSIG proteins. Through a poorly understood process, insulin stimulates trafficking of the SREBP1c-SCAP complex to the Golgi, where SREBP1c is proteolytically processed to generate the active transcription factor. The active form of SREBP1c is sensitive to proteasomal degradation but can enter the nucleus to engage its transcriptional targets, including its own gene promoter and those encoding the major enzymes of fatty acid synthesis [6]. A collection of previous studies has implicated insulin and Akt in controlling different aspects of SREBP1c activation [5]. While the mechanisms remain to be determined, mTORC1 signaling downstream of Akt appears to regulate some aspect of the trafficking or processing of SREBP isoforms, without obvious effects on translation or stability (Chapter 2; [10, 11]).

The role of mTORC1 activation in the metabolic response of the liver to insulin and nutrients is poorly understood [16]. Elevated levels of mTORC1 signaling have been associated with conditions of hepatic insulin resistance [17-19]. *In vitro*, mTORC1 signaling can cause cell-intrinsic insulin resistance through negative feedback mechanisms affecting upstream regulators of Akt [20, 21]. In support of an *in vivo* role for these feedback mechanisms controlling insulin sensitivity, knockout of S6K1, a downstream target activated by mTORC1, leads to an increased response of Akt signaling to insulin in the mouse liver, as well as other metabolic tissues [22]. However, the phenotype of the S6K1 knockout mouse is confounded by a pronounced reduction in adiposity. Therefore, liver-specific genetic models are needed to better define the hepatocyte-intrinsic roles of mTORC1 in controlling insulin signaling and lipogenesis.

Here, we seek to elucidate the role of mTORC1 signaling in the regulation of SREBP1c and lipid metabolism in the liver. We find that mTORC1 activation is required

for the induction of hepatic SREBP1c in response to insulin and feeding. To determine

whether mTORC1 activation is sufficient to drive hepatic lipogenesis, we generate an

mTORC1 gain of function mouse model lacking TSC1 in the liver. Contrary to our

prediction, these mice are protected from both age- and diet-induced hepatic steatosis.

In determining the mechanism of this protection, we find that there is a surprising defect

in the induction of SREBP1c in the livers of these mice stemming from the attenuation of

hepatic Akt signaling. These findings indicate that mTORC1 activity alone cannot

stimulate lipogenesis in the liver and that a second Akt-driven pathway is also required.

Finally, our data indicate that the mTORC1-independent pathway downstream of Akt

involves the suppression of a liver-specific isoform of INSIG [23-25].

RESULTS

Insulin stimulates hepatic SREBP1c in an mTORC1-dependent manner.

As the mechanism of hepatic SREBP1c induction by insulin and Akt is poorly

understood, we sought to determine whether mTORC1 activity contributes to this

induction in primary mouse hepatocytes. Insulin stimulates activating phosphorylation

events on Akt leading to subsequent phosphorylation of the Akt targets FOXO1,

FOXO3a, and TSC2, the latter target of which leads to mTORC1 activation and

phosphorylation of S6K1 (Figure 3-1A and 3-2A). As described for other cell types, we

find that inhibition of mTORC1 with rapamycin enhances the insulin-stimulated

phosphorylation of Akt and its substrates in hepatocytes (Figure 3-1A), presumably

through inhibition of negative feedback mechanisms (reviewed in [12, 21]). In response

to insulin, SREBP1c induces its own expression, as well as genes encoding lipogenic

enzymes, such as FASN [6, 15]. Importantly, despite enhancing Akt signaling, pre-

treatment with rapamycin suppressed the ability of insulin to stimulate *Srebp1c* and *Fasn*

(Figure 3-1B). In contrast, mRNA expression of *Igfbp1* and the gluconeogenic enzyme
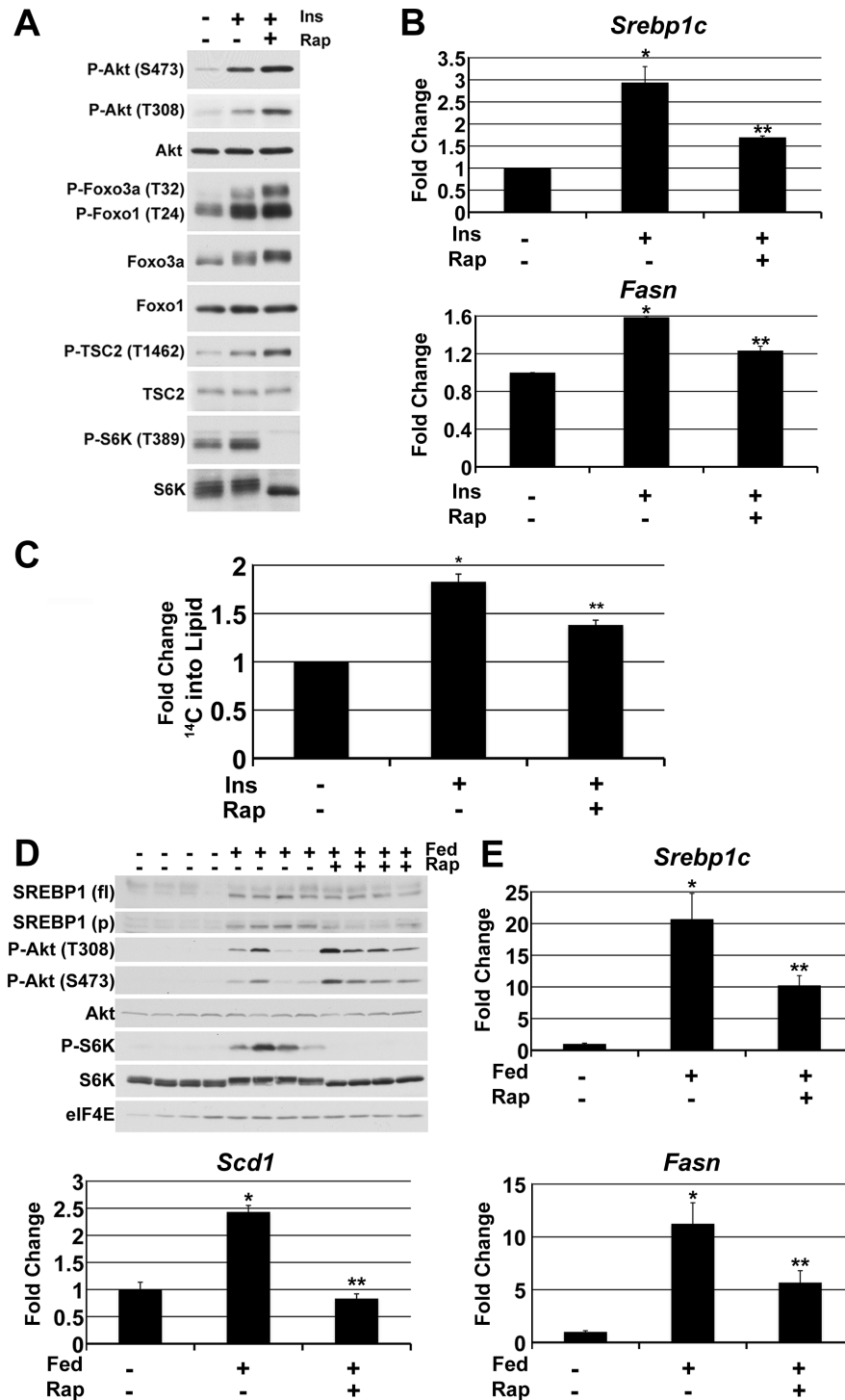
Figure 3-1. mTORC1 activity is required for the insulin-stimulated induction of hepatic SREBP1c and *de novo* lipogenesis. (JLY)

A) Primary hepatocytes were serum starved overnight, pretreated for 30 min with vehicle or rapamycin (Rap; 20 nM), and stimulated for 6 h with insulin (Ins; 10 nM), as indicated.

Figure 3-1 continued

B) Hepatocytes were treated as in (A), and mRNA expression was measured by qRT-PCR. Transcript levels are shown relative to untreated controls. *P<0.006 (*Srebp1c*) and P<4x10^{-7} (*Fasn*) compared to unstimulated; **P<0.03 (*Srebp1c*) and P<0.002 (*Fasn*) compared to insulin-stimulated, vehicle-treated.

C) Hepatocytes treated as in (A) were labeled with ^{14}C-acetate and the levels of ^{14}C incorporation into the lipid fraction are shown relative to untreated controls. *P<5x10^{-5} and **P<0.004 for the comparisons described in (B). Data are presented as the mean ± SEM from three (B) or four (C) independent experiments.

(D,E) 8 week-old mice were fasted overnight (-) and then refed for 6 h (+) following a 30-min pre-treatment with vehicle or rapamycin (10mg/kg). N=4 mice per condition. (D) Liver lysates were immunoblotted for markers of mTORC1 signaling and full length (fl) and processed (p) SREBP1. (E) Gene expression was measured by qRT-PCR. Data are shown as mean ± SEM relative to untreated controls. *P<0.003 (*Srebp1c*), P<0.002 (*Fasn*) and P<0.0007 (*Scd1*) compared to fasted; **P<0.03 (*Srebp1c*), P<0.05 (*Fasn*), and P<0.0001 (*Scd1*) compared to fed, vehicle-treated.
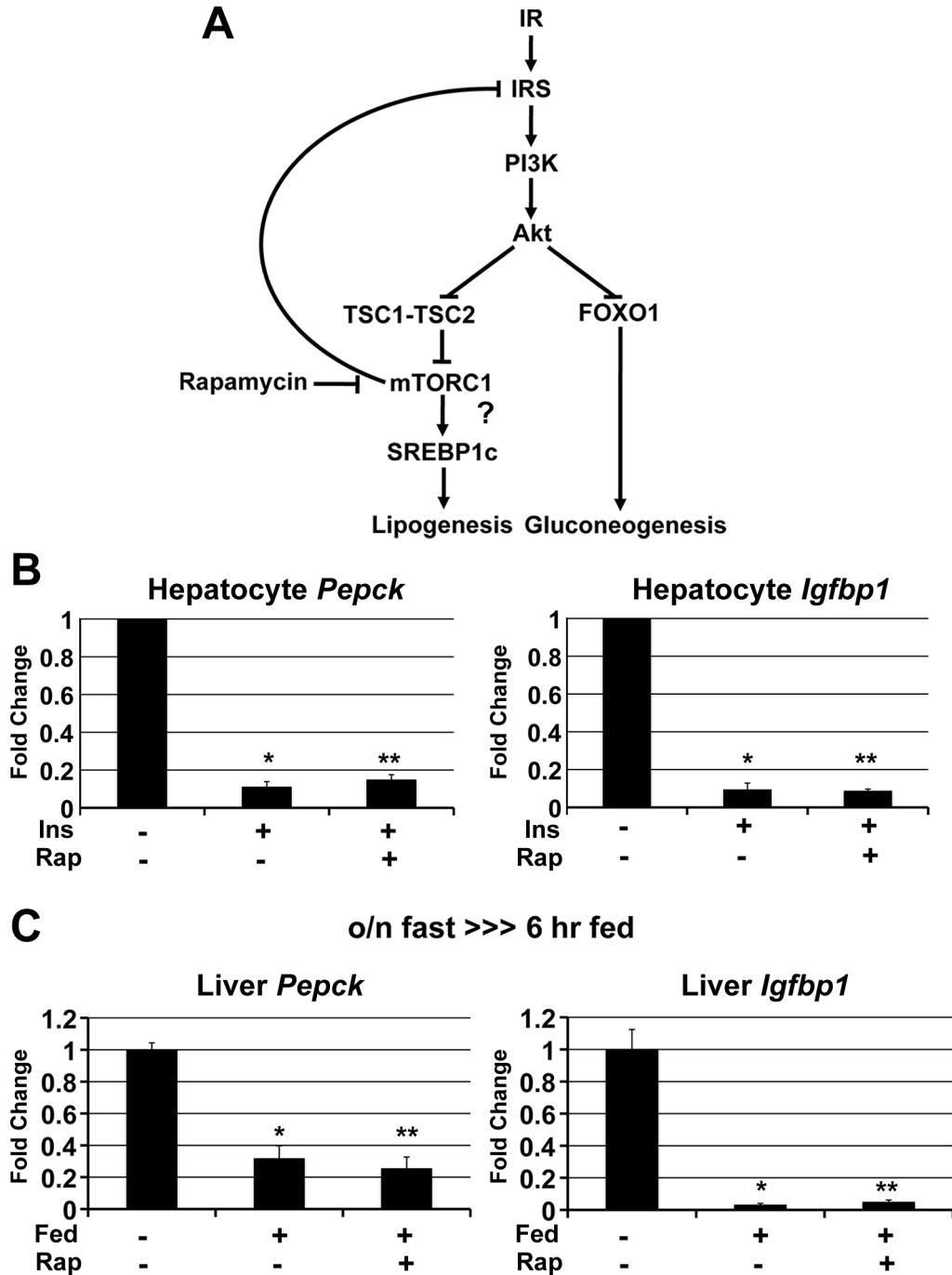
Figure 3-2. mTORC1 activity is dispensable for insulin-mediated suppression of FOXO1 targets. (JLY)

A) Model depicting the proposed pathways through which insulin suppresses gluconeogenesis and stimulates lipogenesis in the liver (see text for details).

Figure 3-2 continued

B,C) mTORC1 activity is not required for insulin-mediated suppression of FOXO1

targets. (B) Primary hepatocytes were serum starved overnight, pretreated for 30 min

with vehicle (DMSO) or rapamycin (Rap; 20 nM), and then stimulated for 6 h with insulin

(Ins; 10 nM), as indicated. mRNA expression was measured by qRT-PCR. Transcript

levels are shown relative to untreated controls and are presented as mean ± SEM from

three independent experiments. *$P<1\times10^{-5}$ compared to unstimulated; **$P<5\times10^{-6}$

compared to unstimulated for both targets. (C) 8 week-old mice were fasted overnight (-)

and then refed for 6 hours (+) with or without 30 min pre-treatment with rapamycin

(10mg/kg), where indicated (n=4 per group). RNA was isolated from livers and gene

expression was measured by qRT-PCR. Data are shown as mean ± SEM relative to

untreated controls. *$P<0.001$ (*Pepck*) and $P<0.002$ (*Igfbp1*) compared to fasted;

**$P<0.0005$ (*Pepck*) and $P<0.0003$ (*Igfbp1*) compared to fasted. Note: There is no

significant difference between the fold suppression by insulin in the presence or absence

of rapamycin in hepatocytes (B) and livers (C).

Pepck, two canonical FOXO1 targets, was inhibited by insulin but not affected by rapamycin (Figure 3-2B). These findings are consistent with those described recently for rat hepatocytes [13] and demonstrate that mTORC1 is required for proper insulin stimulation of SREBP1c. Consistent with this effect on SREBP1c, rapamycin also significantly impairs the ability of insulin to stimulate *de novo* lipid synthesis in hepatocytes (Figure 3-1C). To determine the relevance of these findings *in vivo*, we subjected mice to an overnight fast followed by refeeding. Feeding activates hepatic Akt and mTORC1 signaling and promotes the expression and processing of SREBP1 and increased expression of its targets (Figure 3-1D,E; [26]). Importantly, SREBP1c activation was blocked by treatment with rapamycin just prior to feeding (Figure 3-1D,E), without effects on FOXO1 targets (Figure 3-2C). Taken together with studies in other settings [10, 11], these results indicate that mTORC1 is a critical effector downstream of insulin and Akt for the induction of SREBP1c in hepatocytes.

Liver-specific deletion of *Tsc1* results in insulin-independent activation of mTORC1.

To further define the role of mTORC1 in the regulation of hepatic lipid metabolism, we employed a liver-specific gain of function model to disconnect mTORC1 activation from its normal control by insulin. As insulin signals to mTORC1 through Akt-mediated inhibition of the TSC1-TSC2 complex, loss of TSC1 or TSC2 leads to Akt-independent activation of mTORC1 signaling. To delete *Tsc1* specifically in hepatocytes, we used a previously described floxed allele of *Tsc1* (*Tsc1^fl^*; Figure 3-3A; [27]), backcrossed onto a pure C57Bl/6J background. Following Cre-induced recombination, exons 17 and 18 of the *Tsc1^fl^* allele are deleted, and this has been demonstrated to generate a null allele [27]. Hepatocyte-specific deletion of this allele was achieved by crossing these mice to those expressing Cre from the albumin promoter (*Alb-Cre*; [28]).
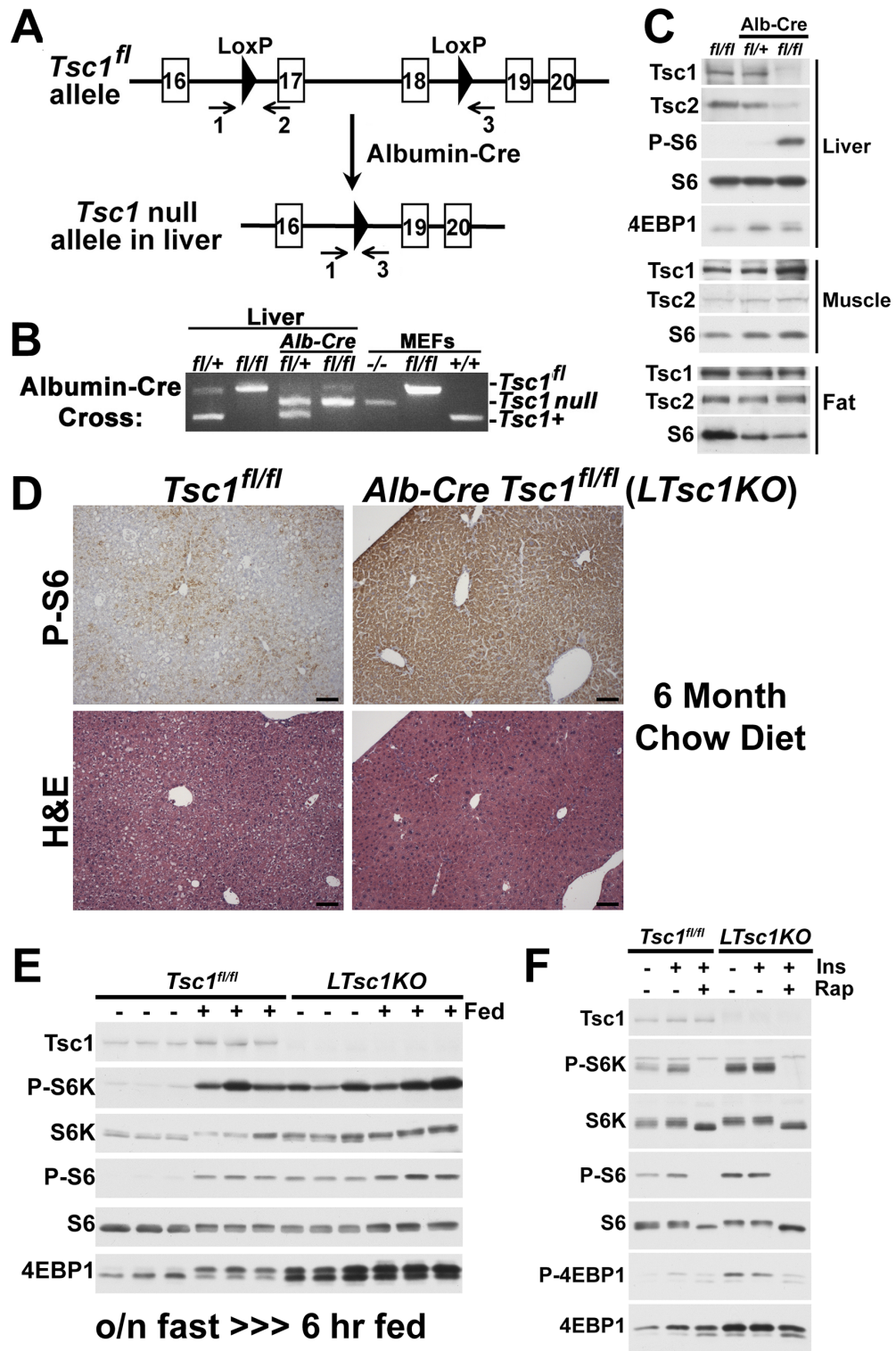
Figure 3-3. Liver-specific *Tsc1* deletion renders hepatic mTORC1 signaling constitutive and insulin independent.

Figure 3-3 continued

A) Schematic of the *Tsc1fl* allele and resulting null allele following Cre-mediated excision. The position of the three PCR primers used for genotyping are shown with arrows.

B) Representative PCR genotyping of liver tissue from the offspring of a cross between *Tsc1fl/fl* and *Albumin* (*Alb*)-*Cre Tsc1fl/+* mice using the primers shown in (A). Genomic DNA from MEFs of the given genotype was used as controls for the three *Tsc1* alleles. **(AIL)**

C) Immunoblots of liver, muscle, and fat tissue extracts from *ad libitum*-fed mice of the given genotypes are shown. **(JLY, HZ)**

D) Immunohistochemistry of phospho-S6 (S240/244) and staining with hematoxylin and eosin (H&E) were performed on adjacent liver sections from *ad libitum*-fed, 6 month-old mice of the given genotypes. **(SM, HZ)**

E) 8 week-old *Tsc1fl/fl* and *LTsc1KO* mice were fasted overnight (-) and then re-fed for 6 h (+), where indicated (N=3 mice per condition). Immunoblots of liver extracts from these mice are shown. **(JLY)**

F) Primary hepatocytes from *Tsc1fl/fl* and *LTsc1KO* mice were serum-starved overnight and stimulated for 6 h with insulin (Ins; 10 nM) in the presence or absence of a 30-min pretreatment with rapamycin (Rap; 20 nM). **(JLY)**

Genomic appearance of the null allele and liver-specific loss of TSC1 protein

were confirmed by PCR genotyping (Figure 3-3B) and immunoblotting (Figure 3-3C),

respectively, of liver extracts from littermates of different genotypes. Mice with

homozygous loss of *Tsc1* in their livers (*Alb-Cre Tsc1*$^{fl/fl}$; referred to as *LTsc1KO*) were

born at Mendelian ratios and exhibited no loss of viability out to 9 months of age. As

TSC1 stabilizes TSC2, *LTsc1KO* livers also exhibit a near complete loss of TSC2 protein

(Figure 3-3C). Importantly, only *LTsc1KO* livers exhibited increased phosphorylation of

S6 and 4EBP1, reflected by decreased electrophoretic mobility, which are common

readouts of mTORC1 signaling (Figures 3-3C,D). Hepatic mTORC1 signaling was

sustained even under fasting conditions in the *LTsc1KO* mice, and the level of activation

was comparable to control *Tsc1*$^{fl/fl}$ mice just after feeding (Figure 3-3E). Likewise,

primary hepatocytes isolated from *LTsc1KO* mice exhibited insulin-independent

activation of mTORC1 signaling (Figure 3-3F). Therefore, the *LTsc1KO* mice provide a

model of hepatic mTORC1 activation that occurs independent of the upstream insulin-

signaling pathway.

LTsc1KO mice are protected from age- and diet-induced hepatic steatosis.

To begin to understand the role of mTORC1 signaling in the control of hepatic

lipid metabolism, we examined the histological features of livers from cohorts of *Tsc1*$^{fl/fl}$

and *LTsc1KO* mice. Contrary to our expectations, *LTsc1KO* mice were protected from

age-induced hepatic steatosis at 9 months, exhibiting significantly lower levels of liver

triglycerides (TGs; Figure 3-4A-C). A relative decrease in lipid accumulation in *LTsc1KO*

livers was also evident in H&E-stained liver sections at 6 months (e.g., see Figure 3-3D).

Given the surprising decrease in lipid accumulation in the livers of *LTsc1KO* mice fed a

normal chow diet, we challenged the *LTsc1KO* mice with a lard-based high fat diet

(HFD) to further examine this phenotype. As on a chow diet (data not shown), there was
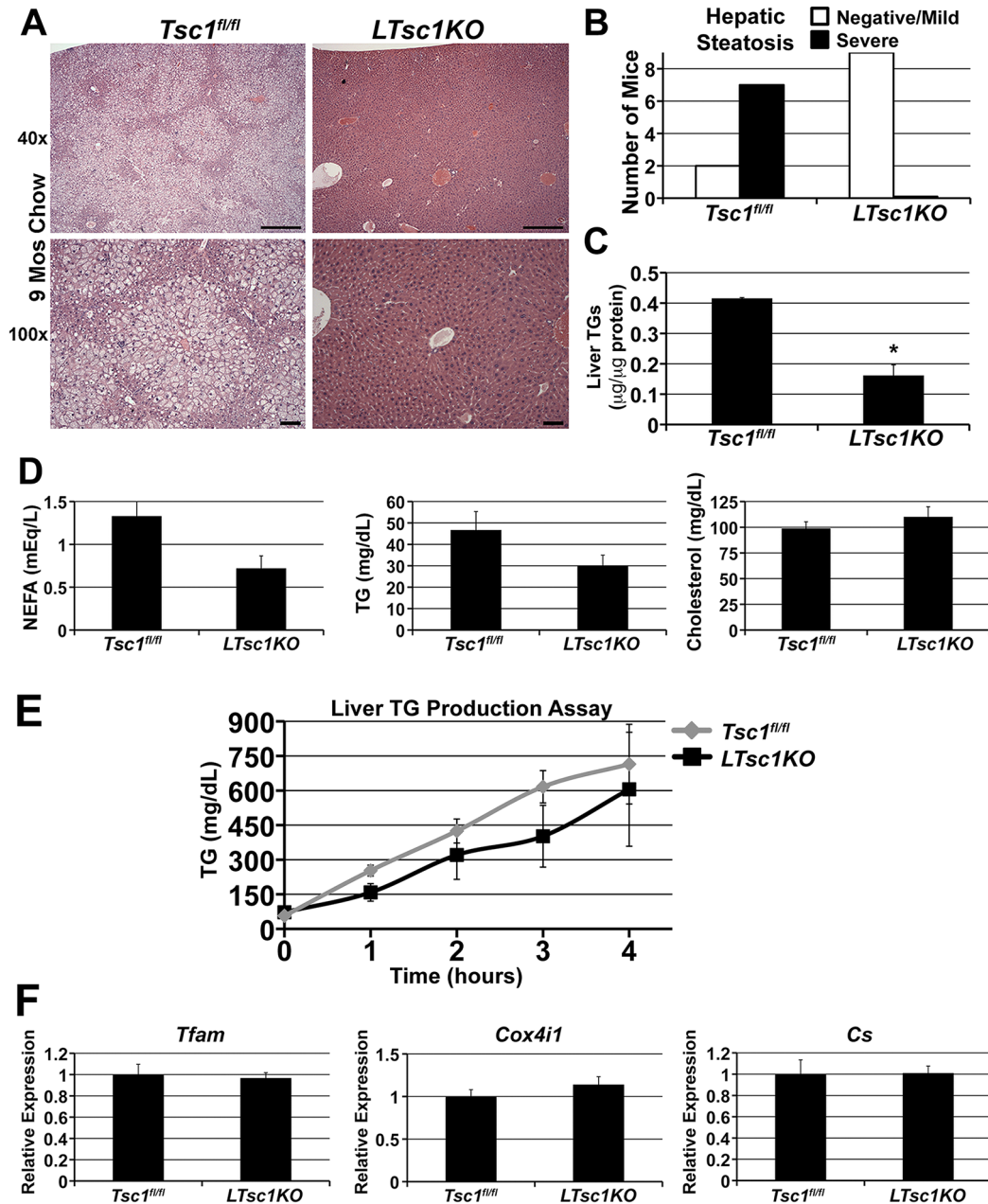
Figure 3-4. Further characterization of lipid metabolism in *LTsc1KO* mice.

A,B,C) *LTsc1KO* mice are protected from age-induced steatosis. Liver sections from 9 month-old *Tsc1^{fl/fl}* (n=9) and *LTsc1KO* (n=9) mice were stained with H&E. (A) Representative sections from these mice are shown with steatosis in *Tsc1^{fl/fl}* livers but not in *LTsc1KO* livers (scale bars: 500 μM (40X), 100 μM (100X). (B) The results from blinded scoring of the H&E-stained liver sections for steatosis are provided.

Figure 3-4 continued

(C) Liver triglycerides (TG) were measured in *ad libitum*-fed *Tsc1*$^{fl/fl}$ (n=2) and *LTsc1KO* (n=4) aged mice on chow diet, as in (A,B). TG levels are shown normalized to protein concentration and are presented as the mean ± SEM. *P<0.007 **(HZ)**

D) *LTsc1KO* mice have normal serum levels of triglyceride (TG), non-esterified fatty acid (NEFA), and cholesterol. Blood collected from *ad libitum*-fed *Tsc1*$^{fl/fl}$ (n=5) and *LTsc1KO* (n=5) mice after HFD was assayed for levels of TGs, NEFAs, and cholesterol. Data and are presented as the mean ± SEM. **(JLY)**

E) *LTsc1KO* mice do not have differences in hepatic triglyceride (TG) output. Hepatic TG production was measured in a cohort of chow-fed *Tsc1*$^{fl/fl}$ (n=5) and L*Tsc1*KO (n=5) mice following a 4 h fast and injection with Tyloxapol (2 g/kg bodyweight) to inhibit lipolysis. Serum TG levels were measured and are plotted over time as mean ± SEM. **(JLY)**

F) *LTsc1KO* livers do not display increased mitochondrial gene expression. RNA was isolated from livers of *ad libitum*-fed male *Tsc1*$^{fl/fl}$ (n=4) and *LTsc1KO* (n=4) mice after HFD and gene expression was measured by qRT-PCR. Data and are presented as the mean ± SEM relative to *Tsc1*$^{fl/fl}$. **(JLY)**

no significant difference in weight gain between the $Tsc1^{fl/fl}$ and *LTsc1KO* mice on the

HFD (Figure 3-5A). Dual-energy X-ray absorptiometry (DEXA) indicated that there was

no difference in percentage body fat after 16 weeks of HFD (Figure 3-5B). However, the

LTsc1KO mice exhibited protection from HFD-induced hepatic steatosis (Figure 3-5C).

Blinded scoring of liver sections by a pathologist indicated that all $Tsc1^{fl/fl}$ mice had

moderate to severe steatosis, while the majority of *LTsc1KO* mice exhibited negative to

mild lipid accumulation (Figure 3-5D). Consistent with these histological findings,

LTsc1KO livers had significantly reduced levels of TGs (Figure 3-5E). Therefore,

constitutive mTORC1 signaling in the *LTsc1KO* livers is accompanied by a decrease,

rather than the predicted increase, in hepatic lipid accumulation.

LTsc1KO mice have defects in hepatic induction of SREBP1c and lipogenesis.

To determine the mechanism of protection from hepatic steatosis in the *LTsc1KO*

mice, we examined candidate pathways involved in lipid mobilization and metabolism.

For instance, increased TG export could account for decreased accumulation in the liver.

However, serum levels of TGs, non-esterified fatty acids (NEFAs), and cholesterol were

not significantly different in mice fed a HFD, but TG and NEFA levels trended down in

*LTsc1*KO compared to $Tsc1^{fl/fl}$ mice (Figure 3-4D). Furthermore, *LTsc1KO* mice did not

display significant differences in hepatic TG output under fasting conditions, and again,

these levels trended lower relative to controls (Figure 3-4E). Consistent with the lack of

physiological evidence supporting a role for increased TG mobilization, transcript levels

of proteins involved in these processes, such as *Mttp*, *Dgat1*, and *Dgat2*, were not

significantly changed in *LTsc1KO* livers (Figure 3-5F). To address the possibility that

LTsc1KO livers burn more lipid than controls, we measured expression of genes

important for the β-oxidation of fatty acids. We found that transcript levels of *Pparα*,

Mcad, and *Cpt1a* were not increased in the *LTsc1KO* livers, and in fact, *Mcad*
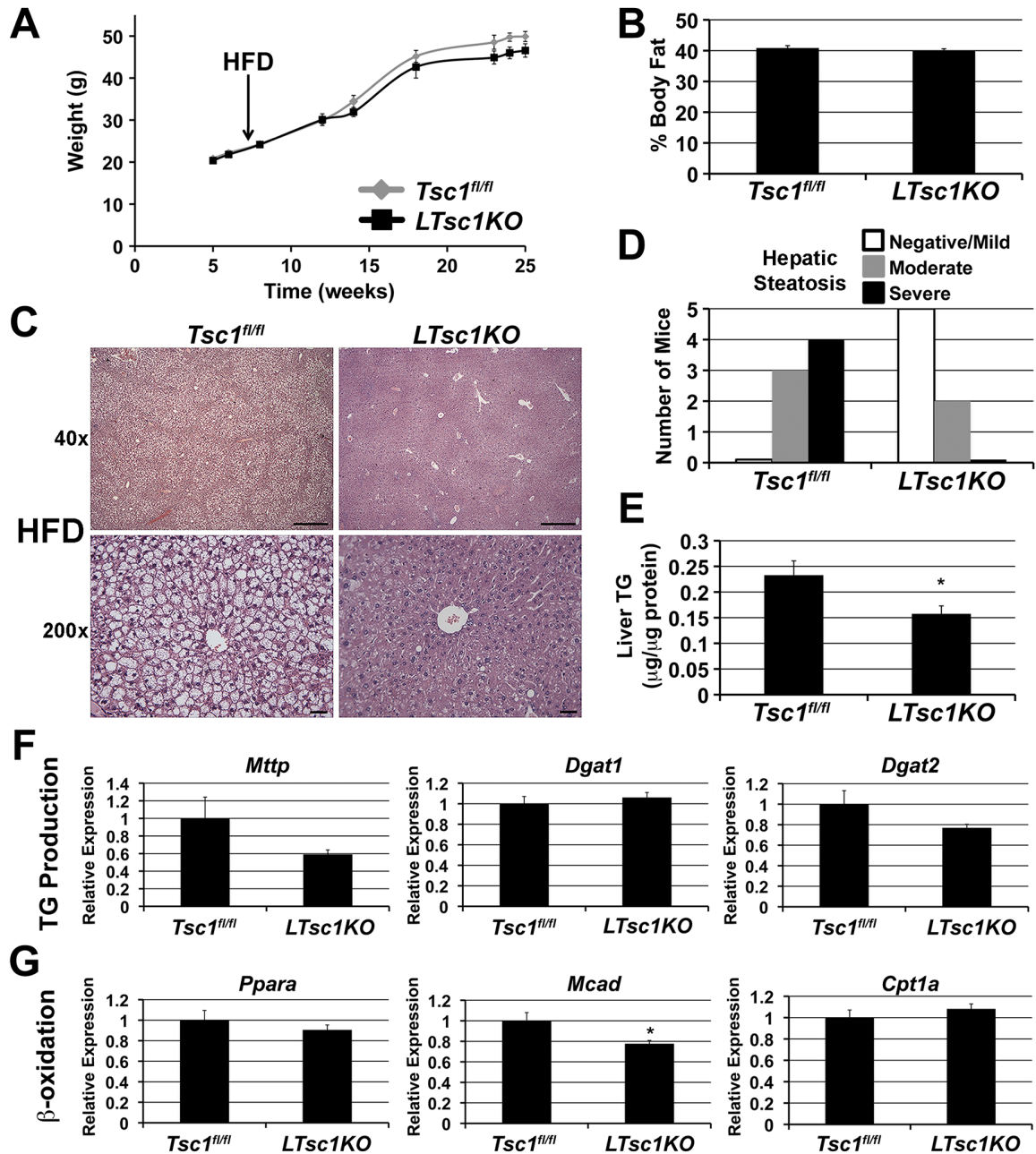
Figure 3-5. *LTsc1KO* mice are protected from diet-induced hepatic steatosis.

A) A cohort of male *Tsc1^{fl/fl}* (n=3) and *LTsc1KO* (n=4) mice were weighed between the ages of 5 and 25 weeks, while being fed a high-fat diet (HFD) for the final 16 weeks. **(HZ)**

B) HFD-fed male *Tsc1^{fl/fl}* (n=6) and *LTsc1KO* (n=6) mice were subjected to DEXA scanning. **(CG, HZ)**

Figure 3-5 continued

C,D) Liver sections from 6-month old $Tsc1^{fl/fl}$ (n=7) and $LTsc1KO$ (n=7) mice fed a HFD, as in (A), were stained with H&E. (C) Representative sections from these mice are shown (scale bars: 500 μM (40X), 50 μM (200X). D) The results from blinded scoring of the H&E-stained liver sections for negative/mild, moderate, or severe steatosis are provided. **(RB, HZ)**

E) Liver triglycerides (TG) were measured in *ad libitum*-fed $Tsc1^{fl/fl}$ (n=5) and $LTsc1KO$ (n=5) mice on a HFD, as in (A). TG levels are shown normalized to protein concentration and are presented as the mean ± SEM. *P<0.05 **(HZ)**

F,G) Expression of mRNA in the livers of *ad libitum*-fed $Tsc1^{fl/fl}$ (n=4) and $LTsc1KO$ (n=4) mice on a HFD, as in (A), was measured by qRT-PCR for the given genes, and levels are presented as mean ± SEM relative to $Tsc1^{fl/fl}$. *P<0.05 (*Mcad*). **(JLY)**

expression was significantly reduced in these livers relative to controls (Figure 3-5G).

This is consistent with recent findings that mTORC1 signaling decreases the expression

of β-oxidation genes in the liver [29]. As mitochondria are the major site of β-oxidation

and mTORC1 signaling has been proposed to promote mitochondrial biogenesis [30],

we also measured levels of mitochondrial markers. However, transcripts encoding the

major mitochondrial transcription factor TFAM and the mitochondrial enzymes COX-IV

and citrate synthase were not different (Figure 3-4F). Collectively, these results suggest

that neither an increase in hepatic lipid output nor consumption underlie the protection

from steatosis exhibited by the *LTsc1KO* mice.

Previous studies have demonstrated that mTORC1 signaling can drive

lipogenesis through activation of SREBP isoforms (Chapter 2; [10, 11]), and a similar

role in the liver is supported by our findings above (Figure 3-1). However, like *LTsc1KO*

mice, *Srebp1* knockout mice are protected from hepatic steatosis despite normal

increases in adiposity [31]. Therefore, we considered the possibility that *LTsc1KO* livers

might have a defect in SREBP1c induction that could account for their decreased TG

levels. Indeed, we found that the expression of *Srebp1c* and its lipogenic targets, *Fasn*

and *Scd1*, were significantly reduced in the livers of *LTsc1KO* mice (Figure 3-6A).

Consistent with a defect in SREBP1c activation, a more pronounced decrease in the

levels of processed, active SREBP1 relative to full-length, inactive SREBP1 was

detected in the *LTsc1KO* livers (Figure 3-6B). Reduced levels of FASN and SCD1

protein were also evident in these livers. The differences in lipogenic gene expression

were not restricted to the HFD-fed group, but were also detected in young mice (9

weeks) fed a normal chow diet (Figure 3-7A). Furthermore, young *LTsc1KO* mice

displayed defects in the hepatic induction of processed SREBP1 in response to feeding

(Figure 3-6C). The decreased ratio of processed to full length SREBP1 in the *LTsc1KO*

livers is also reflected in decreased induction of its lipogenic targets at the protein and
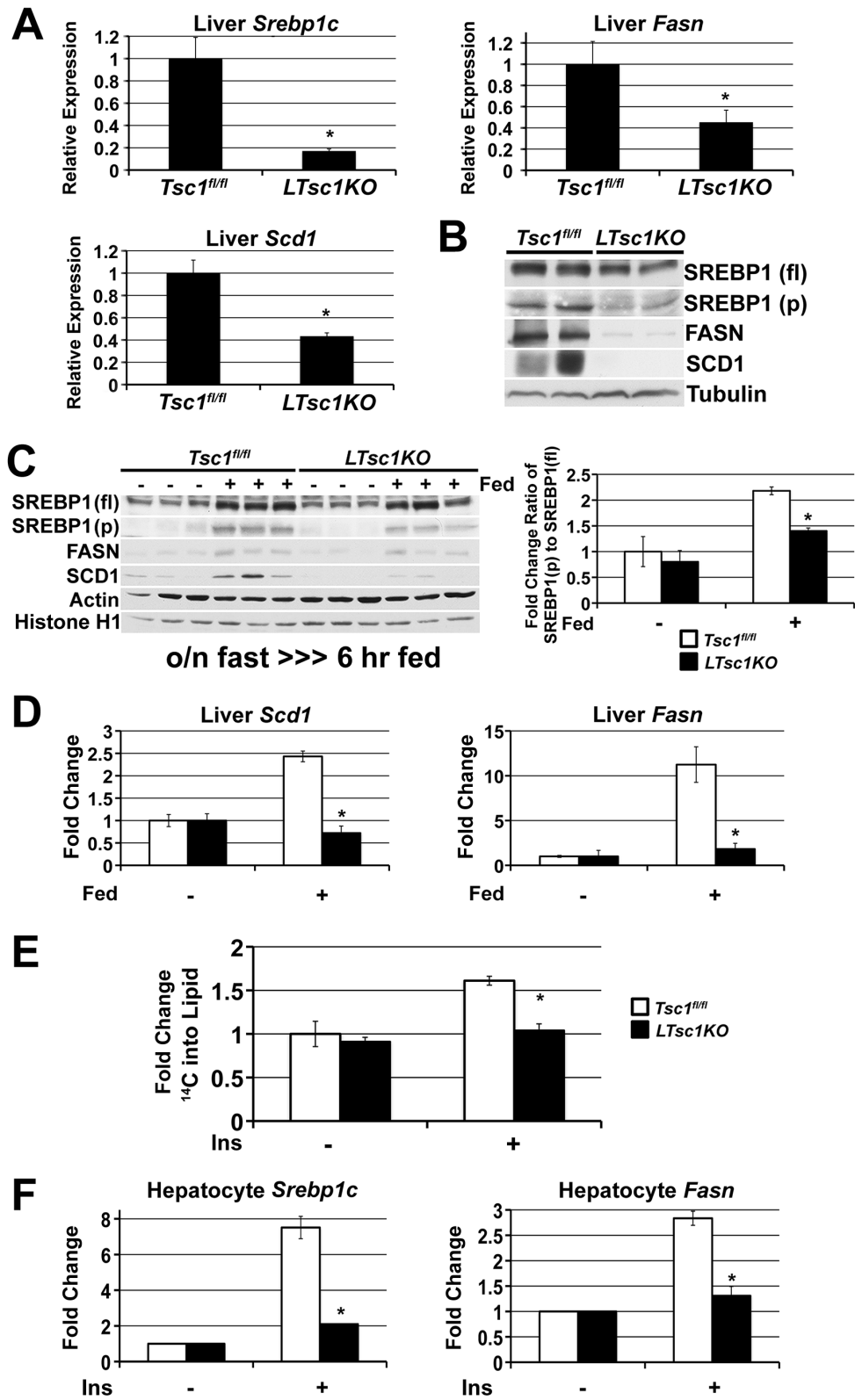
Figure 3-6. *LTsc1KO* **livers and hepatocytes have defects in the induction of**

SREBP1c expression and *de novo* **lipogenesis.**

Figure 3-6 continued

A) Expression of mRNA in the livers of male *ad libitum*-fed *Tsc1$^{fl/fl}$* (n=4) and *LTsc1KO* (n=4) mice on a HFD was measured by qRT-PCR for the given genes, and levels are presented as mean ± SEM relative to *Tsc1$^{fl/fl}$*. *P<0.005 (*Srebp1c*), P<0.05 (*Fasn*), and P<0.004 (*Scd1*). **(JLY)**

B) Immunoblots of full-length (fl) and processed (p) SREBP1, FASN, and SCD1 are shown in liver lysates from mice described in (A). **(JLY)**

(C, D) 8 week-old *Tsc1$^{fl/fl}$* and *LTsc1KO* mice were fasted overnight (-) with or without refeeding for 6 h (+), as indicated (N=4 per condition). (C) Liver lysates from *Tsc1$^{fl/fl}$* and *LTsc1KO* mice were immunoblotted for full length (fl) and processed (p) SREBP1 and its targets. The ratio of SREBP1(p) to SREBP1(fl) in the fasted and refed state was quantified for both genotypes and is presented as mean ± SEM relative to fasted wild-type samples. *P<0.01 for the fold induction by feeding compared to *Tsc1$^{fl/fl}$* livers. (D) RNA was isolated from the livers of these mice and gene expression was measured by qRT-PCR and is shown as mean ± SEM relative to fasted samples for each genotype. *P<0.0005 (*Scd1*) and P<0.003 (*Fasn*) for the fold induction by feeding compared to *Tsc1$^{fl/fl}$* livers. Note: There are no significant differences in fasted expression levels between *Tsc1$^{fl/fl}$* and *LTsc1KO* livers. **(JLY)**

E) Primary hepatocytes from *Tsc1$^{fl/fl}$* and *LTsc1KO* mice were serum starved overnight followed by insulin stimulation (Ins; 10 nM) for 6 h. Cells were labeled with ^{14}C-acetate for the final 4 h, and its incorporation into the lipid fraction was measured. Data are presented as mean ± SEM relative to unstimulated wild-type samples. *P<0.01 for the fold induction by insulin compared to *Tsc1$^{fl/fl}$* hepatocytes. **(JLY)**

F) Expression of mRNA from primary hepatocytes treated as described in (E) was analyzed by qRT-PCR for the given genes, and levels are presented as mean ± SEM

Figure 3-6 continued

relative to the unstimulated samples for each genotype. *P<0.013 (*Srebp1c*) and

P<0.023 (*Fasn*) for the fold induction by insulin compared to *Tsc1*$^{fl/fl}$ hepatocytes. Data in

(E) and (F) are representative of three independent experiments. **(JLY)**
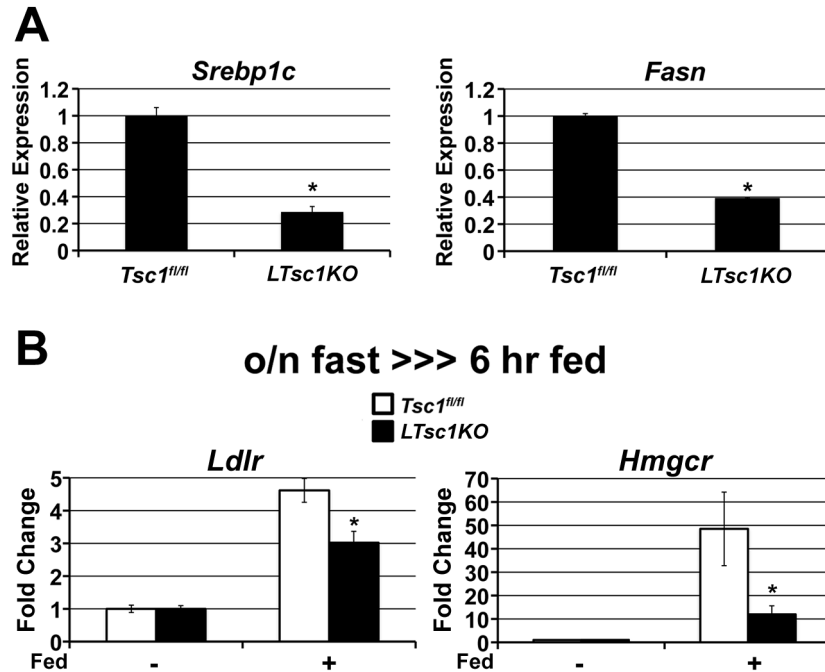
A

B

o/n fast >>> 6 hr fed

Figure 3-7. *LTsc1KO* **livers from young, chow-fed mice display decreased lipogenic gene expression and defects in the induction of SREBP2 targets by feeding. (JLY)**

A) Livers from fasted 8 week-old male *Tsc1*^{fl/fl} (n=4) and *LTsc1KO* (n=4) mice, fed a normal chow diet, were analyzed for mRNA expression by qRT-PCR. Data and are presented as the mean ± SEM relative to *Tsc1*^{fl/fl}. *P<0.004 (*Srebp1c*) and P<0.01 (*Fasn*) comparing *Tsc1*^{fl/fl} and *LTsc1KO*.

B) 8 week-old *Tsc1*^{fl/fl} (n=4) and *LTsc1KO* (n=4) mice were fasted overnight (-) with or without refeeding for 6 hours (+), as indicated. RNA was isolated from livers and gene expression was measured by qRT-PCR. Expression levels of transcripts are shown as mean ± SEM relative to fasted samples for each genotype. *P<0.026 (*Ldlr*) and *P<0.044 (*Hmgcr*) compared to the fold induction in *Tsc1*^{fl/fl} livers.

transcript levels (Figure 3-6C,D). *LTsc1KO* mice also exhibit defects in the feeding-induced expression of canonical SREBP2 target genes, including *Ldlr* and *Hmgcr* (Figure 3-7B; [6]). Importantly, a hepatocyte-intrinsic defect in the induction of *de novo* lipid synthesis is detected in primary hepatocytes from *LTsc1KO* livers (Figure 3-6E), and there was a corresponding defect in the insulin-stimulated expression of *Srebp1c* and its target *Fasn* (Figure 3-6F). Taken together with our previous findings, these data indicate that mTORC1 activation is required but not sufficient to induce SREBP1c and lipogenesis in hepatocytes and suggest that defects in the induction of SREBP1c might underlie the protection of *LTsc1KO* mice from hepatic steatosis.

Elevated hepatic mTORC1 signaling attenuates insulin signaling to Akt.

Decreases in hepatic lipid accumulation and steatosis accompanied by decreases in SREBP1c and *de novo* lipogenesis are phenotypes described for the liver-specific knockout of Akt2 [3]. It has been well established in cell culture models that mTORC1 activation stimulates negative feedback mechanisms that can dampen the response of cells to insulin, resulting in decreased Akt signaling (reviewed in [12, 21]). However, it is unknown whether mTORC1 activation in the liver can cause hepatic insulin resistance. Indeed, *LTsc1KO* mice display decreased phosphorylation of Akt and its downstream target FOXO1 in their livers (Figure 3-8A). In contrast, phosphorylation of GSK3α and β was not substantially different in *Tsc1$^{fl/fl}$* and *LTsc1KO* livers, consistent with the fact that additional protein kinases can phosphorylate these Akt substrates [32-35]. Atypical PKCs have also been implicated in the promotion of hepatic lipogenesis downstream of the insulin receptor [36, 37]. However, the activating phosphorylation of PKCζ/λ was increased, rather than decreased, in the *LTsc1KO* livers (Figure 3-9A), perhaps suggesting a compensatory mechanism. As the AMP-dependent protein kinase (AMPK) has recently been found to block the processing of SREBP isoforms [38], we
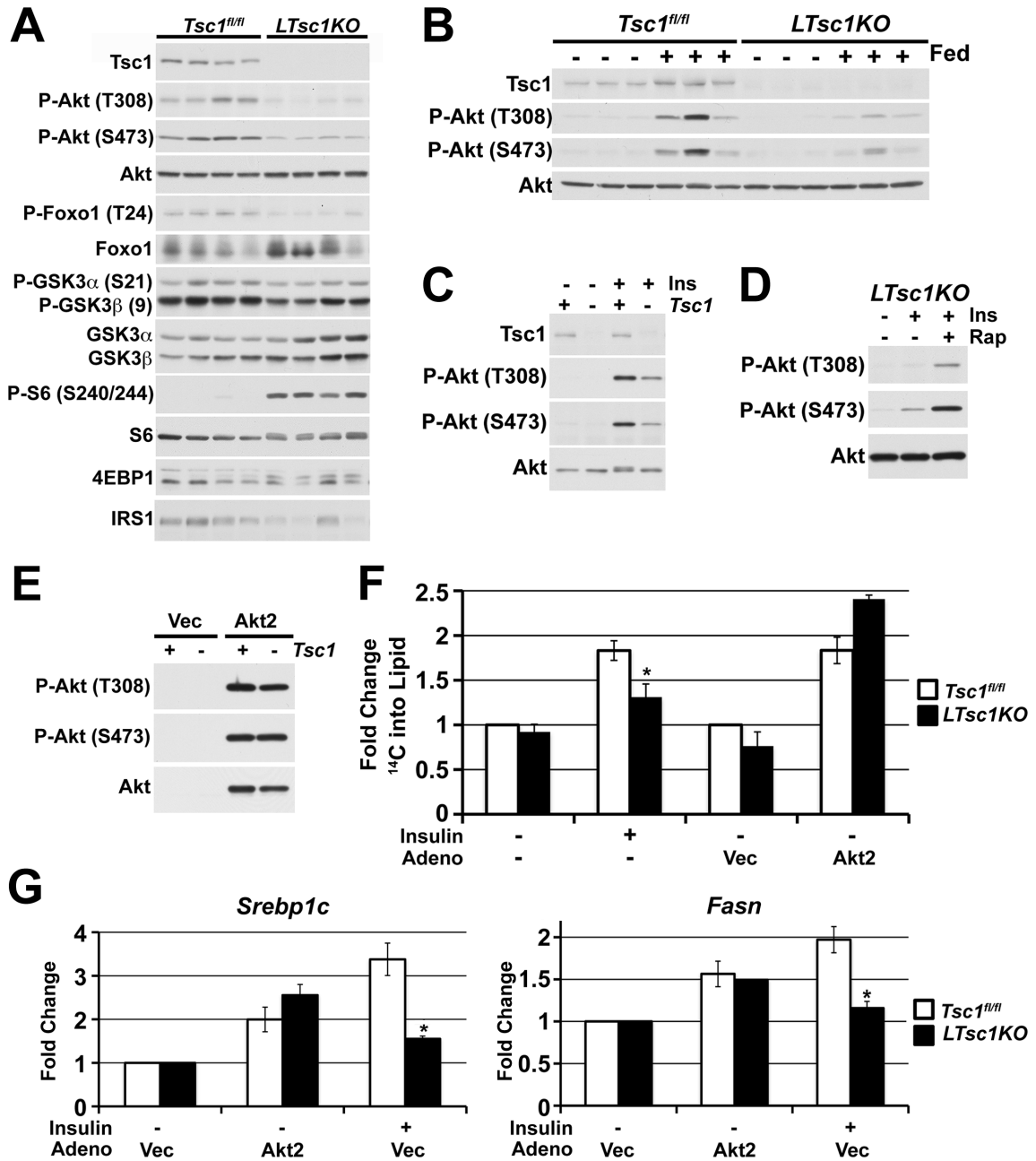
Figure 3-8. Attenuation of Akt signaling in *LTsc1KO* livers and hepatocytes is responsible for the defect in SREBP1c induction. (JLY)

A) Immunoblots of liver lysates from *ad libitum*-fed male *Tsc1^fl/fl* and *LTsc1KO* mice following a 16-week HFD are shown for the indicated phospho-(P) and total proteins.

(B) 8 week-old *Tsc1^fl/fl* and *LTsc1KO* mice were fasted overnight (-) with or without refeeding for 6 h (+), as indicated, prior to immunoblot analysis of liver lysates.

Figure 3-8 continued

C) Primary hepatocytes from $Tsc1^{fl/fl}$ (+) and $LTsc1KO$ (-) mice were serum starved overnight and then stimulated with insulin (Ins; 10 nM) for 1 h, where indicated.

D) Following overnight serum starvation, $LTsc1KO$ hepatocytes were treated with rapamycin (Rap; 20 nM) for 30 min, where indicated, prior to insulin stimulation (10 nM) for 6 h.

E) Primary hepatocytes from $Tsc1^{fl/fl}$ and $LTsc1KO$ mice were infected with adenovirus expressing either empty vector (Vec) or myr-Akt2 (Akt2), and 6 h post-infection, cells were serum starved overnight before lysis and immunoblotting.

F) Following overnight serum starvation, uninfected cells were stimulated with insulin (10 nM) for 6 h, whereas cells infected as in (E) were left unstimulated. Cells were labeled with ^{14}C-acetate for the final 4 h, and its incorporation into the lipid fraction was measured. Data are presented as mean $\pm$ SEM relative to unstimulated $Tsc1^{fl/fl}$ samples for the uninfected group or to the vector-expressing $Tsc1^{fl/fl}$ samples for the infected group for at least two independent experiments. *P<0.05 for the difference in fold induction by insulin compared to $Tsc1^{fl/fl}$ hepatocytes.

G) Primary hepatocytes were infected as described in (E), with vector-expressing cells being treated with insulin (10 nM) for 6 h, where indicated. Expression of mRNA was measured by qRT-PCR for the given genes, and levels are presented as mean $\pm$ SEM relative to the unstimulated vector-expressing group for each genotype. *P<0.027 ($Srebp1c$) and P<0.024 ($Fasn$) for the fold induction by insulin compared to $Tsc1^{fl/fl}$ hepatocytes.
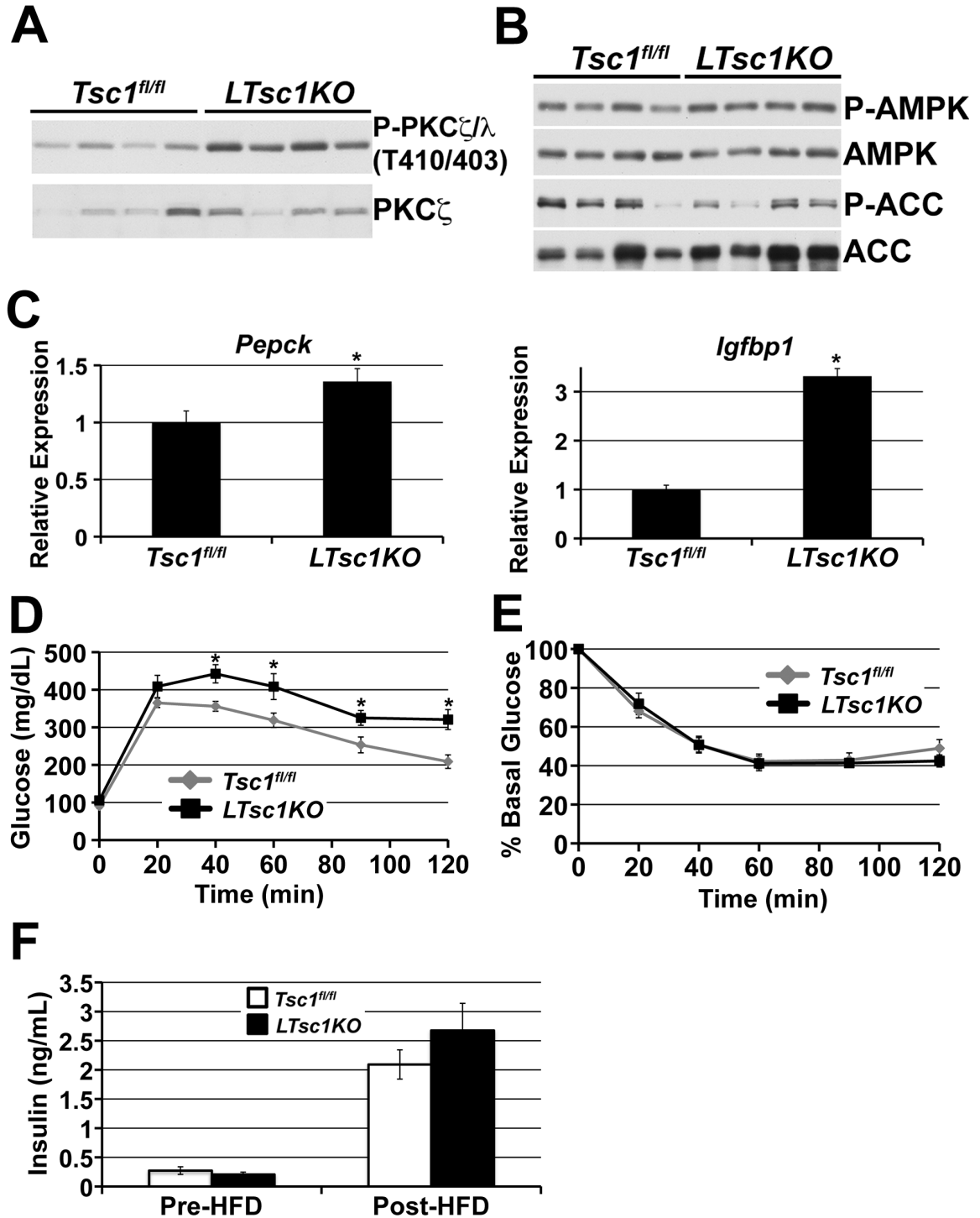
Figure 3-9. Further characterization of signaling and metabolic phenotypes of *LTsc1KO* mice.

Figure 3-9 continued

A) Atypical PKC phosphorylation is not attenuated in *LTsc1KO* livers. Liver lysates from

ad libitum-fed male *Tsc1$^{fl/fl}$* and *LTsc1KO* mice after a 16-week HFD were

immunoblotted for the indicated phospho- (P) and total proteins. **(JLY)**

B) *LTsc1KO* livers do not display increased activation of AMPK. Immunoblots of liver

lysates from *ad libitum*-fed male *Tsc1$^{fl/fl}$* and *LTsc1KO* mice following a 16-week HFD

are shown for the indicated phospho- (P) and total proteins. **(JLY)**

C) Expression of FOXO1 targets is elevated in *LTsc1KO* livers. Expression of mRNA in

the livers of *Tsc1$^{fl/fl}$* (n=4) and *LTsc1KO* (n=4) mice, described in (A), was measured by

qRT-PCR for the given genes, and levels are presented as mean ± SEM relative to

Tsc1$^{fl/fl}$. *P<0.032 (*Pepck*) and P<0.005 (*Igfbp1*) comparing *Tsc1$^{fl/fl}$* and *LTsc1KO* levels.

(JLY)

D,E) Relative to controls, *LTsc1KO* mice exhibit more severe glucose intolerance, but

the same insulin tolerance, on a HFD. Glucose (D) and insulin (E) tolerance tests were

performed at 25 and 26 weeks of age, respectively, following a 16-week HFD on the

same cohort of fasted *Tsc1$^{fl/fl}$* (n=12) and *LTsc1KO* (n=7) mice. (D) P<0.007 for area

under the curve analysis comparing *Tsc1$^{fl/fl}$* to *LTsc1KO*. *Significance for individual time

points: P<0.004 (40 min), P<0.024 (60 min), P<0.04 (90 min), and P<0.003 (120 min).

(HZ)

F) *LTsc1KO* mice do not exhibit differences in serum insulin levels on chow or high-fat

diet. Serum insulin was measured from overnight fasted *Tsc1$^{fl/fl}$* and *LTsc1KO* mice (n ≥

6 per genotype) before and after HFD. NOTE: There is no difference between genotypes

on either diet, but HFD increased serum insulin significantly in both genotypes P<2x10^{-5}

(*Tsc1$^{fl/fl}$*) and P<0.0003 (*LTsc1KO*). **(HZ)**

also examined AMPK activation but found no difference between the control and

LTsc1KO livers (Figure 3-9B). One feedback mechanism by which mTORC1 activation

is thought to inhibit insulin signaling is through the downregulation of IRS1 protein levels

(reviewed in [21]), and indeed, IRS1 levels were reduced in *LTsc1KO* livers (Figure 3-

8A). As would be expected from the defect in Akt-mediated phosphorylation of FOXO1,

LTsc1KO mice exhibit a significant increase in hepatic expression of the FOXO1 targets

Pepck and *Igfbp1* (Figure 3-9C) and a decrease in glucose tolerance (Figure S4D)

relative to controls. However, *LTsc1KO* mice do not display differences in insulin

tolerance (Figure 3-9E). Young *LTsc1KO* mice on a normal chow diet also exhibit

attenuation of Akt activation in response to feeding (Figure 3-8B). Finally, a cell-intrinsic

reduction in the ability of insulin to stimulate Akt was confirmed in primary hepatocytes

from *LTsc1KO* livers (Figure 3-8C), and this was rescued by pretreatment with

rapamycin (Figure 3-8D). The hepatocyte-intrinsic defect in insulin sensitivity in

LTsc1KO mice is further supported by the fact that there are no significant differences in

circulating insulin levels on either a normal chow or high fat diet (Figure 3-9F).

Therefore, uncontrolled mTORC1 activity in the liver causes defects in insulin signaling

to Akt.

**Restoration of Akt signaling to *LTsc1KO* hepatocytes rescues SREBP1c
induction.**

To determine whether the mTORC1-dependent attenuation of Akt signaling

underlies the defect in the ability of insulin to stimulate lipogenesis in *LTsc1KO*

hepatocytes, we employed a membrane-targeted constitutively active allele of Akt2 (myr-

Akt2), which bypasses negative-feedback mechanisms acting on upstream components

in the pathway. Unlike endogenous Akt (Figure 3-8C), adenovirally delivered myr-Akt2 is

phosphorylated to a similar extent in both *Tsc1*$^{fl/fl}$ and *LTsc1KO* hepatocytes (Figure 3-

8E). Interestingly, restoring Akt2 signaling to *LTsc1KO* hepatocytes ameliorated their

defect in lipogenesis. Unlike insulin, myr-Akt2 stimulated similar levels of *de novo* lipid

synthesis in both *Tsc1$^{fl/fl}$* and *LTsc1KO* hepatocytes (Figure 3-8F). As expected from this

rescue of lipogenesis, and in contrast to insulin, myr-Akt2 also induced expression of

Srebp1c and *Fasn* to a similar extent in *Tsc1$^{fl/fl}$* and *LTsc1KO* hepatocytes (Figure 3-8G).

These findings support a model in which Akt2 signaling is essential for the induction of

hepatic SREBP1c and lipogenesis and that, in addition to a requirement for mTORC1

activity, at least one additional parallel pathway downstream of Akt2 is essential for this

induction.

INSIG2a suppression is an mTORC1-independent mechanism regulating SREBP1c downstream of Akt.

      To gain insight into the mTORC1-independent mechanism of SREBP1c induction

downstream of Akt2, we examined the regulation of candidate pathways. Akt and other

kinases phosphorylate and inhibit GSK3α and β, which have been found to regulate the

stability of processed, active SREBP isoforms in cell culture models [39]. However,

unlike Akt and FOXO1, we did not observe substantial differences in the inhibitory

phosphorylation of GSK3 in the livers or hepatocytes of *LTsc1KO* mice (Figure 3-8A and

3-10A). Another potential candidate for SREBP1c regulation downstream of Akt is the

LXR family of nuclear receptors, which can transcriptionally activate *Srebp1c* in

response to insulin [40]. However, no significant differences in the expression of *Lxra* or

Lxrb or their canonical transcriptional target *Abca1* were detected in the *LTsc1KO* livers

(Figure 3-10B).

      Unlike hepatocytes, mTORC1 signaling is both necessary and sufficient to

activate SREBP isoforms in other cell types (Chapter 2; [10, 11]). Therefore, we decided

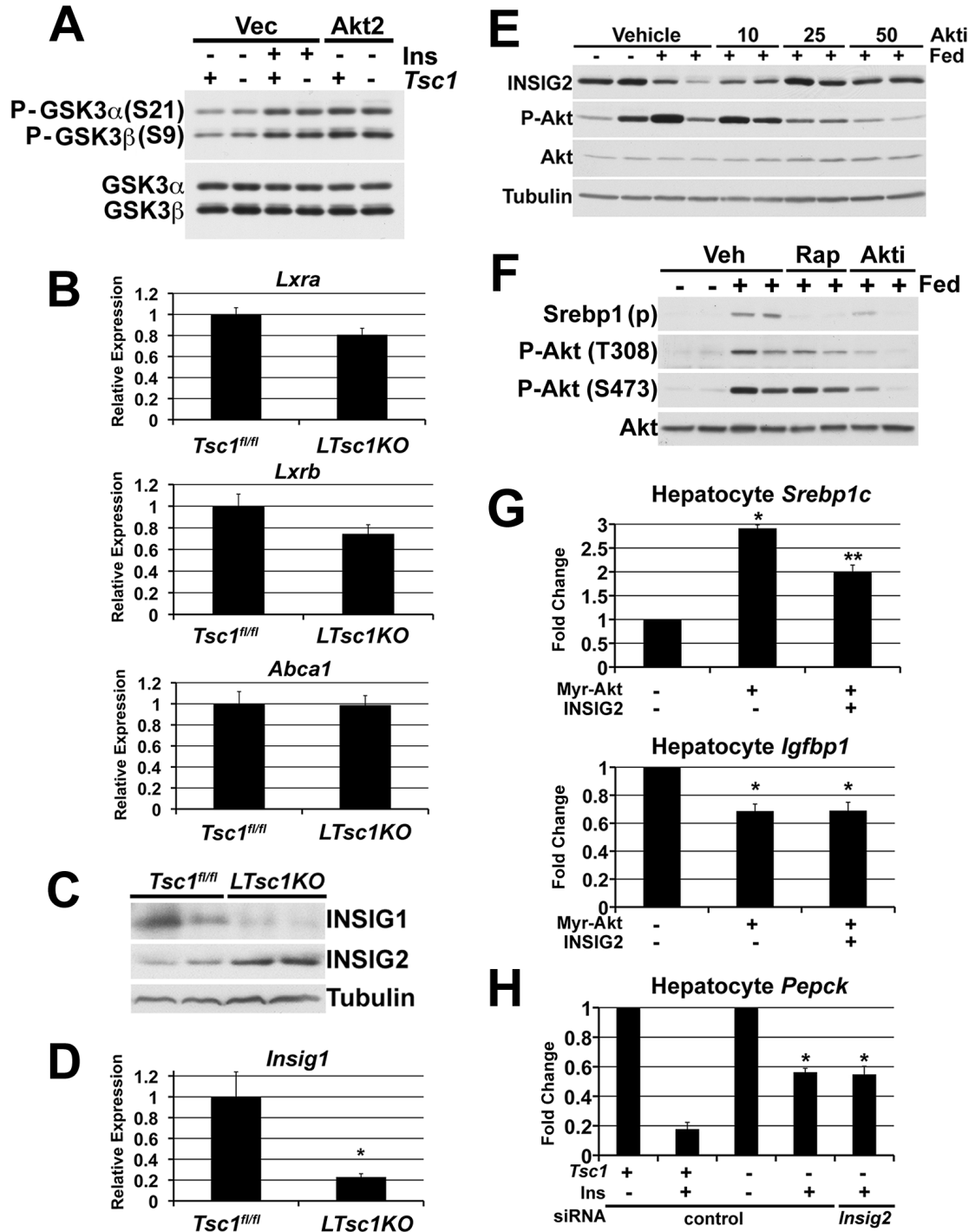to investigate a mechanism of SREBP1c regulation that is believed to be specific to the

Figure 3-10. Additional analysis of the mechanism underlying the defects in SREBP1c induction downstream of Akt in *LTsc1*KO hepatocytes and livers. (JLY)

A) *LTsc1KO* hepatocytes do not have defects in insulin-stimulated GSK3 phosphorylation. Primary hepatocytes from *Tsc1fl/fl* (+) and L*Tsc1*KO (-) mice were

Figure 3-10 continued

infected with adenovirus expressing either empty vector (Vec) or myr-Akt2 (Akt2). After 6

hours of infection, cells were serum starved overnight, then stimulated with insulin (Ins;

10nM) for 1 hour, where indicated, prior to immunoblot analyses.

B) *LTsc1KO* livers express normal levels of *Lxra, Lxrb*, and *Abca1*. RNA was isolated

from livers of *ad libitum*-fed *Tsc1^{fl/fl}* (n=4) and L*Tsc1*KO (n=4) mice after HFD and gene

expression was measured by qRT-PCR. Data are presented as mean ± SEM relative to

Tsc1^{fl/fl} mice.

C) Protein levels of INSIG1 and INSIG2 are respectively decreased and increased in

LTsc1KO livers. Liver lysates of mice described in (B) were immunoblotted for the

indicated proteins.

D) *LTsc1KO* livers express reduced levels of *Insig1.* Expression of RNA from livers of

mice described in (B) was analyzed by qRT-PCR. Data are presented as mean ± SEM

relative to *Tsc1^{fl/fl}* mice. *P <0.02.

E) Suppression of INSIG2 protein by refeeding is blocked by inhibition of Akt in a dose-

dependent manner. 8 week-old mice were fasted overnight (-) and then refed for 6 hours

(+) with or without 30 min pre-treatment with vehicle or three different doses of Aktviii

(Akti; 10, 25 and 50mg/kg), where indicated. Liver lysates were immunoblotted for the

indicated phospho- (P) and total proteins.

F) Akt inhibition blocks refeeding induced activation of SREBP1 processing. 8 week-old

mice were fasted overnight (-) and then refed for 6 hours (+) with or without 30 min pre-

treatment with rapamycin (Rap; 10mg/kg) or Aktviii (Akti; 50mg/kg), where indicated.

Liver lysates were immunoblotted for processed (p) SREBP1 and phospho- (P) and total

Akt.

G) INSIG2 overexpression blocks *Srebp1c* induction by Myr-Akt. Wild-type hepatocytes

were transiently transfected with Myr-Akt and either vector or INSIG2. 24 h post-

Figure 3-10 continued

transfection, cells were serum starved over night, followed by RNA isolation. Expression

was measured by qRT-PCR. Data are presented as mean of technical duplicates ± SEM

relative to vector. *P<0.002 (*Srebp1c*) and P<0.03 *(Igbfp1)* for Myr-Akt compared to

vector and P<0.04 (*Igfbp1*) for Myr-Akt and INSIG2 co-expression compared to vector;

**P<0.03 (*Srebp1c*) for Myr-Akt co-expressed with INSIG2 compared to vector.

H) Inhibition of *Insig2a* does not rescue the defect in insulin-stimulated suppression of

Pepck in *LTsc1KO* hepatocytes. *Tsc1*^fl/fl^ and *LTsc1KO* primary hepatocytes were

transiently transfected with control and *Insig2* siRNA, as indicated. 24 h post-

transfection, cells were serum starved overnight followed by a 6 h stimulation with insulin

(Ins; 10nM) and RNA isolation. *Pepck* expression was measured by qRT-PCR and the

mean ± SEM is graphed as fold-suppression by insulin relative to unstimulated for each

genotype. *P<0.02 and P<0.04 for fold-change between insulin stimulation of *Tsc1*^fl/fl^ and

LTsc1KO hepatocytes with control and *Insig2* siRNA, respectively.

liver. Insulin signaling has been found to suppress a liver-specific transcript encoding the

SREBP-inhibitory protein INSIG2, called *Insig2a* [23-25]. As INSIG proteins can block

the induction of hepatic SREBP1c and lipogenesis [41-43], the suppression of *Insig2a* is

likely to contribute to the activation of SREBP1c in response to insulin [23] . Interestingly,

we found that *LTsc1KO* livers express elevated levels of *Insig2a* transcripts and INSIG2

protein (Figure 3-11A and 3-10C). This is in contrast to *Insig1*, which is a known

transcriptional target of SREBP and, like other targets, is reduced in the *LTsc1KO* livers

(Figure 3-10C,D). Consistent with the insulin-stimulated suppression of *Insig2a*

functioning in a parallel pathway to mTORC1, we found that rapamycin does not effect

Insig2a suppression in intact livers or isolated hepatocytes from wild-type mice (Figure

3-11B,C). However, an Akt-specific inhibitor (Aktviii) completely reversed the

suppression of *Insig2a* in response to feeding or insulin, indicating that this mechanism

occurs downstream of Akt. The feeding-induced suppression of INSIG2 protein levels

was blocked in a dose-dependent manner by the Akt inhibitor (Figure 3-10E). In contrast

to the differential effects on *Insig2a* expression, the Akt inhibitor and rapamycin have

similar inhibitory effects on the induction of SREBP1c processing and expression (Figure

3-10F and 3-11B,C). Consistent with the elevated expression of *Insig2a* in *LTsc1KO*

livers (Figure 3-11A), *LTsc1KO* hepatocytes are defective in the suppression of *Insig2a*

in response to insulin (Figure 3-11D). Importantly, the restoration of Akt signaling to

LTsc1KO hepatocytes completely rescues the suppression of *Insig2a* (Figure 3-11D).

Consistent with Akt-mediated downregulation of *Insig2a* being required for proper

Srebp1c induction, forced expression of *Insig2* significantly decreased the ability of

activated Akt to stimulate *Srebp1c*, while having no effect on its suppression of the

FOXO1 target *Igfbp1* (Figure 3-10G). Finally, siRNA-mediated suppression of *Insig2a* in

LTsc1KO hepatocytes restores the insulin-stimulated induction of *Srebp1c* (Figure 3-

11E), while maintaining the defect in insulin-mediated suppression of *Pepck* (Figure 3-
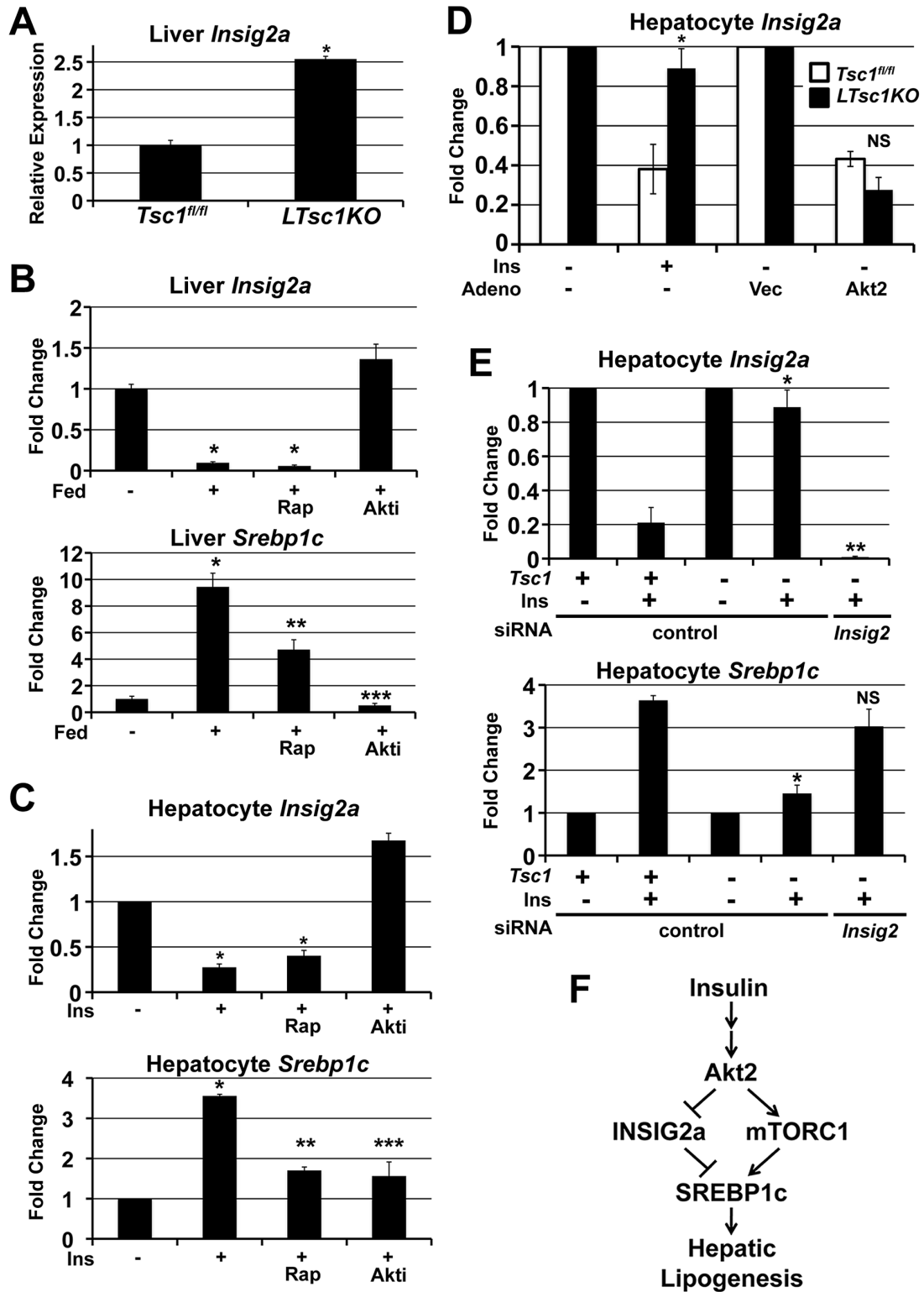
Figure 3-11. The mTORC1-independent pathway to SREBP1c involves Akt-mediated suppression of *Insig2a*. (JLY)

Figure 3-11 continued

A) Expression of *Insig2a* in the livers of *ad libitum*-fed male *Tsc1^{fl/fl}^* (n=4) and *LTsc1KO* (n=4) mice on a HFD was measured by qRT-PCR and levels are presented as mean ± SEM relative to *Tsc1^{fl/fl}^*. *P<0.0002.

B) 8 week-old mice were fasted overnight (-) and then refed for 6 h (+) following a 30-min pre-treatment with vehicle, rapamycin (Rap; 10mg/kg) or Aktviii (Akti; 50mg/kg) (N=4 per condition). Hepatic RNA was isolated and gene expression was measured by qRT-PCR. Data are shown as mean ± SEM relative to fasted controls. *P<3x10^{-6} (*Insig2a*) and P<0.0002 (*Srebp1c*) compared to fasted; **P<0.01 and ***P<0.0008 compared to vehicle-treated fed mice. Note: There is no significant difference between the fold suppression of *Insig2a* by refeeding in the presence or absence of rapamycin or between *Insig2a* levels in fasted mice versus those fed in the presence of Aktviii.

C) *Tsc1^{fl/fl}^* primary hepatocytes were serum starved overnight and pretreated for 30 min with vehicle, rapamycin (20 nM), or Aktviii (10 μM) prior to 6 h stimulation with insulin (Ins; 10 nM), gene expression was measured by qRT-PCR. Data are presented as the mean ± SEM relative to unstimulated cells and are representative of two-independent experiments. *Insig2a*: *P<0.003 for insulin-stimulated suppression and P<0.01 for insulin-stimulated suppression in the presence of rapamycin. Note: There is no significant difference between the fold suppression of *Insig2a* by insulin in the presence or absence of rapamycin. *Srebp1c:* *P<0.0003 compared to unstimulated; **P<0.003 and ***P< 0.03 compared to vehicle-treated, insulin-stimulated samples.

D) Primary hepatocytes from *Tsc1^{fl/fl}^* and *LTsc1KO* mice were left uninfected or were infected with adenovirus expressing either empty vector (Vec) or myr-Akt2 (Akt2), and 6 h post-infection, cells were serum starved overnight. Uninfected cells were stimulated with insulin (10 nM) for 6 h, whereas infected cells were left unstimulated. *Insig2a*

Figure 3-11 continued

expression was measured by qRT-PCR. Data are presented as mean ± SEM relative to

the unstimulated samples for the uninfected group or the vector-expressing samples for

the infected group for each genotype and are representative of at least two independent

experiments. *P<0.05 compared to the fold suppression by insulin in *Tsc1$^{fl/fl}$* cells. The

fold suppression of *Insig2a* induced by Myr-Akt2 in *Tsc1$^{fl/fl}$* and *LTsc1KO* hepatocytes is

not significantly different (NS).

E) *Tsc1$^{fl/fl}$* (*Tsc1* +) and *LTsc1KO* (*Tsc1* -) primary hepatocytes were transiently

transfected with control or *Insig2* siRNA. 24-h post-transfection, cells were serum

starved overnight followed by a 6 h stimulation with insulin (10nM). Gene expression

was measured by qRT-PCR and levels are presented as mean ± SEM relative to

unstimulated controls for each genotype. *P<0.04 (*Insig2a*) and *P<0.01 (*Srebp1c*)

compared to the fold-change in response to insulin in *Tsc1$^{fl/fl}$* hepatocytes treated with

control siRNAs. The insulin-stimulated induction of *Srebp1c* in control siRNA-treated

Tsc1$^{fl/fl}$ and *Insig2* siRNA-treated *LTsc1KO* hepatocytes is not significantly different (NS).

F) Model of two parallel pathways downstream of insulin and Akt2 required for the

induction of hepatic SREBP1c and lipogenesis.

10H). Collectively, these data are consistent with two parallel pathways downstream of Akt2, one involving the suppression of *Insig2a* expression and the other requiring mTORC1 activation, both being essential for insulin-stimulated induction of hepatic SREBP1c (Figure 3-11F).

DISCUSSION

Recent genetic evidence suggests that Akt is a major effector of insulin signaling for the induction of hepatic lipogenesis [3, 7, 8]. Whole-body and liver-specific knockouts of Akt2 are protected from hepatic steatosis under conditions of obesity caused by leptin deficiency (*ob/ob*) or a lard-based HFD [3]. This phenotype is similar to that described for *Srebp1* knockout mice, which are also protected from steatosis in the background of obesity [31]. Importantly, the protection from hepatic lipid accumulation in the Akt2 knockout models is accompanied by reduced expression of *Srebp1c* and decreased *de novo* lipogenesis, suggesting that a defect in SREBP1c induction underlies this phenotype. However, on a coconut oil-based HFD with sucrose (Surwit), the liver-specific Akt2 knockout mice do not exhibit defects in the expression of *Srebp1c* or its lipogenic targets but maintain their reduced levels of hepatic TGs. This suggests that SREBP1c-independent pathways downstream of Akt might also contribute to hepatic lipid content. Interestingly, mice with liver-specific deletion of *Pten*, which exhibit constitutive activation of Akt signaling, develop severe hepatic steatosis on a normal chow diet [44, 45], and this phenotype is dependent on Akt2 and its regulation of lipogenic gene expression downstream of SREBP1c [45]. Likewise, hepatic expression of constitutively active Akt also induces SREBP1c and causes fatty liver disease and hypertriglyceridemia [8], much like transgenic overexpression of SREBP1c itself [46]. While studies have indicated that atypical PKCs might play a parallel role [36, 37], these collective findings demonstrate that Akt is a major insulin-responsive effector in the

induction of hepatic SREBP1c. While this regulation appears to contribute to both physiological and pathological hepatic lipid accumulation, the critical mechanisms downstream of Akt are not well defined.

Together with a recent study in rats [13], our current findings indicate that mTORC1 is an essential downstream target of insulin and Akt signaling for the proper induction of SREBP1c and lipogenesis in the liver. However, the *LTsc1KO* mouse model demonstrates that mTORC1 activation alone is not sufficient to induce SREBP1c. We were particularly surprised to find that chronic mTORC1 signaling, instead, leads to a decrease in the induction of SREBP1c and lipogenesis and protection from both age- and diet-induced hepatic steatosis. The decreased activation of SREBP1c in *LTsc1KO* hepatocytes is the result of mTORC1-driven inhibitory feedback mechanisms causing insulin resistance and attenuation of Akt signaling to its other downstream pathways. Due to the disconnect between Akt and mTORC1 signaling in these mice, the *LTsc1KO* model affords a unique experimental system in which to identify mTORC1-independent pathways and processes downstream of Akt in the liver. Analyses of the *LTsc1KO* mice revealed that Akt stimulates hepatic SREBP1c and lipogenesis through parallel mTORC1-dependent and independent pathways and that the latter pathway involves suppression of a liver-specific inhibitor of SREBP1c.

Although functionally similar, distinct mechanisms regulate the expression and stability of INSIG1 and INSIG2 [14, 15]. SREBP induces the expression of *Insig1*, and the INSIG1 protein is stabilized under sterol-rich conditions, creating an autoinhibitory feedback mechanism [47-49]. In contrast to INSIG1, the *Insig2* gene is not transcriptionally regulated by SREBP, and the INSIG2 protein is much more stable and unaffected by sterols. Importantly, the predominant liver-specific transcript encoding INSIG2, referred to as *Insig2a*, is strongly downregulated at the message level by insulin signaling [23], perhaps facilitating SREBP1c release from the ER and its subsequent

processing and activation. In this study, we find that Akt is responsible for *Insig2a* suppression by insulin and that this occurs independent of mTORC1 signaling. While the pathway by which Akt suppresses *Insig2a* is currently unknown, our data indicate that this is a major mTORC1-independent pathway downstream of Akt in the liver regulating SREBP1c activation. We hypothesize that the failure to suppress *Insig2a* in *LTsc1KO* hepatocytes blocks the pathway to SREBP1c activation at a step prior to that dependent on mTORC1 signaling. Therefore, insulin induces SREBP1c processing and activation through Akt-mediated suppression of *Insig2a* and stimulation of mTORC1 signaling, which both regulate essential but distinct steps in the pathway to full activation of SREBP1c. Future mechanistic studies are needed to define both the signaling pathway by which Akt suppresses *Insig2a* expression and the molecular target of mTORC1 signaling involved in promoting SREBP1c activation.

MATERIALS AND METHODS

Primary hepatocyte cultures.

Primary hepatocytes were isolated from 7 to 9 week-old male mice following portal vein collagenase perfusion (Blenzyme 3; Roche) and percoll gradient purification. For insulin stimulation experiments, hepatocyte cultures were treated as described elsewhere [13]. Infection with adenovirus (Vector Biolabs) was performed 2 h after plating at an moi of 10. After 6 h infection, cells were washed once with PBS before serum starving overnight prior to insulin stimulation. Non-targeting control and *Insig2* siRNAs (ON-TARGETplus, Dharmacon) were transiently transfected into primary hepatocytes 6 h after plating using Lipofectamine 2000 (Invitrogen). 24 h post-transfection, cells were serum starved overnight prior to insulin stimulation.

Measurement of *de novo* lipogenesis.

For the measurement of lipogenesis, primary hepatocytes were cultured and treated as described above. For the final 4 h of a 6-h insulin stimulation, cells were labeled with 1-^{14}C acetic acid (Perkin Elmer). Cells were washed twice with PBS before lysis in 0.5% Triton X-100. The lipid fraction was extracted by the addition of chloroform and methanol (2:1 v/v) with vortexing, followed by the addition of water with vortexing. Samples were centrifuged (1000 rpm, 15 min), and ^{14}C incorporation was measured in the bottom, lipid-containing phase using a Beckman LS6500 scintillation counter. Each condition was assayed in duplicate and normalized to protein concentrations in the original lysates.

Gene expression analysis.

For gene expression analyses, RNA was isolated from mouse tissue using TRIzol (Invitrogen) and from primary hepatocytes using the RNeasy Mini Kit (Qiagen) and was reverse transcribed into cDNA using the Superscript III First Strand Synthesis System for RT-PCR kit (Invitrogen). SYBR green-based quantitative RT-PCR was performed using an Applied Biosystems 7300 Real Time PCR System. Duplicate or triplicate samples were collected for each experimental condition, and triplicate runs of each sample were normalized to Rplp0 (m36b4) mRNA to determine relative expression levels. The sequences for the primer pairs used in this study are listed in Table 3-1.

Immunoblotting and immunohistochemistry.

Lysates from cultured primary hepatocytes were prepared as previously described [50]. Tissue lysates were prepared from tissue that was frozen in liquid nitrogen immediately following resection. Frozen tissue samples were homogenized in NP-40 lysis buffer, and remaining debris was cleared from lysates by subsequent 10 and

Table 3-1 – RT-PCR and PCR primers used in this study.

RT-PCR:	Forward (5'-3')	Reverse (5'-3')
Abca1	GGCAGTGTCCAACATCTGAAAA	CAGGGTTGGAGCCTGCTATTC
Dgat1	CATGCGTGATTATTGCATCC	ACAGGTTGACATCCCGGTAG
Dgat2	GCGCTACTTCCGAGACTACTT	GGGCCTTATGCCAGGAAACT
Cox4i1	TGAATGGAAGACAGTTGTGGG	GATCGAAAGTATGAGGGATGGG
Cpt1a	GGAGAGAATTTCATCCACTTCCA	CTTCCCAAAGCGGTGTGAGT
Cs	GGGACTTGTGTATGAGACTTCG	AGCCAAAATAAGCCCTCAGG
Fasn	AAGGCTGGGCTCTATGGATT	GGAGTGAGGCTGGGTTGATA
Hmgcr	TGTTCACCGGCAACAACAAGA	CCGCGTTATCGTCAGGATGA
Igfbp1	GGAGCCTGTGTACCAGAACC	CCTTTGCCTCTTCATGCTG
Insig1	CACGACCACGTCTGGAACTAT	TGAGAAGAGCACTAGGCTCCG
Insig2a	CCCTCAATGAATGTACTGAAGGATT	TGTGAAGTGAAGCAGACCAATGT
Ldlr	TGACTCAGACGAACAAGGCTG	ATCTAGGCAATCTCGGTCTCC
Lxra	GCCCTGCACGCCTACGT	TAGCATCCGTGGGAACATCA
Lxrb	GCTGATGATCCAGCAGTTAG	CGGAGAAAGATCGTTTGTTG
Mcad	TTTCGAAGACGTCAGAGTGC	TGCGACTGTAGGTCTGGTTC
Mttp	CGTCCACATACAGCCTTGAC	CCACCTGACTACCATGAAGC
Pepck	CCACAGCTGCTGCAGAACA	GAAGGGTCGCATGGCAAA
Ppara	TGTTTGTGGCTGCTATAATTTGC	GCAACTTCTCAATGTAGCCTATGTTT
Scd1	CTGACCTGAAAGCCGAGAAG	GCGTTGAGCACCAGAGTGTA
Srebp1c	GGAGCCATGGATTGCACATT	GCTTCCAGAGAGGAGGCCAG
Tfam	CACCCAGATGCAAAACTTTCAG	CTGCTCTTTATACTTGCTCACAG

Genotyping:

Tsc1	AGGAGGCCTCTTCTGCTACC (1)	CAGCTCCGACCATGAAGTG (2)
		TGGGTCCTGACCTATCTCCTA (3)
Cre	GCGGTCTGGCAGTAAAAACTATC	GTGAAACAGCATTGCTGTCACTT

30 minute spins at 16,000 x g. All primary antibodies were obtained from Cell Signaling Technology, except those to tubulin and actin (Sigma) and histone H1, SREBP1, INSIG1, and INSIG2 (Santa Cruz). For immunohistochemistry, paraffin-embedded sections were stained with phospho-S6 (S240/244) using a tissue staining kit (R&D Biosystems).

Mouse studies.

Mice harboring the *Tsc1*[fl] allele on an FVB background were described previously [27]. For the current study, these mice were crossed onto a C57Bl/6J background through 7 backcrosses. *Alb-Cre* transgenic mice on this same background were described previously [28]. Study cohorts were generated by crossing *Tsc1*^{fl/fl} mice with *Alb-Cre Tsc1*^{fl/+} mice. PCR genotyping for *Tsc1* and *Cre* was performed as described [27]. Mice were fed either a normal chow diet (9% kcal from fat) or a HFD (60% kcal from fat; F3282, Bio-serv). For fasting-refeeding studies, mice were fasted overnight and either euthanized or refed normal chow for 6 h. Vehicle (5% Tween-80, 5% PEG-400 in 1X PBS), rapamycin (10mg/kg), or Aktviii (50mg/kg; EMD) were administered via i.p. injection 30 min prior to refeeding. Histological preparation and analyses was performed in the Dana-Farber/Harvard Cancer Center Rodent Histopathology Core by Dr. R.T. Bronson, an expert rodent pathologist. Liver TGs were measured by enzymatic assay using a kit and were normalized to protein content. Body fat percentage was measured by dual-energy X-ray absorptiometry (DEXA; PIXImus).

Metabolic studies.

For the glucose (GTT) and insulin (ITT) tolerance tests, animals were injected with 1 g glucose/kg body weight after an overnight fast (GTT) or 1.5 units of insulin/kg (ITT) after a 5 h fast, followed by blood glucose measurements from a tail nick using the

OneTouch (Lifescan, Milpitas, CA) glucometer system at the indicated time points. All mouse studies were approved by the Harvard Medical Area Standing Committee on Animals.

Triglyceride production.

Blood was collected via tail bleeding at baseline before injection with Tyloxapol (2 g/kg in PBS; Sigma) followed by subsequent tail nick bleeding every hour for 4 h. Serum triglyceride levels were measured using a colorimetric assay (Infinity Triglycerides, Thermo).

Measurement of serum parameters.

Serum levels of non-esterified fatty acids and total cholesterol were measured using kits (Wako Chemicals and ThermoDMA). Serum insulin levels were measured by ELISA (Linco).

Statistical analyses.

Statistical significance was measured using a Student's two-tailed t-test and a statistical cutoff of $P<0.05$. Data are presented as mean ± SEM. Immunoblot quantification was performed using ImageJ software.

ACKNOWLEDGEMENTS

REFERENCES

1.   Cho, H., Mu, J., Kim, J.K., Thorvaldsen, J.L., Chu, Q., Crenshaw, E.B., 3rd, Kaestner, K.H., Bartolomei, M.S., Shulman, G.I., and Birnbaum, M.J. (2001). Insulin resistance and a diabetes mellitus-like syndrome in mice lacking the protein kinase Akt2 (PKB beta). Science *292*, 1728-1731.

2.   Garofalo, R.S., Orena, S.J., Rafidi, K., Torchia, A.J., Stock, J.L., Hildebrandt, A.L., Coskran, T., Black, S.C., Brees, D.J., Wicks, J.R.*, et al.* (2003). Severe diabetes, age-dependent loss of adipose tissue, and mild growth deficiency in mice lacking Akt2/PKB beta. J Clin Invest *112*, 197-208.

3.   Leavens, K.F., Easton, R.M., Shulman, G.I., Previs, S.F., and Birnbaum, M.J. (2009). Akt2 is required for hepatic lipid accumulation in models of insulin resistance. Cell Metab *10*, 405-418.

4.   Gross, D.N., Wan, M., and Birnbaum, M.J. (2009). The role of FOXO in the regulation of metabolism. Curr Diab Rep *9*, 208-214.

5.   Krycer, J.R., Sharpe, L.J., Luu, W., and Brown, A.J. (2010). The Akt-SREBP nexus: cell signaling meets lipid metabolism. Trends Endocrinol Metab *21*, 268-276.

6.   Horton, J.D., Goldstein, J.L., and Brown, M.S. (2002). SREBPs: activators of the complete program of cholesterol and fatty acid synthesis in the liver. J Clin Invest *109*, 1125-1131.

7.   Fleischmann, M., and Iynedjian, P.B. (2000). Regulation of sterol regulatory-element binding protein 1 gene expression in liver: role of insulin and protein kinase B/cAkt. Biochem J *349*, 13-17.

8.   Ono, H., Shimano, H., Katagiri, H., Yahagi, N., Sakoda, H., Onishi, Y., Anai, M., Ogihara, T., Fujishiro, M., Viana, A.Y.*, et al.* (2003). Hepatic Akt activation induces marked hypoglycemia, hepatomegaly, and hypertriglyceridemia with sterol regulatory element binding protein involvement. Diabetes *52*, 2905-2913.

9.   Brown, M.S., and Goldstein, J.L. (2008). Selective versus total insulin resistance: a pathogenic paradox. Cell Metab *7*, 95-96.

10.   Porstmann, T., Santos, C.R., Griffiths, B., Cully, M., Wu, M., Leevers, S., Griffiths, J.R., Chung, Y.L., and Schulze, A. (2008). SREBP activity is regulated

by mTORC1 and contributes to Akt-dependent cell growth. Cell Metab *8*, 224-236.

11.   Duvel, K., Yecies, J.L., Menon, S., Raman, P., Lipovsky, A.I., Souza, A.L., Triantafellow, E., Ma, Q., Gorski, R., Cleaver, S.*, et al.* (2010). Activation of a metabolic gene regulatory network downstream of mTOR complex 1. Mol Cell *39*, 171-183.

12.   Huang, J., and Manning, B.D. (2009). A complex interplay between Akt, TSC2 and the two mTOR complexes. Biochem Soc Trans *37*, 217-222.

13.   Li, S., Brown, M.S., and Goldstein, J.L. (2010). Bifurcation of insulin signaling pathway in rat liver: mTORC1 required for stimulation of lipogenesis, but not inhibition of gluconeogenesis. Proc Natl Acad Sci U S A *107*, 3441-3446.

14.   Goldstein, J.L., DeBose-Boyd, R.A., and Brown, M.S. (2006). Protein sensors for membrane sterols. Cell *124*, 35-46.

15.   Raghow, R., Yellaturu, C., Deng, X., Park, E.A., and Elam, M.B. (2008). SREBPs: the crossroads of physiological and pathological lipid homeostasis. Trends Endocrinol Metab *19*, 65-73.

16.   Howell, J.J., and Manning, B.D. (2011). mTOR couples cellular nutrient sensing to organismal metabolic homeostasis. Trends Endocrinol Metab *22*, 94-102.

17.   Khamzina, L., Veilleux, A., Bergeron, S., and Marette, A. (2005). Increased activation of the mammalian target of rapamycin pathway in liver and skeletal muscle of obese rats: possible involvement in obesity-linked insulin resistance. Endocrinology *146*, 1473-1481.

18.   Mordier, S., and Iynedjian, P.B. (2007). Activation of mammalian target of rapamycin complex 1 and insulin resistance induced by palmitate in hepatocytes. Biochem Biophys Res Commun *362*, 206-211.

19.   Koketsu, Y., Sakoda, H., Fujishiro, M., Kushiyama, A., Fukushima, Y., Ono, H., Anai, M., Kikuchi, T., Fukuda, T., Kamata, H.*, et al.* (2008). Hepatic overexpression of a dominant negative form of raptor enhances Akt phosphorylation and restores insulin sensitivity in K/KAy mice. Am J Physiol Endocrinol Metab *294*, E719-725.

20.   Dibble, C.C., Asara, J.M., and Manning, B.D. (2009). Characterization of Rictor phosphorylation sites reveals direct regulation of mTOR complex 2 by S6K1. Mol Cell Biol *29*, 5657-5670.

21.   Harrington, L.S., Findlay, G.M., and Lamb, R.F. (2005). Restraining PI3K: mTOR signalling goes back to the membrane. Trends Biochem Sci *30*, 35-42.

22.	Um, S.H., Frigerio, F., Watanabe, M., Picard, F., Joaquin, M., Sticker, M., Fumagalli, S., Allegrini, P.R., Kozma, S.C., Auwerx, J., *et al.* (2004). Absence of S6K1 protects against age- and diet-induced obesity while enhancing insulin sensitivity. Nature *431*, 200-205.

23.	Yabe, D., Komuro, R., Liang, G., Goldstein, J.L., and Brown, M.S. (2003). Liver-specific mRNA for Insig-2 down-regulated by insulin: implications for fatty acid synthesis. Proc Natl Acad Sci U S A *100*, 3155-3160.

24.	Yellaturu, C.R., Deng, X., Cagen, L.M., Wilcox, H.G., Park, E.A., Raghow, R., and Elam, M.B. (2005). Posttranslational processing of SREBP-1 in rat hepatocytes is regulated by insulin and cAMP. Biochem Biophys Res Commun *332*, 174-180.

25.	Yellaturu, C.R., Deng, X., Park, E.A., Raghow, R., and Elam, M.B. (2009). Insulin enhances the biogenesis of nuclear sterol regulatory element-binding protein (SREBP)-1c by posttranscriptional down-regulation of Insig-2A and its dissociation from SREBP cleavage-activating protein (SCAP).SREBP-1c complex. J Biol Chem *284*, 31726-31734.

26.	Horton, J.D., Bashmakov, Y., Shimomura, I., and Shimano, H. (1998). Regulation of sterol regulatory element binding proteins in livers of fasted and refed mice. Proc Natl Acad Sci U S A *95*, 5987-5992.

27.	Kwiatkowski, D.J., Zhang, H., Bandura, J.L., Heiberger, K.M., Glogauer, M., el-Hashemite, N., and Onda, H. (2002). A mouse model of TSC1 reveals sex-dependent lethality from liver hemangiomas, and up-regulation of p70S6 kinase activity in TSC1 null cells. Hum Mol Genet *11*, 525-534.

28.	Postic, C., and Magnuson, M.A. (2000). DNA excision in liver by an albumin-Cre transgene occurs progressively with age. Genesis *26*, 149-150.

29.	Sengupta, S., Peterson, T.R., Laplante, M., Oh, S., and Sabatini, D.M. (2010). mTORC1 controls fasting-induced ketogenesis and its modulation by ageing. Nature *468*, 1100-1104.

30.	Cunningham, J.T., Rodgers, J.T., Arlow, D.H., Vazquez, F., Mootha, V.K., and Puigserver, P. (2007). mTOR controls mitochondrial oxidative function through a YY1-PGC-1alpha transcriptional complex. Nature *450*, 736-740.

31.	Yahagi, N., Shimano, H., Hasty, A.H., Matsuzaka, T., Ide, T., Yoshikawa, T., Amemiya-Kudo, M., Tomita, S., Okazaki, H., Tamura, Y., *et al.* (2002). Absence of sterol regulatory element-binding protein-1 (SREBP-1) ameliorates fatty livers but not obesity or insulin resistance in Lep(ob)/Lep(ob) mice. J Biol Chem *277*, 19353-19357.

32. Cross, D.A., Alessi, D.R., Cohen, P., Andjelkovich, M., and Hemmings, B.A. (1995). Inhibition of glycogen synthase kinase-3 by insulin mediated by protein kinase B. Nature *378*, 785-789.

33. Eldar-Finkelman, H., Seger, R., Vandenheede, J.R., and Krebs, E.G. (1995). Inactivation of glycogen synthase kinase-3 by epidermal growth factor is mediated by mitogen-activated protein kinase/p90 ribosomal protein S6 kinase signaling pathway in NIH/3T3 cells. J Biol Chem *270*, 987-990.

34. Fang, X., Yu, S., Tanyi, J.L., Lu, Y., Woodgett, J.R., and Mills, G.B. (2002). Convergence of multiple signaling cascades at glycogen synthase kinase 3: Edg receptor-mediated phosphorylation and inactivation by lysophosphatidic acid through a protein kinase C-dependent intracellular pathway. Mol Cell Biol *22*, 2099-2110.

35. Zhang, H.H., Lipovsky, A.I., Dibble, C.C., Sahin, M., and Manning, B.D. (2006). S6K1 regulates GSK3 under conditions of mTOR-dependent feedback inhibition of Akt. Mol Cell *24*, 185-197.

36. Matsumoto, M., Ogawa, W., Akimoto, K., Inoue, H., Miyake, K., Furukawa, K., Hayashi, Y., Iguchi, H., Matsuki, Y., Hiramatsu, R.*, et al.* (2003). PKClambda in liver mediates insulin-induced SREBP-1c expression and determines both hepatic lipid content and overall insulin sensitivity. J Clin Invest *112*, 935-944.

37. Taniguchi, C.M., Kondo, T., Sajan, M., Luo, J., Bronson, R., Asano, T., Farese, R., Cantley, L.C., and Kahn, C.R. (2006). Divergent regulation of hepatic glucose and lipid metabolism by phosphoinositide 3-kinase via Akt and PKClambda/zeta. Cell Metab *3*, 343-353.

38. Li, Y., Xu, S., Mihaylova, M.M., Zheng, B., Hou, X., Jiang, B., Park, O., Luo, Z., Lefai, E., Shyy, J.Y.*, et al.* (2011). AMPK Phosphorylates and Inhibits SREBP Activity to Attenuate Hepatic Steatosis and Atherosclerosis in Diet-Induced Insulin-Resistant Mice. Cell Metab *13*, 376-388.

39. Sundqvist, A., Bengoechea-Alonso, M.T., Ye, X., Lukiyanchuk, V., Jin, J., Harper, J.W., and Ericsson, J. (2005). Control of lipid metabolism by phosphorylation-dependent degradation of the SREBP family of transcription factors by SCF-FBW7. Cell Metabolism *1*, 379-391.

40. Hegarty, B.D., Bobard, A., Hainault, I., Ferre, P., Bossard, P., and Foufelle, F. (2005). Distinct roles of insulin and liver X receptor in the induction and cleavage of sterol regulatory element-binding protein-1c. Proc Natl Acad Sci U S A *102*, 791-796.

41. Engelking, L.J., Kuriyama, H., Hammer, R.E., Horton, J.D., Brown, M.S., Goldstein, J.L., and Liang, G. (2004). Overexpression of Insig-1 in the livers of transgenic mice inhibits SREBP processing and reduces insulin-stimulated lipogenesis. J Clin Invest *113*, 1168-1175.

42.   Takaishi, K., Duplomb, L., Wang, M.Y., Li, J., and Unger, R.H. (2004). Hepatic insig-1 or -2 overexpression reduces lipogenesis in obese Zucker diabetic fatty rats and in fasted/refed normal rats. Proc Natl Acad Sci U S A *101*, 7106-7111.

43.   Engelking, L.J., Liang, G., Hammer, R.E., Takaishi, K., Kuriyama, H., Evers, B.M., Li, W.P., Horton, J.D., Goldstein, J.L., and Brown, M.S. (2005). Schoenheimer effect explained--feedback regulation of cholesterol synthesis in mice mediated by Insig proteins. J Clin Invest *115*, 2489-2498.

44.   Stiles, B., Wang, Y., Stahl, A., Bassilian, S., Lee, W.P., Kim, Y.J., Sherwin, R., Devaskar, S., Lesche, R., Magnuson, M.A.*, et al.* (2004). Liver-specific deletion of negative regulator Pten results in fatty liver and insulin hypersensitivity [corrected]. Proc Natl Acad Sci U S A *101*, 2082-2087.

45.   He, L., Hou, X., Kanel, G., Zeng, N., Galicia, V., Wang, Y., Yang, J., Wu, H., Birnbaum, M.J., and Stiles, B.L. (2010). The critical role of AKT2 in hepatic steatosis induced by PTEN loss. Am J Pathol *176*, 2302-2308.

46.   Shimano, H., Horton, J.D., Shimomura, I., Hammer, R.E., Brown, M.S., and Goldstein, J.L. (1997). Isoform 1c of sterol regulatory element binding protein is less active than isoform 1a in livers of transgenic mice and in cultured cells. J Clin Invest *99*, 846-854.

47.   Yang, T., Espenshade, P.J., Wright, M.E., Yabe, D., Gong, Y., Aebersold, R., Goldstein, J.L., and Brown, M.S. (2002). Crucial step in cholesterol homeostasis: sterols promote binding of SCAP to INSIG-1, a membrane protein that facilitates retention of SREBPs in ER. Cell *110*, 489-500.

48.   Horton, J.D., Shah, N.A., Warrington, J.A., Anderson, N.N., Park, S.W., Brown, M.S., and Goldstein, J.L. (2003). Combined analysis of oligonucleotide microarray data from transgenic and knockout mice identifies direct SREBP target genes. Proc Natl Acad Sci U S A *100*, 12027-12032.

49.   Gong, Y., Lee, J.N., Lee, P.C., Goldstein, J.L., Brown, M.S., and Ye, J. (2006). Sterol-regulated ubiquitination and degradation of Insig-1 creates a convergent mechanism for feedback control of cholesterol synthesis and uptake. Cell Metab *3*, 15-24.

50.   Manning, B.D., Tee, A.R., Logsdon, M.N., Blenis, J., and Cantley, L.C. (2002). Identification of the tuberous sclerosis complex-2 tumor suppressor gene product tuberin as a target of the phosphoinositide 3-kinase/Akt pathway. Mol Cell *10*, 151-162.

CHAPTER 4

Discussions and Future Directions

Adapted from:

[1]Department of Genetics and Complex Diseases, Harvard School of Public Health, Boston, MA 02115

[2]Genetics Division, Department of Medicine, Brigham and Women's Hospital, Boston, MA 02115

[3]Harvard Medical School, Boston, MA, 02115

[4]Ludwig Center at Dana-Farber/Harvard Cancer Center, Boston, MA 02115

[5]Department of Medical Oncology, Dana-Farber Cancer Institute, Boston, MA 02115

[6]Ben May Institute for Cancer Research, The University of Chicago, Chicago, IL 60637

[7]Department of Pathology, Harvard Medical School, Boston, MA 02115

[8]Division of Matrix Biology, Beth Israel Deaconess Medical Center, Boston, MA 02115

[9]Infinity Pharmaceuticals, 780 Memorial Drive, Cambridge, MA 02139

JLY performed all experiments.

SREBP as a key effector of mTORC1 signaling

The data from our studies and other recent studies have demonstrated that the SREBPs are major downstream effectors of mTORC1 (Chapters 2 and 3; [1, 2, 3]). SREBPs play an important role in both the physiological and pathological regulation of lipid metabolism. Because aberrant lipid and cholesterol production can be detrimental to cells and tissues, activation of SREBP is a complex, highly regulated process. SREBPs are synthesized as inactive precursors that reside in the endoplasmic reticulum (ER). Signals that indicate the need to produce lipids and sterols, such as insulin or decreased intracellular levels of cholesterol, induce SREBP to traffic to the Golgi where it is proteolytically processed, releasing the active transcription factor form, which then translocates to the nucleus to turn on target genes [4]. Previous studies suggest that SREBP activation is controlled by growth factors through the PI3K-Akt pathway [5, 6]. Akt has been proposed to regulate SREBP, in part, by promoting the stability of its processed form through inhibition of glycogen synthase kinase 3 (GSK3), which has been shown to phosphorylate the processed active form of SREBP1 and target it for proteasomal degradation [7]. However, consistent with our findings, Akt has also been demonstrated to activate SREBP in a manner dependent on mTORC1 [1]. We and others have also found that the physiological induction of SREBP1c by insulin in hepatocytes is sensitive to rapamycin (Chapter 3; [3, 8]). We find that mTORC1 signaling also increases the transcript levels of both *Srebp1* and *Srebp2* [2]. However, SREBP1 is known to strongly induce its own transcription [9], and this is further demonstrated in our study (Chapter 2; [2]). Importantly, a specific increase in the levels of processed active SREBP1 is detected in cells lacking the TSC1-TSC2 complex, and this increase is sensitive to rapamycin [2]. The mTORC1-stimulated increase in processed SREBP1 occurs independent of GSK3 or effects on SREBP1 protein stability. Knockdown experiments demonstrated that S6K1 is required downstream of mTORC1

for accumulation of processed SREBP1 and expression of its target genes in this setting. In hepatocytes, the small molecule inhibitor PF-4708671, which is an S6K1-specific inhibitor [10], blocks the insulin-stimulated activation of *Srebp1c* expression (Figure 4-1). A role for S6K1 in the activation of SREBP is consistent with genetic studies in *Drosophila*, where the orthologs of both S6K1 and SREBP have been found to be critical for the ability of TORC1 to promote an increase in cell and organ size [1, 11].

While the mechanism is currently unknown, our data are consistent with S6K1 regulating a step in the complex processing of the SREBPs. A previous study has suggested that a pathway downstream of PI3K and Akt stimulates the trafficking of full-length SREBP2 to the golgi, where it is processed and activated [12]. It has also been reported that ER stress can promote SREBP trafficking and activation in an adaptive mechanism to expand the ER [13-15]. However, despite elevated basal levels of ER stress in cells and tumors lacking the TSC1-TSC2 complex due to uncontrolled mTORC1 signaling [16], this mechanism does not appear to contribute to the activation of SREBP, as knockdown of S6K1 blocks SREBP1 activation without relieving ER stress in these cells (J.L.Y. and B.D.M, unpublished). We hypothesize that S6K1 plays a more direct role, phosphorylating and regulating one of the many proteins involved in ER retention, trafficking, or proteolytic processing of SREBP. However, at this stage, additional S6K-independent mechanisms regulating SREBP activation downstream of mTORC1 cannot be ruled out. For example, a recent study demonstrated that mTORC1, through direct phosphorylation, regulates the localization of a phosphatidic acid phosphatase called lipin to modulate SREBP promoter activity and nuclear protein accumulation [17]. Future studies will undoubtedly reveal potential additional molecular mechanism(s). Ultimately, the existence of several mTORC1-dependent mechanisms of SREBP regulation further illustrates the importance of this target as a major transcriptional effector of mTORC1 signaling.
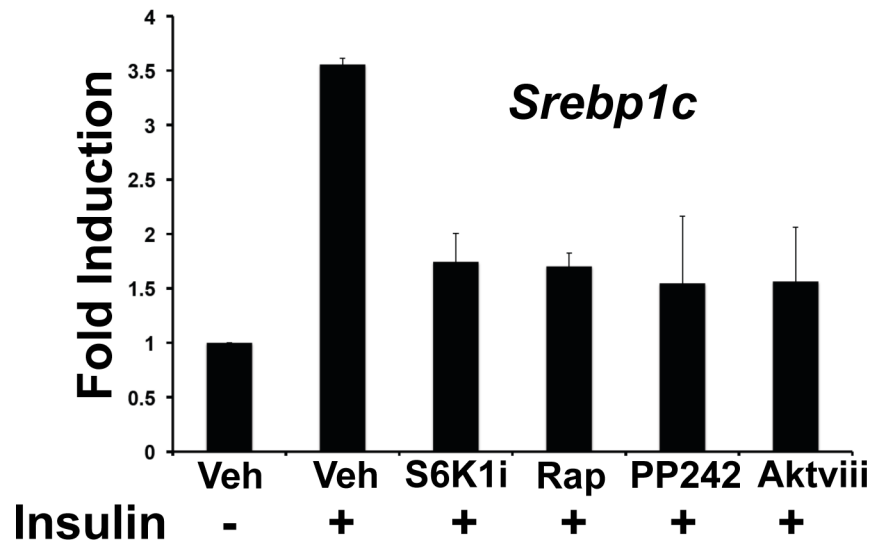
Figure 4-1. S6K1 is required for induction of hepatic *Srebp1c* expression by insulin. Primary hepatocytes were serum starved overnight, pretreated for 30 min with vehicle, PF-4708671 (S6K1i; 20 μM), rapamycin (Rap; 20 nM), PP242 (2.5 μM), or Aktviii (10 μM) and stimulated for 6 h with insulin (Ins; 10 nM), as indicated. mRNA expression was measured by qRT-PCR. Transcript levels are shown relative to untreated controls.

mTORC1-dependent regulation of SREBP in hepatic lipid metabolism

Selective insulin resistance has been proposed to explain the paradox of type 2 diabetes mellitus (T2DM), in which patients exhibit insulin resistance with respect to hepatic production of glucose, but not lipid. The induction of hepatic lipogenesis is selectively maintained in T2DM, leading to pathological production of triglycerides and the development of nonalcoholic fatty liver disease and hypertriglyceridemia. In contrast to individuals with T2DM, patients and mice exhibiting hepatic loss of insulin receptor function are completely resistant to all functions of insulin on the liver. Therefore, while they similarly fail to suppress hepatic glucose production and become hyperglycemic, they also fail to stimulate lipogenesis and are protected from hepatic lipid accumulation [18, 19]. Brown and Goldstein have proposed that there must exist a branch point downstream of the insulin receptor that regulates hepatic glucose and lipid production independently to account for this selectivity [20].

Recent genetic evidence suggests that this bifurcation in insulin signaling occurs somewhere downstream of Akt but upstream of the key lipogenic transcription factor SREBP1c. Whole-body and liver-specific knockouts of Akt2 are protected from hepatic steatosis under conditions of obesity caused by leptin deficiency (*ob/ob*) or a lard-based HFD, which is accompanied by reduced expression of *Srebp1c* and decreased de novo lipogenesis [21]. However, on a coconut oil-based HFD with sucrose (Surwit), the liver-specific Akt2 knockout mice do not exhibit defects in the expression of *Srebp1c* or its lipogenic targets but maintain their reduced levels of hepatic TGs [21]. In a model of acute refeeding with a high carbohydrate diet (HCD), Wan et al. found that liver-specific loss of Akt led to lower levels of lipid synthesis without defects in mTORC1 or SREBP1c activation or suppression of INSIG2a [22]. This suggests that SREBP1c-independent pathways downstream of Akt might also contribute to hepatic lipid content. Overall, these

findings support Akt as the main insulin-responsive effector driving induction of hepatic SREBP1c resulting in both physiological and pathological lipogenesis. However, the critical pathway(s) downstream of Akt responsible is not well defined.

Recently, mTORC1 has been proposed to be this bifurcation point downstream of Akt [3]. Our findings in primary mouse hepatocytes are consistent with this model, as the insulin-stimulated induction of lipogenic gene expression and lipogenesis were sensitive to rapamycin, whereas the suppression of gluconeogenic genes was not affected by rapamycin. This result is also consistent with previous studies showing that mTORC1 activation is sufficient to stimulate an SREBP-dependent increase in lipid synthesis (Chapter 2; [2]) and that raptor-deficient livers have decreased de novo lipogenesis [22]. However, the *LTsc1KO* mouse model, which results in the insulin and Akt-independent activation of hepatic mTORC1 signaling, demonstrates that constitutive mTORC1 activation is not sufficient to induce SREBP1c and drive hepatic lipid accumulation and it actually leads to a decrease in lipid production and protection from both age and diet-induced hepatic steatosis (Chapter 3; [8]). We find that the decreased induction of SREBP1c is the result of mTORC1-driven feedback mechanisms causing hepatic insulin resistance and attenuation of Akt signaling to its other downstream pathways.

As disruption of the TSC1-TSC2 complex completely disconnects mTORC1 activation from its regulation by insulin and Akt and results in attenuation of normal Akt signaling, the *LTsc1KO* model provides a unique experimental system in which to identify mTORC1-independent pathways downstream of Akt in the liver. After examining some obvious candidates for SREBP1c regulation downstream of Akt, such as GSK3 and LXR, we focused on the INSIG proteins, as key negative regulators of SREBP1c. Although functionally similar, distinct mechanisms regulate the expression of different INSIG isoforms [23, 24]. *Insig1* is a transcriptional target of the SREBPs, creating in an

autoinhibitory feedback mechanism [25-27]. However, a liver-specific transcript encoding INSIG2, referred to as *Insig-2a*, is strongly downregulated at the message level by insulin signaling [28], thereby facilitating SREBP1c release from the ER and its subsequent processing and activation. Importantly, we found that Akt is responsible for *Insig2a* suppression by insulin and that this occurs independent of mTORC1 signaling (Chapter 3; [8]). While the pathway by which Akt suppresses *Insig2a* is currently unknown, we predict that this is the major mTORC1-independent pathway downstream of Akt in the liver regulating SREBP1c activation. We hypothesize that the failure to suppress *Insig2a* in *LTsc1KO* hepatocytes blocks the pathway to SREBP1c activation at a step prior to that dependent on mTORC1 signaling. Therefore, insulin induces SREBP1c processing and activation through Akt-mediated suppression of *Insig2a* and stimulation of mTORC1 signaling, which both regulate essential, but distinct, steps in the pathway to full activation of SREBP1c.

It is interesting to note that the *LTsc1KO* mice described in this study phenocopy liver-specific knockouts of the insulin receptor and Akt2 [18, 21]. While the overall phenotype is milder than these other models, disruption of the TSC1-TSC2 complex and constitutive activation of mTORC1 results in a phenotype resembling total hepatic insulin resistance, with loss of control over both gluconeogenesis and lipogenesis. This finding lends strong *in vivo* support to cell culture studies demonstrating that mTORC1 activation can cause cell-intrinsic insulin resistance (Reviewed in [29, 30]) and is consistent with the enhanced peripheral insulin sensitivity described for whole-body knockouts of the mTORC1 target S6K1 [31]. The *LTsc1KO* phenotype also suggests that the phenomenon of selective insulin resistance is unlikely to be due soley to sustained activation of hepatic mTORC1 signaling. Our studies on SREBP1c regulation downstream of insulin and Akt suggest that mechanisms leading to the suppression of *Insig2a* might also be intact under conditions of insulin resistance, thereby allowing

sustained activation of hepatic SREBP1c and lipogenesis. It is clear that genetic mouse models, such as the *LTsc1KO* mice, which provide *in vivo* tools to manipulate the insulin signaling network in distinct ways, will continue to reveal tissue-specific mechanisms affecting systemic metabolic homeostasis under both physiological and pathological states.

Transcriptional Control of Cellular Metabolism by mTOR Signaling: Implications for mTORC1-driven cancer

Tumor cells are characterized by adaptations in cellular metabolism that afford growth and proliferative advantages over normal cells and thus contribute to cancer pathophysiology. There is an increasing appreciation that oncogenic signaling controls the metabolic reprogramming of cancer cells, however, the mechanisms and critical players are only beginning to be elucidated. Recent studies have revealed that the mammalian target of rapamycin complex 1 (mTORC1), a master regulator of cell growth and proliferation downstream of oncogenic signaling pathways, controls specific aspects of cellular metabolism through the induction of metabolic gene expression. mTORC1 activation is sufficient to promote flux through glycolysis and the oxidative branch of the pentose phosphate pathway, as well as to stimulate de novo lipogenesis, all processes that are important in tumor biology. As mTORC1 signaling is aberrantly elevated in the majority of genetic tumor syndromes and sporadic cancers, this pathway is poised to be a major driver of the metabolic conversion of tumor cells.

Transcriptional control of tumor cell metabolism

Cancer researchers have known for over 80 years that the metabolic processes at work within tumors are vastly different from those of their tissue of origin [32]. This metabolic shift promotes bioenergetic and anabolic changes that provide a growth and

proliferation advantage to tumor cells under the suboptimal growth conditions of the

tumor microenvironment. This distinction between the behavior of normal and tumor

cells, by definition, represents a therapeutic opportunity to selectively target tumor cells.

However, there is a substantial void in our knowledge of how oncogenic events alter the

metabolic program of cancer cells and how best to take advantage of these differences

for the development of specific anti-tumor therapies. Our laboratory has recently found

that the mammalian target of rapamycin (mTOR) signaling pathway, which is frequently

activated in genetic tumor syndromes and cancers, induces the expression of a

metabolic gene regulatory network (Chapter 2; [2]). The potential implications of these

finding for tumor cell metabolism, growth, and viability are discussed below.

Toward understanding the consequences of aberrant mTORC1 signaling

The ser/thr kinase mTOR exists within two distinct protein complexes, and we

focus here on mTOR complex 1 (mTORC1), which senses the availability of growth

factors, nutrients, and cellular stress to coordinate anabolic processes promoting cell

growth and proliferation [33]. Most of the signals that regulate mTORC1 are transmitted

through upstream signaling pathways that converge upon a small G protein switch. Rheb

is a Ras-related small G protein that, when in its GTP-bound state, is a potent and

essential activator of mTORC1. In general, signals impinging on mTORC1 regulation

generally alter the GDP/GTP-bound status of Rheb by regulating the TSC1-TSC2

complex, which has GTPase activating protein (GAP) activity towards Rheb. Therefore,

when the TSC1-TSC2 complex is active, it stimulates the intrinsic GTPase activity of

Rheb, effectively converting Rheb to its GDP-bound state and shutting down mTORC1

activity [30]. Growth promoting conditions inhibit the TSC1-TSC2 complex to stimulate

mTORC1, while poor growth conditions activate the TSC1-TSC2 complex to suppress

mTORC1 signaling. The TSC1-TSC2 complex is encoded by the two tumor suppressor

genes mutated in the genetic tumor syndrome tuberous sclerosis complex (TSC).

Importantly, within the network of signaling pathways that regulate mTORC1 activity

upstream of the TSC1-TSC2 complex are numerous oncogenes and tumors

suppressors, including those most commonly affected in human malignancies (Figure 4-

2). In fact, aberrant activation of mTORC1 signaling is a frequent occurrence in the most

common types of human cancer and a variety of genetic tumor syndromes [34].

While we have made enormous progress in understanding the upstream

signaling pathways that regulate mTORC1, relatively little is known about the

downstream consequences of mTORC1 activation. The two best-characterized, direct

targets of mTORC1 are the ribosomal S6 kinases (S6K1 and S6K2) and eukaryotic

initiation factor 4E (eIF4E)-binding proteins (4EBP1 and 4EBP2), which are respectively

activated and inhibited by mTORC1. Through these targets, and likely others, mTORC1

regulates specific aspects of cap-dependent translation initiation. In addition, through

poorly understood mechanisms, mTORC1 activation promotes ribosome biogenesis,

thereby enhancing the protein synthetic capacity of the cell. Through mechanisms that

are emerging, but incompletely elucidated, mTORC1 is also a key inhibitor of the

catabolic process of autophagy. For more information on these broad subject areas

related to mTOR, see reviews from Ma and Blenis [35], Mayer and Grummt [36], and

Neufeld [37]. Given its common activation in human cancers, there is much interest in

elucidating other downstream processes controlled by mTORC1 to better understand its

contributions to cancer pathogenesis and to identify novel therapeutic avenues.

To elucidate the cell intrinsic effects of mTORC1 activation, we recently used a

reductionist approach to isolate mTORC1 signaling from the many branching pathways

lying upstream (Chapter 2 [2]). We took advantage of the fact that loss of TSC1 or TSC2

results in constitutive Rheb-GTP loading and mTORC1 activation, even in the absence

of growth factors. Therefore, cell lines lacking TSC1 or TSC2 represent a genetic gain of
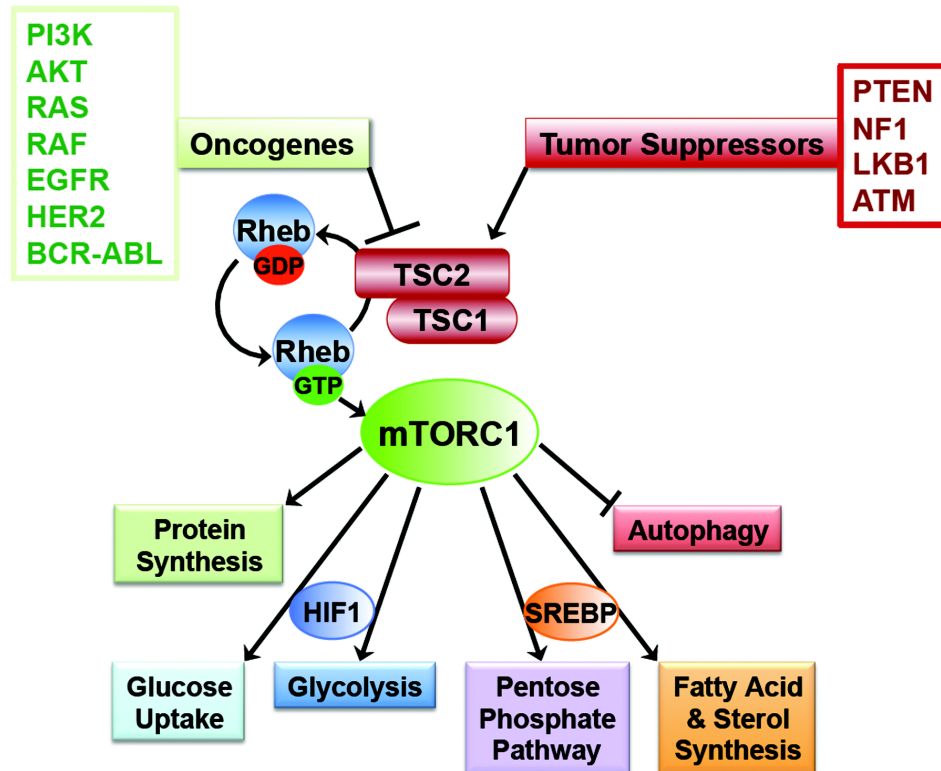
Figure 4-2. Model of the small G protein switch controlling mTORC1 activation downstream of common oncogenes and tumors suppressors and the effects on cell physiology. A network of upstream signaling pathways comprised of the oncogenes and tumor suppressors listed control the activation status of mTORC1 by regulating the TSC1-TSC2 complex. Oncogenic signaling events inhibit the TSC1-TSC2 complex to promote the accumulation of Rheb-GTP and subsequent activation of mTORC1. Reciprocally, through their inhibitory effects on oncogenic signaling, tumor suppressors in effect stimulate the TSC1-TSC2 complex to inhibit the activation of mTORC1 by Rheb. In addition to its previously defined roles in promoting protein synthesis and blocking autophagy, mTORC1 activation can drive specific metabolic processes through regulation of metabolic gene expression. These include glucose uptake and glycolysis through HIF1α and the pentose phosphate pathway and lipid biosynthesis through SREBP (see text for details).

function model, where mTORC1 activation is uncoupled from regulation by upstream

pathways that normally converge upon the TSC1-TSC2 complex. Combining the

analysis of these cells with the use of rapamycin, a highly specific pharmacological

inhibitor of mTORC1, provides an approach to identify cellular processes that mTORC1

activation alone is sufficient to regulate.

Transcriptional control of metabolic pathways downstream of mTORC1

We employed unbiased genomic and metabolomic analyses to identify

mTORC1-regulated transcripts and metabolites (Chapter 2; [2]). Gene expression arrays

were used to compare *Tsc1*- and *Tsc2*-deficient mouse embryo fibroblasts (MEFs) to

their littermate-derived wild-type counterparts under serum-free growth conditions,

where mTORC1 is inactive in wild-type cells and fully stimulated in both *Tsc1* and *Tsc2*

null cells. A time course of rapamycin treatment was included to establish a role for

mTORC1 in any changes detected. Transcripts were classified as being induced by

mTORC1 signaling only if they were significantly elevated in both *Tsc1* and *Tsc2* null

cells relative to wild-type and reduced toward wild-type levels by rapamycin treatment.

Only 130 genes met these highly stringent criteria. Gene set enrichment analysis

revealed significant over-representation of genes from three specific metabolic pathways

amongst those induced by mTORC1 signaling: glycolysis, the pentose phosphate

pathway, and lipid and sterol biosynthesis. To determine whether the stimulation of

these metabolic genes downstream of mTORC1 altered cellular metabolism, we used

both focused metabolic assays and metabolomic approaches. Steady state and

metabolic flux analyses revealed that mTORC1 activity promotes flux through glycolysis

and, specifically, the NADPH-producing oxidative arm of the pentose phosphate

pathway. Finally, we found that *Tsc2*-deficient cells demonstrate an mTORC1-

dependent increase in *de novo* lipogenesis. Therefore, the robust pathway-specific

induction of metabolic genes by mTORC1 signaling drives corresponding metabolic changes in cells.

To gain insight into how mTORC1 controls metabolic gene expression and thereby affects cellular metabolism, we used a bioinformatic apporach to identify overrepresented transcription factor binding motifs in the promoters of mTORC1-regulated genes (Chapter 2; [2]). Interestingly, the two most significantly enriched cis-regulatory elements amongst rapamycin-sensitive genes in this study were for sterol regulatory element binding protein (SREBP) and Myc, both of which are global regulators of cellular metabolism. Importantly, c-Myc and hypoxia-inducible factor 1 (HIF1) recognize an overlapping motif and are both known to promote the transcription of glycolytic genes [38]. We found that, in the setting of TSC gene disruption, mTORC1 signaling drives glucose uptake and glycolysis through up-regulation of HIF1α. On the other hand, the SREBPs (SREBP1a, 1c, and 2) are known to stimulate the expression of a large number of lipid and sterol biosynthesis genes [4]. We demonstrated that these transcription factors are, indeed, essential for the mTORC1-induced expression of these genes and for the promotion of de novo lipogenesis by mTORC1 signaling (Chapter 2; [2]). Interestingly, SREBP1 was also found to be required for the mTORC1-dependent increase in the expression of glucose-6-phosphate dehydrogenase (*G6pd*), the rate-limiting enzyme of the oxidative branch of the pentose phosphate pathway. This suggests that mTORC1 can coordinate *de novo* lipogenesis and the generation of reducing equivalents required to fuel this anabolic process through regulation of this transcription factor. Importantly, two previous studies demonstrated that activated alleles of Akt, which potently activate mTORC1, can stimulate HIF1α and the SREBPs to respectively induce expression of glycolytic and lipogenic gene sets similar to those

identified in our study [39, 40]. This suggests that activation of mTORC1 through upstream oncogenic pathways, will also promote these metabolic changes.

Normoxic induction of HIF1α by mTORC1

HIF1α protein levels are elevated in many human cancers through genetic events or intratumoral hypoxia that promote its stability, and increased HIF1α levels correlate poorly with patient survival [41]. We find that mTORC1 activation alone is sufficient to drive increases in HIF1α levels under normoxic conditions (Chapter 2; [2]), without effects on its stability (S. Menon and B.D.M., unpublished). Consistent with previous findings [42, 43], we show that, through phosphorylation and inhibition of 4EBP1, mTORC1 can stimulate cap-dependent translation from the 5'-untranslated region of the HIF1α mRNA. However, we also found increases in both HIF1α and HIF2α transcripts, suggesting either additional mechanisms of regulation or auto-regulation of their expression. The ability of mTORC1 to promote elevated normoxic levels of HIF1α suggests that even oxygenated regions of tumors characterized by high mTORC1 activity could display HIF1α-dependent metabolic changes, resulting in aerobic glycolysis (more commonly referred to as the "Warburg effect"). The ability of mTORC1 to promote glucose uptake and gylcolytic flux through HIF1α also suggests that FDG-PET positivity may be a useful indicator for monitoring mTOR-driven tumors, a notion supported by genetic tumor models in mice [39, 44]. Like HIF1α, c-Myc can also induce the expression of genes involved in glucose uptake and glycolysis [38] and can be translated in an mTORC1-dependent manner in some settings [45]. Therefore, it is possible that in such settings, mTORC1 might enhance glycolytic gene expression through c-Myc rather than HIF1α.

__Implications for tumor development, progression, and treatment__

Increased aerobic glycolysis (the Warburg effect) and *de novo* lipogenesis are

the two most commonly detected metabolic changes in tumors and can be considered

the metabolic hallmarks of cancer. Our study to uncover the downstream consequences

of mTORC1 activation, a common event in human cancer [34], demonstrates that

mTORC1 signaling is sufficient to drive these metabolic processes (Chapter 2; [2]).

mTORC1 promotes these metabolic changes through induction of a transcriptional

program affecting metabolic gene targets of HIF1α and SREBP1 and 2. While the

glucose transporters and glycolytic enzymes encoded by HIF1α are well known to be

upregulated in tumors [41], less is known regarding the expression status of the diverse

array of SREBP targets. One notable exception is fatty acid synthase (FASN), which

encodes a multifunctional enzyme complex that converts acetyl-CoA to the 16-carbon

saturated fatty acid palmitate. Since most normal tissues do not undergo substantial

levels of *de novo* lipid biosynthesis, obtaining lipids from dietary sources instead, FASN

levels are low in most tissues. However, FASN is transcriptionally upregulated in most

types of human cancer [46]. Oncogenic activation of the PI3K-Akt pathway has been

implicated in the increased expression of FASN in ovarian and prostate cancer [47]. Our

findings that mTORC1 signaling can stimulate FASN expression through SREBP

suggest that mTORC1 might play a critical role in FASN expression and lipogenesis in

human cancers characterized by activation of the PI3K-Akt pathway. Interestingly, we

found that the SREBPs are essential for mTORC1-driven cell proliferation (Chapter 2;

[2]), suggesting that specific enzymes encoded by gene targets of these transcription

factors could represent novel targets for cancer therapeutics. To this end, there have

been many studies suggesting efficacy of FASN inhibitors in pre-clinical tumor models

[48]. Inhibiting lipid biosynthesis may be particularly effective in settings of aberrantly

high mTOR activity, which drives uncontrolled protein synthesis, as lipids are required

for biogenesis of not only plasma membrane but also endoplasmic reticulum. Indeed,

knockdown of SREBP1 and SREBP2 in TSC2-deficient cells further exacerbates mTOR-

driven ER stress (J.L.Y. and B.D.M. unpublished).

In addition to lipogenesis, there are a number of other processes induced by

SREBP that could contribute to the tumor-promoting activities of mTORC1. SREBP

stimulates the expression of genes involved in the synthesis of isoprenoids, which

modify many signaling proteins, including members of the Ras superfamily, and could

contribute to cancer pathogenesis. The observation that acetyl-CoA derived from the

reaction catalyzed by the SREBP target ATP-citrate lyase (ACLY) is required for histone

acetylation [49] suggests a potential role for global regulation of chromatin downstream

of mTORC1. Perhaps most notable is our finding that mTORC1 increases flux through

the oxidative arm of the pentose phosphate pathway and regulates expression of the

rate-limiting enzyme in this pathway (G6PD) through SREBP1. Relative to glycolysis and

lipogenesis, dysregulation of the pentose phosphate pathway in cancer has received

much less attention in the field of tumor cell metabolism, despite mounting evidence for

the importance of this pathway in tumor development and progression. A causal role for

G6PD in tumorigenesis was demonstrated by its ability to transform NIH-3T3 cells [50],

and G6PD has been found to be elevated in animal tumor models [51, 52] and human

neoplasms of the breast, endometrium, cervix, lung and prostate [53-57]. Through the

production of NADPH, upregulation of the oxidative pentose phosphate pathway is likely

to represent an important mechanism by which some tumor cells meet the unique

metabolic demands of rapid anabolic growth and proliferation. In addition, G6PD-

produced NADPH is important for regenerating reduced glutathione oxidized in the

protection against reactive oxygen species (ROS). Tumor cells may benefit from

upregulation of this pathway to control elevated ROS levels resulting from the fluctuating

availability of oxygen and nutrients in the tumor microenvironment. It will be important for future studies to determine whether there are also SREBP-independent inputs into the regulation of the pentose phosphate pathway downstream of mTORC1 and whether mTORC1 signaling promotes resistance to oxidative stress.

Given the shear number of oncogenes and tumor suppressors lying upstream of mTORC1, it will be important to identify the oncogenic settings in which mTORC1 signaling is the major driver of these common metabolic changes. It seems likely that parallel pathways downstream of oncogenes such as PI3K and RAS will also contribute to the control over these metabolic parameters within different tumors. It is this complexity that we must understand in order to develop therapeutic strategies aimed at tumor-specific cell metabolism.

Studies toward defining the role of the mTOR-SREBP connection in tumor cell metabolism

We explored whether mTORC1 regulates SREBP in cancers and tumor syndromes driven by aberrant activation of mTORC1. In cells, mTORC1 activation upon loss of TSC1-TSC2 complex function is sufficient to drive activation of SREBP, its target genes, and lipogenesis. Similar activation of mTORC1 results when $Tsc2^{+/-}$ mice lose the wild-type allele of Tsc2 in renal epithelial cells, leading to the development of renal cystadenomas [58]. These tumors are characterized by elevated mTORC1 signaling and are sensitive to treatment with rapamycin [59]. Loss of heterozygosity events also cause TSC patients to develop a kidney lesion known as angiomyolipoma (AML), which contains fat, smooth muscle, and vascular components, and these tumors are also partially sensitive to rapamycin [60]. While TSC-associated AMLs are distinct from the epithelium-derived tumors in the $Tsc2^{+/-}$ mice, the mouse model affords a system to

study tumors driven by mTORC1 activation and caused by genetic lesions similar to the

human TSC disease.

In an analysis of kidney tumors from $Tsc2^{+/-}$ mice, aged 12 months, treated for 36

hours with either rapamycin or vehicle (n=2 per treatment), we found that SREBP

targets, including fatty acid synthase (FASN), glucose 6-phosphate dehydrogenase

(G6PD), and acetyl-CoA carboxylase (ACC), are elevated relative to adjacent normal

tissue (Figure 4-3A). The increased immuno-staining of FASN and ACC in the tumor

relative to the surrounding normal tissue was eliminated upon treatment with rapamycin

(Figure 4-3B). AMLs from four TSC patients diplayed increased FASN staining in the

adipocytes from these lesions compared to normal adipose, and the smooth muscle

component also showed elevated expression of FASN (Figure 4-3C). This suggests that

mTORC1 dependent activation of lipogenic genes may be relevant to the pathogenesis

of TSC and that inhibiting lipogenic pathways could be therapeutically effective.

To extend these observations in other settings relevant to common forms of

human cancer, we explored SREBP activation in lung tumor models, driven by activating

mutations in $PIK3CA$ (H10474, $PIK3CA^{H1047R}$) and $Kras$ (G12D, $Kras^{G12D}$) (n=2-4 per

condition, courtesy of Drs. Jeffrey Engleman and Kwok-Kin Wong, Massachusetts

General Hospital and Harvard Medical School). Interestingly, IHC demonstrated that

SREBP targets, including Fasn and G6PD, are elevated in the tumors from both of these

models relative to surrounding normal tissue (Figure 4-4A). It will be import to determine

whether rapamycin reduces the increased expression of lipogenic genes in these lung

tumors. Interestingly, unlike the TSC-deficient cystadenomas, the $PIK3CA$ and $Kras$

tumors are not sensitive to rapamycin [61], although loss of $Tsc1$ sensitizes the Kras-

driven tumors [62]. It will be interesting to determine whether rapamycin-sensitive

changes in SREBP activity correlate with drug sensitivity. If so, this would suggest that

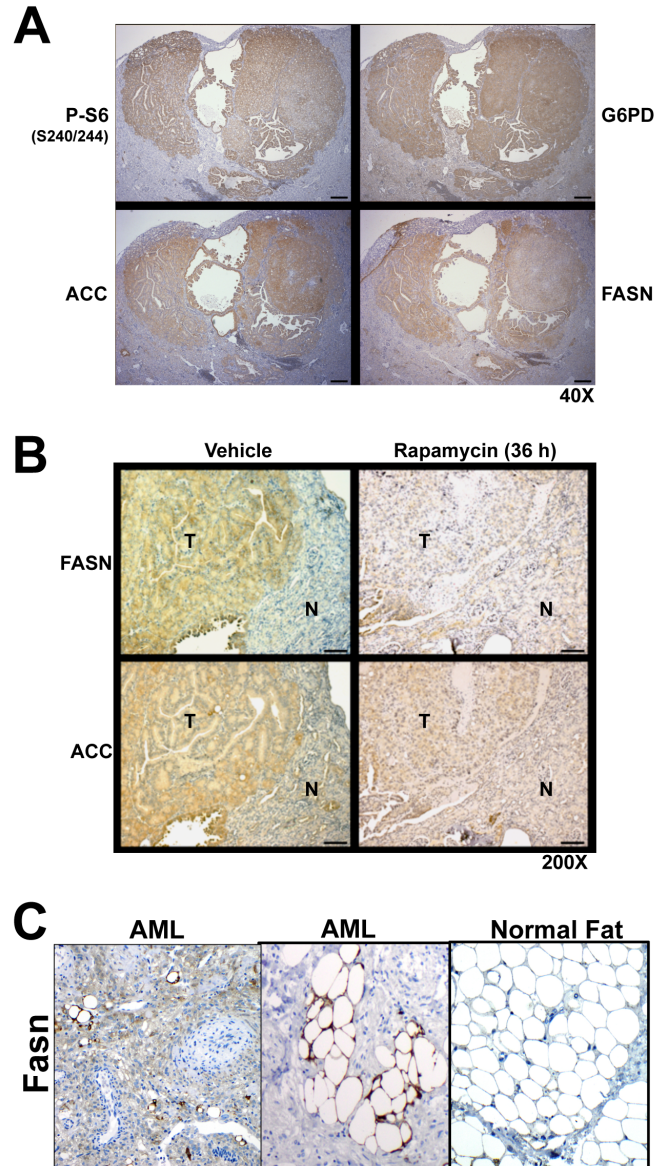SREBP targets could be used as biomarkers for treatment efficacy.

Figure 4-3. TSC-deficiency activates SREBP through mTORC1.

A) Kidney sections from *Tsc2*$^{+/-}$ mice were stained for phospho-S6, as a marker of mTORC1 activation, and SREBP targets FASN, ACC, and G6PD.

B) *Tsc2*$^{+/-}$ mice were treated with either vehicle or rapamycin (10mg/kg) for 36 hours. Kidney sections were stained for FASN and ACC.

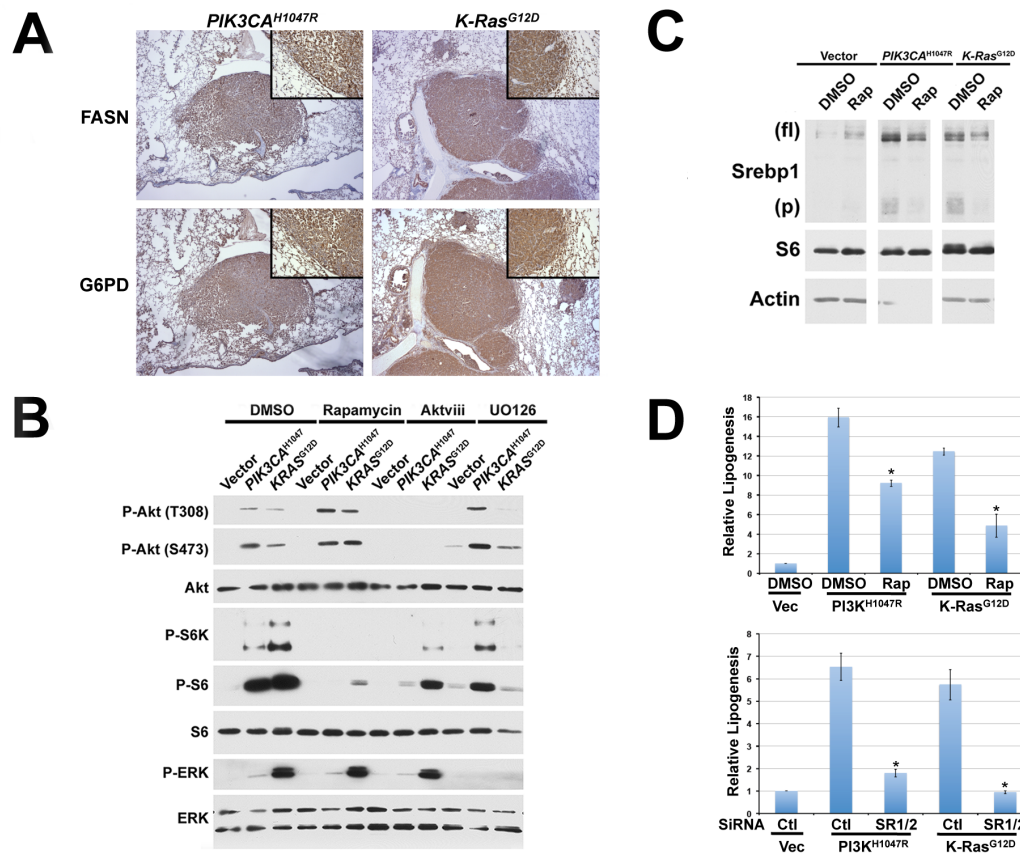C) Human angiomyolipomas and normal adipose tissue were stained for FASN.

Figure 4-4. Oncogenic PIK3CA and KRas induce SREBP and lipogenesis through mTORC1.

A) *PIK3CA*[H1047R] and *K-Ras*[G12D] lung tumors treated with vehicle for 2 weeks were stained for G6pd and Fasn.

B,C) MCF-10A lines transformed with *PIK3CA*[H1047R] and *K-Ras*[G12D] were serum starved in the presence of vehicle, rapamycin (20nM), Aktviii (20uM), and UO126 () for 16 hours. Western blots for the indicated proteins. NOTE: Images shown are from the same western blot, but conditions that are not relevant were excised.

D) Cells treated as in (B,C; top) or transfected with either control or SREBP1 and SREBP2 for 48h (bottom) were labeled with ^{14}C-acetate and the levels of ^{14}C incorporation into the lipid fraction are shown relative to untreated controls.

To follow up these in vivo findings in an isogenic, cell-based system that enables one to study transforming events that lead to mTORC1 activation, I have used MCF10A cells, a non-transformed breast epithelial cell line, that have been transformed by expression of either *PIK3CA*^{H1047R} or *Kras*^{G12D}. We confirmed that mTORC1 signaling is activated as expected upon transformation and is appropriately reduced in response to the inhibitors (Figure 4-4B). Levels of processed active SREBP1 are elevated in transformed lines and strongly reduced toward parental levels by treatment with rapamycin (Figure 4-4C). Importantly, this mTORC1-dependent activation of SREBP1 correlates with oncogene-induced, mTORC1-dependent changes in de novo lipogenesis, a process that depends on SREBPs (Figure 4D). Currently, these experiments are being repeated and followed up by another graduate student in the lab.

In a recent collaboration with the laboratory of Dr. Karen Cichowski (Brigham and Women's Hospital, Harvard Medical School), we explored the relevance of mTORC1-induced PPP in a Ras-driven cancer, *Nf1*-deficient malignant peripheral nerve sheath tumors (MPNSTs). It was found that three ER stress-inducing agents, including the HSP90 inhibitor IPI-504, triggered rapid tumor regression in the MPNST mouse model, but only when combined with the mTOR inhibitor rapamycin [63]. Consistent with cellular studies showing that SREBP1 is regulated by mTOR (Chapter 2; [1, 2]), rapamycin significantly decreased the expression of known SREBP targets including SREBP1 itself, ACC, and FASN in MNPSTs within 7 hours of treatment (Figure 4-5A,B). Treatment with IPI-504 alone slightly suppressed SREBP1, but together both agents reduced SREBP1 expression by 92% and effectively suppressed ACC and FASN (Figure 4-5A,B). Rapamycin also potently suppressed G6PD mRNA levels in MPNST tumor tissue (Figure 4-5C). However, rapamycin alone had inconsistent effects on G6PD protein levels (Figure 4-5B), perhaps reflecting a slower turnover of G6PD protein within this

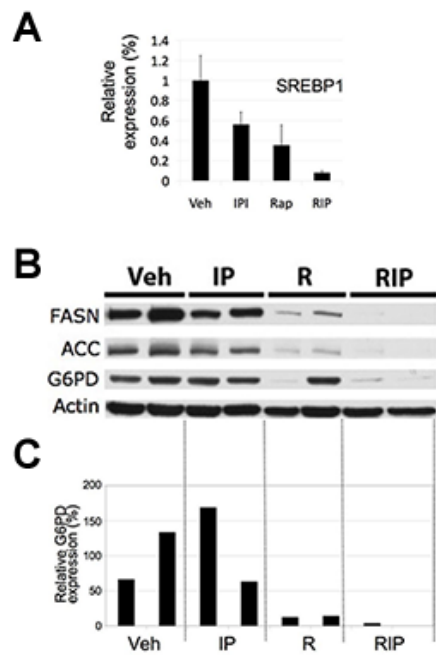**Figure 4-5. Oxidative stress plays a critical role in mediating the therapeutic response to IPI-504 and rapamycin.**

(A) SREBP1 mRNA levels in tumors from animals that were treated for 7 hr as indicated.

(B) Immunoblots showing expression of FASN, ACC, and G6PD in tumors from animals treated for 7 hr as indicated. Actin serves as a loading control.

(C) G6PD mRNA levels in individual tumors treated as described in (B).

short time frame. Nevertheless, rapamycin and IPI-504 together dramatically suppressed both G6PD mRNA and protein expression in MPNSTs in vivo (Figure 4-5B,C). Accordingly, rapamycin/IPI-504 caused a 34% decrease in reduced glutathione levels in these tumors, demonstrating the functional consequence of this suppression of SREBP-driven G6pd [63]. Rapamycin and IPI-504 synergize by promoting irresolvable ER stress. The drug combination causes catastrophic ER and mitochondrial damage. This process is further fueled by oxidative stress, induced by the IPI-504-dependent production of reactive oxygen species (ROS) and the simultaneous rapamycin-dependent suppression of an important endogenous antioxidant pathway. The mechanism by which these agents cooperate reveals a therapeutic paradigm that can be expanded to develop additional combinations for Ras-driven malignancies.

Our findings demonstrate that mTORC1 activation alone is sufficient to drive specific metabolic processes that are frequently detected in human cancers. Aberrant activation of mTORC1 occurs in the most common human cancers, suggesting that mTORC1 signaling contributes to the metabolic reprogramming of cancer cells, thereby affording survival and proliferative advantages. Targeting these downstream metabolic pathways may provide effective therapeutic approaches for mTORC1-driven tumor syndromes (e.g., Tuberous Sclerosis Complex) and sporadic cancers. Inhibitors targeting the metabolic enzymes comprising these pathways are unlikely to elicit the same unwanted feedback signaling events that have been proposed to limit the usefulness of rapamycin and its analogs in the clinic. Therefore, it is possible that such metabolic inhibitors would elicit selective cytotoxic responses in the tumor, rather than the cytostatic effects routinely seen with rapamycin [64].

Future Directions

We and others have recently identified a role for mTORC1 in the regulation of SREBPs and lipid metabolism, which has implications for disease states in which mTORC1 is aberrantly activated and de novo lipogenesis is misregulated, including cancer and type 2 diabetes. In cultured and tumor cells characterized by TSC deficiency, mTORC1 activation is both necessary and sufficient to stimulate expression of lipogenic and pentose phosphate pathway SREBP targets. Future studies are required to understand the molecular mechanism(s) by which mTORC1 regulates SREBP. It will also be important to understand which oncogenes and tumors suppressors drive SREBP activation and lipogenesis through mTORC1 and to determine which tumorigenic settings require activation of SREBPs for cell growth, survival, and proliferation. Understanding which SREBP targets are required for tumorigenic properties will offer insights into novel therapeutic approaches targeting tumor cell metabolism. Importantly, we found that the regulation of SREBP1c and lipogenesis in hepatocytes is different than cultured cells, as parallel mTORC1-dependent an independent pathways downstream of Akt are required for hepatic lipogenesis. Future mechanistic studies are needed to define both the signaling pathway by which Akt suppresses *Insig2a* expression and the molecular target of mTORC1 signaling involved in promoting hepatic SREBP1c activation. Our findings that SREBP is a major transcriptional effector or mTORC1 will be enhanced by the proposed future studies to ultimately better understand and ideally treat disease characterized by aberrant mTORC1 signaling.

ACKNOWLEDGEMENTS

REFERENCES

1.   Porstmann, T., Santos, C.R., Griffiths, B., Cully, M., Wu, M., Leevers, S., Griffiths, J.R., Chung, Y.L., and Schulze, A. (2008). SREBP activity is regulated by mTORC1 and contributes to Akt-dependent cell growth. Cell Metab *8*, 224-236.

2.   Duvel, K., Yecies, J. L., Menon, S., Raman, P., Lipovsky, A. I., Souza, A. L., Triantafellow, E., Ma, Q., Gorski, R., Cleaver, S., Vander Heiden, M. G., MacKeigan, J. P., Finan, P. M., Clish, C. B., Murphy, L. O. and Manning, B. D. (2010). Activation of a metabolic gene regulatory network downstream of mTOR complex 1. Mol Cell *39*, 171-183.

3.   Li, S., Brown, M.S., and Goldstein, J.L. (2010). Bifurcation of insulin signaling pathway in rat liver: mTORC1 required for stimulation of lipogenesis, but not inhibition of gluconeogenesis. Proc Natl Acad Sci U S A *107*, 3441-3446.

4.   Espenshade, P.J., and Hughes, A.L. (2007). Regulation of sterol synthesis in eukaryotes. Annual review of genetics *41*, 401-427.

5.   Demoulin, J.B., Ericsson, J., Kallin, A., Rorsman, C., Ronnstrand, L., Heldin, C.H. (2004). Platelet-derived growth factor stimulates membrane lipid synthesis through activation of phosphatidylinositol 3-kinase and sterol regulatory element-binding proteins. J Biol Chem *279*, 35392–402.

6.   Zhou, R.H., Yao, M., Lee, T.S., Zhu, Y., Martins-Green, M., Shyy, J.Y. (2004). Vascular endothelial growth factor activation of sterol regulatory element binding protein: a potential role in angiogenesis. Circ Res *95*, 471–8.

7.   Sundqvist, A., Bengoechea-Alonso, M.T., Ye, X., Lukiyanchuk, V., Jin, J., Harper, J.W., and Ericsson, J. (2005). Control of lipid metabolism by phosphorylation-dependent degradation of the SREBP family of transcription factors by SCF(Fbw7). Cell Metab *1*, 379-391.

8.   Yecies, J.L., Zhang, H.H., Menon, S., Liu, S., Yecies, D., Lipovsky, A.I., Gorgun, C., Kwiatkowski, D.J., Hotamisligil, G.S., Lee, C.H., and Manning, B.D. (2011). Akt stimulates hepatic SREBP1c and lipogenesis through parallel mTORC1-dependent and independent pathways. *Cell Metab* 14, 21-32.

9.   Horton, J.D., Shah, N.A., Warrington, J.A., Anderson, N.N., Park, S.W., Brown, M.S., and Goldstein, J.L. (2003). Combined analysis of oligonucleotide microarray data from transgenic and knockout mice identifies direct SREBP target genes. Proc Natl Acad Sci U S A *100*, 12027-12032.

10.   Pearce, L.R., Alton, G.R., Richter, D.T., Kath, J.C., Lingardo, L., Chapman, J., Hwang, C., and Alessi, D.R. (2010). Characterization of PF-4708671, a novel and highly specific inhibitor of p70 ribosomal S6 kinase (S6K1). Biochem J *431*, 245-255.

11.   Zhang, H., Stallock, J.P., Ng, J.C., Reinhard, C., Neufeld, T.P. (2000). Regulation of cellular growth by the Drosophila target of rapamycin dTOR. Genes Dev *14*, 2712-24.

12.   Du, X., Kristiana, I., Wong, J., and Borwn, A.J. (2006). Involvement of Akt in ER-to-Golgi Transport of SCAP/SREBP: A Link between a Key Cell Proliferative Pathway and Membrane Synthesis Mol Biol Cell *17*, 2735-2745.

13.   Werstruck, G.H., Lentz, S.R., Dayal, S., Hossain, G.S., Sood, S.K., Shi, Y.Y, Maeda, N. Drisans, S.K., Malinow, M.R., and Austin, R.C. (2001). Homocysteine-induced endoplasmic reticulum stress causes dysregulation of the cholesterol and triglyceride biosynthetic pathways. J Clin Invest. 107, 1263-1273.

14.   Lee, J.N. and Ye, J. (2004) Proteolytic activation of sterol regulatory element-binding protein induced by cellular stress through depletion of Insig-1. J. Biol. Chem. 279, 45257–45265.

15.   Kammoun H.L., Chabanon H, Hainault I., Luquet S., Magnan c., Koike T., Ferré P., and Foufelle F. (2009) GRP78 expression inhibits insulin and ER stress–induced SREBP-1c activation and reduces hepatic steatosis in mice. JCI *119,* 1201-1215.

16.   Ozcan, U., Ozcan, L., Yilmaz, E., Duvel, K., Sahin, M., Manning, B.D., and Hotamisligil, G.S. (2008). Loss of the Tuberous Sclerosis Complex Tumor Suppressors Triggers the Unfolded Protein Response to Regulate Insulin Signaling and Apoptosis. Mol Cell *29*, 541–551.

17.   Peterson, T.R., Sengupta, S.S., Harris, T.E., Carmack, A.E., Kang, S.A., Balderas, E., Guertin, D.A., Madden, K.L., Carpenter, A.E., Finck, B.N.*, et al.* (2011). mTOR complex 1 regulates lipin 1 localization to control the SREBP pathway. Cell *146*, 408-420.

18.   Biddinger, S.B., Hernandez-Ono, A., Rask-Madsen, C., Haas, J.T., Aleman, J.O., Suzuki, R., Scapa, E.F., Agarwal, C., Carey, M.C., Stephanopoulos, G.*, et al.* (2008). Hepatic insulin resistance is sufficient to produce dyslipidemia and susceptibility to atherosclerosis. Cell Metab *7*, 125-134.

19.   Semple, R.K., Sleigh, A., Murgatroyd, P.R., Adams, C.A., Bluck, L., Jackson, S., Vottero, A., Kanabar, D., Charlton-Menys, V., Durrington, P.*, et al.* (2009). Postreceptor insulin resistance contributes to human dyslipidemia and hepatic steatosis. J Clin Invest *119*, 315-322.

20.   Brown, M.S., and Goldstein, J.L. (2008). Selective versus total insulin resistance: a pathogenic paradox. Cell Metab *7*, 95-96.

21.   Leavens, K.F., Easton, R.M., Shulman, G.I., Previs, S.F., and Birnbaum, M.J. (2009). Akt2 Is Required for Hepatic Lipid Accumulation in Models of Insulin Resistance. Cell Metab. *10*, 405–418.

22.   Wan, M., Leavens, K.F., Saleh, D., Easton, R.M., Guertin, D.A., Peterson, T.R., Kaestner, K.H., Sabatini, D.M., and Birnbaum, M.J. (2011). Postprandial hepatic lipid metabolism requires signaling through Akt2 independent of the transcription factors FoxA2, FoxO1, and SREBP1c. Cell Metab *14*, 516-527.

23.   Goldstein, J.L., DeBose-Boyd, R.A., and Brown, M.S. (2006). Protein sensors for membrane sterols. Cell *124*, 35-46.

24.   Raghow, R., Yellaturu, C., Deng, X., Park, E.A., and Elam, M.B. (2008). SREBPs: the crossroads of physiological and pathological lipid homeostasis. Trends Endocrinol Metab *19*, 65-73.

25.   Yang, T., Espenshade, P.J., Wright, M.E., Yabe, D., Gong, Y., Aebersold, R., Goldstein, J.L., and Brown, M.S. (2002). Crucial step in cholesterol homeostasis: sterols promote binding of SCAP to INSIG-1, a membrane protein that facilitates retention of SREBPs in ER. Cell *110*, 489-500.

26.   Horton, J.D., Shah, N.A., Warrington, J.A., Anderson, N.N., Park, S.W., Brown, M.S., and Goldstein, J.L. (2003). Combined analysis of oligonucleotide microarray data from transgenic and knockout mice identifies direct SREBP target genes. Proc Natl Acad Sci U S A *100*, 12027-12032.

27.   Gong, Y., Lee, J.N., Lee, P.C., Goldstein, J.L., Brown, M.S., and Ye, J. (2006). Sterol-regulated ubiquitination and degradation of Insig-1 creates a convergent mechanism for feedback control of cholesterol synthesis and uptake. Cell Metab *3*, 15-24.

28.   Yabe, D., Komuro, R., Liang, G., Goldstein, J.L., and Brown, M.S. (2003). Liver-specific mRNA for Insig-2 down-regulated by insulin: implications for fatty acid synthesis. Proc Natl Acad Sci U S A *100*, 3155-3160.

29.   Harrington, L.S., Findlay, G.M., and Lamb, R.F. (2005). Restraining PI3K: mTOR signalling goes back to the membrane. Trends Biochem Sci *30*, 35-42.

30.   Huang, J., and Manning, B.D. (2008). The TSC1-TSC2 complex: a molecular switchboard controlling cell growth. Biochem J *412*.

31.   Um, S.H., Frigerio, F., Watanabe, M., Picard, F., Joaquin, M., Sticker, M., Fumagalli, S., Allegrini, P.R., Kozma, S.C., Auwerx, J.*, et al.* (2004). Absence of S6K1 protects against age and diet-induced obesity while enhancing insulin sensitivity. Nature *431*, 200-205.

32.   Vander Heiden, M. G., Cantley, L. C. and Thompson, C. B. (2009). Understanding the Warburg effect: the metabolic requirements of cell proliferation. Science *324*, 1029-1033.

33. Guertin, D.A., Sabatini, D.M. (2007). Defining the role of mTOR in cancer. Cancer Cell *12*, 9–22.

34. Menon, S. and Manning, B. D. (2008). Common corruption of the mTOR signaling network in human tumors. Oncogene *27*, S43-S51.

35. Ma, X. M. and Blenis, J. (2009). Molecular mechanisms of mTOR-mediated translational control. Nat Rev Mol Cell Biol *10*, 307-318.

36. Mayer, C., and Grummt, I. (2006). Ribosome biogenesis and cell growth: mTOR coordinates transcription by all three classes of nuclear RNA polymerases. Oncogene *25*, 6384-6391.

37. Neufeld, T.P. (2010). TOR-dependent control of autophagy: biting the hand that feeds. Curr Opin Cell Biol *22*, 157-168.

38. Gordan, J. D., Thompson, C. B. and Simon, M. C. (2007). HIF and c-Myc: sibling rivals for control of cancer cell metabolism and proliferation. Cancer Cell *12*, 108-113.

39. Majumder, P. K., Febbo, P. G., Bikoff, R., Berger, R., Xue, Q., McMahon, L. M., Manola, J., Brugarolas, J., McDonnell, T. J., Golub, T. R., Loda, M., Lane, H. A. and Sellers, W. R. (2004). mTOR inhibition reverses Akt-dependent prostate intraepithelial neoplasia through regulation of apoptotic and HIF-1-dependent pathways. Nat Med *10*, 594-601.

40. Porstmann, T., Griffiths, B., Chung, Y. L., Delpuech, O., Griffiths, J. R., Downward, J. and Schulze, A. (2005). PKB/Akt induces transcription of enzymes involved in cholesterol and fatty acid biosynthesis via activation of SREBP. Oncogene *24*, 6465-6481.

41. Semenza, G.L. (2003). Targeting HIF-1 for cancer therapy. Nature Rev Cancer *3*, 721–32.

42. Laughner, E., Taghavi, P., Chiles, K., Mahon, P. C. and Semenza, G. L. (2001). HER2 (neu) signaling increases the rate of hypoxia-inducible factor 1alpha (HIF-1alpha) synthesis: novel mechanism for HIF-1-mediated vascular endothelial growth factor expression. Mol Cell Biol *21*, 3995-4004.

43. Thomas, G.V., Tran, C., Mellinghoff, I.K., Welsbie, D.S., Chan, E., Fueger, B., Czernin, J., and Sawyers, C.L. (2006). Hypoxia-inducible factor determines sensitivity to inhibitors of mTOR in kidney cancer. Nat Med *12*, 122-127.

44. Shackelford, D.B., Vasquez, D.S., Corbeil, J., Wu, S., Leblanc, M., Wu, C.L., Vera, D.R., and Shaw, R.J. (2009). mTOR and HIF-1alpha-mediated tumor metabolism in an LKB1 mouse model of Peutz-Jeghers syndrome. Proc Natl Acad Sci U S A *106*, 11137-11142.

45. West, M. J., Stoneley, M. and Willis, A. E. (1998). Translational induction of the c-myc oncogene via activation of the FRAP/TOR signalling pathway. Oncogene *17*, 769-780.

46.   Menendez, J. A. and Lupu, R. (2007). Fatty acid synthase and the lipogenic phenotype in cancer pathogenesis. Nature Reviews *7*, 763-777.

47.   Swinnen, J.V., Brusselmans, K., and Verhoeven, G. (2006). Increased lipogenesis in cancer cells: new players, novel targets. Curr Opin Clin Nutr Metab Care *9*, 358-365.

48.   Lupu, R., and Menendez, J.A. (2006). Pharmacological inhibitors of Fatty Acid Synthase (FASN)--catalyzed endogenous fatty acid biogenesis: a new family of anti-cancer agents? Curr Pharm Biotechnol *7*, 483-493.

49.   Wellen, K.E., Hatzivassiliou, G., Sachdeva, U.M., Bui, T.V., Cross, J.R., and Thompson, C.B. (2009). ATP-citrate lyase links cellular metabolism to histone acetylation. Science *324*, 1076-1080.

50.   Kuo, W., Lin, J., and Tang, T.K. (2000). Human glucose-6-phosphate dehydrogenase (G6PD) gene transforms NIH 3T3 cells and induces tumors in nude mice. Int J Cancer *85*, 857-864.

51.   Roy, D., and Liehr, J.G. (1988). Characterization of drug metabolism enzymes in estrogen-induced kidney tumors in male Syrian hamsters. Cancer Res *48*, 5726-5729.

52.   Simile, M., Pascale, R.M., De Miglio, M.R., Nufris, A., Daino, L., Seddaiu, M.A., Muroni, M.R., Rao, K.N., and Feo, F. (1995). Inhibition by dehydroepiandrosterone of growth and progression of persistent liver nodules in experimental rat liver carcinogenesis. Int J Cancer *62*, 210-215.

53.   Bokun, R., Bakotin, J., and Milasinovic, D. (1987). Semiquantitative cytochemical estimation of glucose-6-phosphate dehydrogenase activity in benign diseases and carcinoma of the breast. Acta Cytol *31*, 249-252.

54.   Hughes, E.C. (1976). The effect of enzymes upon metabolism, storage, and release of carbohydrates in normal and abnormal endometria. Cancer *38*, 487-502.

55.   Dutu, R., Nedelea, M., Veluda, G., and Burculet, V. (1980). Cytoenzymologic investigations on carcinomas of the cervix uteri. Acta Cytol *24*, 160-166.

56.   Zampella, E.J., Bradley, E.L., Jr., and Pretlow, T.G., 2nd (1982). Glucose-6-phosphate dehydrogenase: a possible clinical indicator for prostatic carcinoma. Cancer *49*, 384-387.

57.   Dessi, S., Batetta, B., Cherchi, R., Onnis, R., Pisano, M., and Pani, P. (1988). Hexose monophosphate shunt enzymes in lung tumors from normal and glucose-6-phosphate-dehydrogenase-deficient subjects. Oncology *45*, 287-291.

58.   Onda, H., Lueck, A., Marks, P.W. Warren, H.B., and Kwiatkowski, D.J. (1999). *Tsc2+/–* mice develop tumors in multiple sites that express gelsolin and are influenced by genetic background. J Clin Invest 104, 687-695.

59.   Woodrum, C., Nobil, A., and Dabora, S.L. (2010). Comparison of three rapamycin dosing schedules in A/J Tsc2+/- mice and improved survival with angiogenesis inhibitor or asparaginase treatment in mice with subcutaneous tuberous sclerosis related tumors. J Transl Med. *8*, 14.

60.   Bissler, J.J., McCormack, F.X., Young, L.R., Elwing, J.M., Chuck, G., Leonard, J.M., Schmithorst, V.J., Laor, T., Brody, A.S., Bean, J., Salisbury, S., and Franz, D.N. (2008). Sirolimus for Angiomyolipoma in Tuberous Sclerosis Complex or Lymphangioleiomyomatosis. M Engl J Med *358*, 140-151.

61.   Engelman, J.A., Chen, L., Tan, X., Crosby, K., Guimaraes, A.R., Upadhyay, R., Maira, M., McNamara, K., Perera, S.A, Song, Y, Chirieac, L.R., Kaur, R., Lightbown, A., Simendinger, J., Li, T., Padera, R.F.,Garcı´a-Echeverrı´a, C., Weissleder, R., Mahmood, U., Cantley, L.C., and Wong, K. (2008). Effective use of PI3K and MEK inhibitors to treat mutant K-Ras G12D and PIK3CA H1047R murine lung cancers. Nat Med *14*, 1351-1356.

62.   Liang, M., Ma, J., Kzolowski, P., Qin, W., Li, D., Goto, J. Shimamura, T., Hayes, D.N., Meyerson, M., Kwiatkowski, D.J., and Wong, K. (2010). TSC1 loss synergizes with K-RAS activation in lung cancer development in the mouse and confers rapamycin sensitivity. Oncogene 29, 1588–1597.

63.   De Raedt, T., Walton, Z., Yecies, J.L., Li, D., Chen, Y., Malone C.F., Maertens, O., Jeong, S.M., Bronson, R.T., Lebleu, V., Kalluri, R., Normant, E., Haigis, M.C., Manning, B.D., Wong, K.K., Macleod, K.F., and Cichowski, K. (2011). Exploiting cancer cell vulnerabilities to develop a combination therapy for Ras-driven tumors.

64.   Guertin, D. A. and Sabatini, D. M. (2009). The pharmacology of mTOR inhibition. Science Signaling *2*, pe24.

APPENDIX

Chewing the Fat on Tumor Cell Metabolism

Adapted from:

Yecies, J.L.[1] and Manning, B.D[1]. (2010). Chewing the fat on tumor cell metabolism. *Cell* 140, 28-30.

[1]Department of Genetics and Complex Diseases, Harvard School of Public Health, Boston, MA 02115, USA

SUMMARY

Tumor cells undergo a metabolic shift toward specific bioenergetic (glycolysis) and anabolic (protein and lipid synthesis) processes that promote rapid growth. Nomura et al. (2010) now demonstrate that an increase in monoacylglycerol lipase (MAGL) drives tumorigenesis through the lipolytic release and remodeling of free fatty acids [1].

DISCUSSION

The re-emergence of the field of tumor cell metabolism has yielded important new insights into the metabolic reprogramming of cells that accompanies their oncogenic transformation (for recent reviews, see [2, 3]). The fundamental differences in both the catabolic and anabolic properties of a tumor cell relative to its tissue of origin could provide opportunities for selective therapeutic approaches. How cancer cells sense and use nutrients also impacts our understanding of dietary influences on tumor development and progression. To date, the majority of research on cancer metabolism has focused on the nearly ubiquitous catabolic switch of tumor cells (and other rapidly proliferating cells) from oxidative to glycolytic metabolism even in the presence of oxygen. This is referred to as aerobic glycolysis or, more popularly, the Warburg effect. However, tumor cells also commandeer anabolic processes resulting in elevated rates of protein, nucleic acid, and lipid biosynthesis. For instance, tumor cells exhibit a pronounced increase in *de novo* fatty acid synthesis, whereas normal cells are thought to acquire fatty acids primarily from dietary sources [4, 5]. Nomura et al. demonstrate an unexpected role for lipolytic remodeling of lipid species in promoting the tumorigenic properties of cancer cells [1].

A functional screen for differences in the activity of serine hydrolases in a small number of human cancer cell lines revealed that the activity of monoacyglycerol lipase

(MAGL) was elevated in those lines classified as more aggressive [1]. MAGL activity was also elevated in ovarian tumor tissue from patients with more advanced disease. This enzyme hydrolyzes monoacyl glycerols (MAGs) to release glycerol and a free fatty acid (FFA), and its best-characterized substrate is 2-arachidonoylglycerol, an endocannabinoid MAG [6]. Interestingly, the more aggressive cancer cell lines and high-grade primary tumors contained elevated FFA levels, which could be substantially reduced by pharmacological and short-hairpin RNA-mediated attenuation of MAGL activity. This surprising finding suggests that MAGL-dependent hydrolysis of MAGs is a major source of intracellular FFAs in aggressive cancer cells.

The MAGL-dependent remodeling of lipids appears to contribute to the transformed properties of tumor cells [1]. Using *in vitro* cell-based assays, the authors found that inhibition of MAGL activity impaired the enhanced migration and invasive capabilities of aggressive cancer cells and diminished their survival upon growth factor withdrawal. Interestingly, exogenous addition of the saturated FFAs palmitate (C16) or stearate (C18) to MAGL-inhibited cells rescued the migration defects. Reciprocally, overexpression of MAGL or addition of FFAs could enhance these phenotypes in less aggressive cancer cell lines exhibiting low MAGL activity. MAGL knockdown or pharmacological inhibition also blunted xenograft tumor growth in mice, and this was accompanied by a significant decrease in FFA levels within the tumors. Strikingly, these *in vivo* effects of MAGL inhibition on tumor growth and lipid levels were reversed by feeding the mice a high-fat diet. Collectively, these data demonstrate that MAGL promotes the oncogenic properties of tumor cells by increasing FFA levels.

To determine the mechanism of action of the FFA products of MAGL activity, the investigators took a lipidomics approach to identify lipid species sensitive to increases or decreases in MAGL activity in cancer cells [1]. This profile revealed that MAGL activity not only decreases MAGs and increases FFAs, but also leads to an increase in specific

FFA-derived signaling lipids, such as phosphatidic acid (PA), lysophosphatidic acid

(LPA), and prostaglandin E2 (PGE$_2$). The authors propose that these lipids activate

tumor-promoting signaling events, and they demonstrate that LPA and PGE$_2$ can rescue

the migration defects of cancer cells with attenuated MAGL activity. Interestingly, both

LPA and PGE$_2$ stimulate G protein-coupled receptor-mediated signaling events and

promote multiple oncogenic properties in tumor cells [7]. This study suggests that MAGL

activity plays a major role in the production of signaling lipids, which then stimulate tumor

cells in an autocrine manner.

The relationship between the synthesis, storage, and use of FFAs in tumor cells

is poorly understood. Most cancer cells express elevated levels of fatty acid synthase, a

multi-functional enzyme that converts malonyl-CoA to palmitate, thereby explaining the

increase in *de novo* lipogenesis in these cells [4, 5]. However, the Nomura et al. study

makes a compelling case that hydrolysis of acylglycerols, such as MAG, is a major

source of FFAs in tumor cells (Figure A-1). The authors propose that newly synthesized

FFAs are immediately converted into neutral lipid stores and that the use of FFAs is

dependent on their lipolytic release, with MAGL being the critical lipase. However,

further investigation regarding the fate of newly synthesized FFAs versus those released

by hydrolysis of acylglycerols in tumor cells is needed. Through *in vitro* assays, Nomura

et al. focus primarily on the contribution of MAGL-derived lipid mediators to cancer cell

migration. However, the tumor-promoting effects of MAGL in the *in vivo* xenograft model

are more likely to depend on increased cell growth and proliferation. These are

processes predicted to rely on lipid remodeling for new membrane biosynthesis and,

perhaps, beta-oxidation for energy production to support accompanying anabolic

processes. Although the bioenergetic needs of cancer cells are predominantly met

through glycolysis, the oxidation of FFAs offers an alternative route (e.g., [8, 9]). Again,

the question is whether the *in vivo* fates of FFAs derived from *de novo* synthesis versus
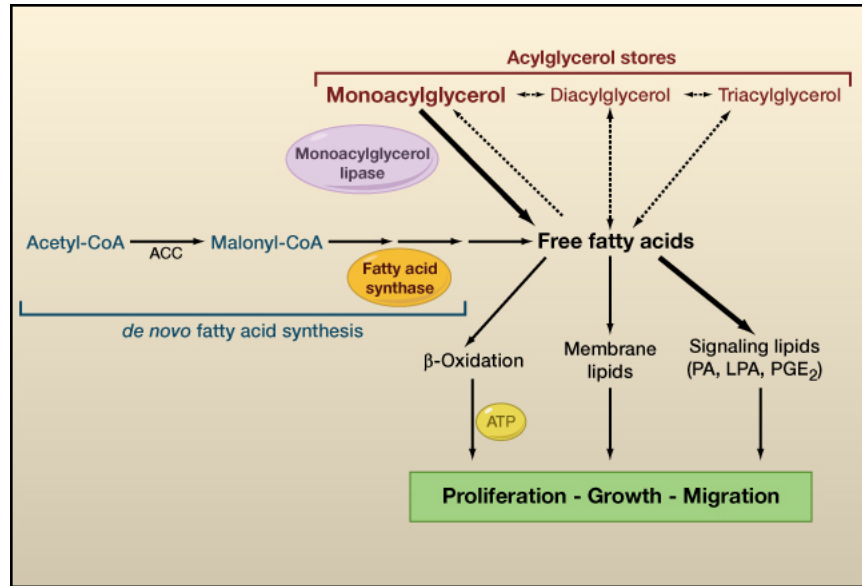
Figure A-1. Free fatty acids in tumor cells. Tumor cells display elevated rates of *de novo* free fatty acid (FFA) synthesis due, in large part, to their increased expression of fatty acid synthase (FASN). Newly synthesized FFAs are believed to be converted to neutral lipid stores, including mono- (MAG), di- (DAG), or tri- (TAG) acylglycerols. The activity of monoacylglycerol lipase (MAGL), which catalyzes the lipolytic release of FFAs from MAGs, is elevated in more aggressive tumor cells (Nomura et al., 2010). MAGL plays a critical role in maintaining the increase in FFAs in such cells and in promoting the production of FFA-derived signaling lipids, such as phosphatidic acid (PA), lysophosphatidic acid (LPA), and prostaglandin E2 (PGE_2). Other potential fates of newly synthesized or released FFAs include conversion to specific lipid species for incorporation into cellular membranes or β-oxidation for the production of ATP. FFA remodeling and utilization contribute to tumor cell proliferation, growth, and migration.

lipolytic release differ or whether FFAs ultimately enter the same pool for remodeling or catabolic use.

Many exciting new questions arise from the findings reported by Nomura and colleagues regarding the role of both MAGL and exogenous lipids in tumor development and progression. For instance, how is MAGL expression and activity regulated in tumor cells, and how widespread is its activation in cancer? Is MAGL a metastasis factor and can its activity be used as a biomarker to predict the influence of dietary fats and obesity on tumor progression? Although MAGL was found to increase cell migration and invasion *in vitro*, the effects on tumor metastasis were not examined in this study (Nomura et al., 2010). Interestingly, the inhibitory effects of MAGL attenuation on tumor growth were reversed by feeding the mice a high fat diet, which has been shown to promote metastasis in other xenograft tumor models (e.g., [10]). It will be interesting to determine whether conditions of obesity lead to increased levels of FFA-derived signaling lipids, such as LPA, within tumors. Finally, the antitumor effects of the MAGL-selective inhibitor used in this study suggest that MAGL is a promising therapeutic target for treating cancer. However, the critical role of MAGL in attenuating endocannabinoid signaling in the brain could lead to behavioral side effects that are unique amongst cancer drugs [6]. It is clear that we are just beginning to understand the molecular contributions of alterations in lipid metabolism to the pathology of cancer.

REFERENCES

1.   Nomura, D.K., Long, J.Z., Niessen, S., Hoover, H.S., Ng, S.W., and Cravatt, B.F. (2010). Monoacylglycerol lipase regulates a fatty acid network that promotes cancer pathogenesis. Cell *140*, 49-61.

2.   Hsu, P.P., and Sabatini, D.M. (2008). Cancer **cell** metabolism: Warburg and beyond. Cell *134*, 703-707.

3.   Vander Heiden, M.G., Cantley, L.C., and Thompson, C.B. (2009). Understanding

the Warburg effect: the metabolic requirements of cell proliferation. Science *324*, 1029-1033.

4.   Medes, G., Thomas, A., and Weinhouse, S. (1953). Metabolism of neoplastic tissue. IV. A study of lipid synthesis in neoplastic tissue slices in vitro. Cancer Res *13*, 27-29.

5.   Menendez, J.A., and Lupu, R. Fatty acid synthase and the lipogenic phenotype in cancer pathogenesis. (2007). Nat. Rev. Cancer *7*, 763-777.

6.   Long, J.Z., Li, W., Booker, L., Burston, J.J., Kinsey, S.G., Schlosburg, J.E., Pavon, F.J., Serrano, A.M., Selley, D.E., Parsons, L.H.*, et al.* (2009). Selective blockade of 2-arachidonoylglycerol hydrolysis produces cannabinoid behavioral effects. Nat. Chem. Biol. *5*, 37-44.

7.   Dorsam, R.T., and Gutkind, J.S. (2007). G-protein-coupled receptors and cancer. Nat. Rev. Cancer *7*, 79-94.

8.   Buzzai, M., Bauer, D.E., Jones, R.G., Deberardinis, R.J., Hatzivassiliou, G., Elstrom, R.L., and Thompson, C.B. (2005). The glucose dependence of Akt-transformed cells can be reversed by pharmacologic activation of fatty acid beta-oxidation. Oncogene *24*, 4165-4173.

9.   Schafer, Z.T., Grassian, A.R., Song, L., Jiang, Z., Gerhart-Hines, Z., Irie, H.Y., Gao, S., Puigserver, P., and Brugge, J.S. (2009). Antioxidant and oncogene rescue of metabolic defects caused by loss of matrix attachment. Nature *461*, 109-113.

10.   Rose, D.P., Connolly, J.M., and Meschter, C.L. (1991). Effect of dietary fat on human breast cancer growth and lung metastasis in nude mice. J. Natl. Cancer Inst. *83*, 1491-1495.